CHARACTERIZING THE EMISSIONS OF FINE PARTICULATE MATTER IN THE VICINITY OF A RAIL YARD

A Dissertation
Presented to
The Academic Faculty

by

Boris Galvis Remolina

In Partial Fulfillment
of the Requirements for the Degree
Doctor of Philosophy in the
School of Civil and Environmental Engineering

Georgia Institute of Technology
December, 2013

CHARACTERIZING THE EMISSIONS OF FINE PARTICULATE MATTER IN THE VICINITY OF A RAIL YARD

Approved by:

Dr. Armistead G. Russell, Advisor
School of School of Civil and Environmental Engineering
Georgia Institute of Technology

Dr. James A. Mulholland
School of School of Civil and Environmental Engineering
Georgia Institute of Technology

Dr. Michael H. Bergin
School of School of Civil and Environmental Engineering
Georgia Institute of Technology

Dr. Rodney J. Weber
School of Earth and Atmospheric Sciences
Georgia Institute of Technology

Dr. Nga Lee Ng
School of Earth and Atmospheric Sciences
Georgia Institute of Technology

Date Approved: August 09, 2013

To Luz Dary, Santiago, Hannah and to all my family

ACKNOWLEDGEMENTS

I want to express my immense gratitude to Dr. Ted Russell for generously giving me his keen insight and putting all his vast experience and support behind my work. His patience and openness have shown me by example how to be a mentor. I also want to thank Dr. Mike Bergin for giving me encouragement, and showing me his contagious curiosity and undying capacity of amazement. Thanks to Dr. Jim Mulholland, Dr. Rodney Weber and Dr. Nga Lee Ng for their guidance, their time, their insightful comments, and thoughtful advice for my dissertation.

I wish to thank my wife Luz Dary for giving up everything to come in this quest with me, for always been there, motivating me to go on. To my son Santiago for all the inspiration he has given me and to my daughter Hannah for the pure stream of joy she endlessly offers me. To my mother, father and siblings and to my aunt Esperanza, for all their support.

I also like to express my appreciation to Alejandro Caro, Gina Rodriguez, Eva Caro, Fernando Garcia and Adriana San Miguel for becoming part of my family.

Thanks to Marcus Trail, Jorge Pachon, Jeremiah Redman, Brandon Strellis, Sunny Ivey, Rawan E-Afifi, Kyle Digby, Mariel Friberg, Aika Yano Davis, Rish Vaidyanathan, Sivaraman Balachandran, Marissa Maier, Peng Liu, Neel Kotra, Laura King, Gretchen Goldman, Xiaolu Zhang, Zakiya Seymour, Ricardo Morales, Natasha Isable and Wenxian Zhang who trudge with me through the perils and vicissitudes of graduate school and academic life.

My heartfelt thanks to my colleagues and friends Heather Holmes, Gayle Hagler, Yongtao Hu and Talat Odman for their collaboration and example.

I wish to acknowledge Hermano Carlos Alberto Gomez and Dr. Camilo Guaqueta Rodriguez and all the officials at Universidad de La Salle in Colombia for igniting my dream to earn a Doctoral degree in the United States. Also thanks to the Colombian Institute for the Development of Science and Technology (COLCIENCAS) and the Academic and Professional Programs for the Americas (LASPAU) for making possible my aspiration of studying in the United States.

This project was funded by the Congestion Mitigation and Air Quality Improvement (CMAQ) Program through Georgia DOT, and Georgia DNR. Funding also was provided by Georgia Power, the Southern Company, and the Colombian Institute for the Development of Science and Technology COLCIENCIAS. We thank Dr. Michelle Bergin and Dr. Gil Grodzinsky at Georgia EPD for their help.

TABLE OF CONTENTS

Page

ACKNOWLEDGEMENTS iv

LIST OF TABLES ix

LIST OF FIGURES x

SUMMARY xiii

CHAPTER

1 INTRODUCTION 1

1.1. References 4

2 FUEL–BASED FINE PARTICULATE AND BLACK CARBON EMISSION FACTORS FROM A RAIL YARD IN ATLANTA 7

2.1. Abstract 7

2.2. Implications 8

2.3. Introduction 8

2.4. Experimental Methods 12

2.4.1. Monitoring sites 12

2.4.2. Air pollutant measurements 14

2.4.3. Data Analysis 15

2.5. Results 18

2.5.1. Concentrations of BC and $PM_{2.5}$ 18

2.5.2. Wind speed and direction and pollutants 20

2.5.3. Downwind–upwind differences and high-frequency components 23

2.5.4. Emission factors 23

2.6. References 29

3 IMPACTS ON FINE PARTICULATE MATTER, BLACK CARBON AND HEALTH OF CONVERTING RAIL YARD LOCOMOTIVES TO LOWER EMISSION TECHNOLOGIES 34

3.1. Abstract 34

3.2. Introduction 35

3.3. Material and Methods 38

3.3.1. Study location 38

3.3.2. Dispersion modeling 40

3.3.3. Sources 41

3.3.3. Emissions 42

3.3.3. Background concentrations 47

3.3.3. Health Impacts 47

3.4. Results and Discussion 48

3.4.1. Model evaluation 48

3.4.2. Source apportionment 51

3.4.3. Air quality impact evaluation 52

3.4.4. Health Incidence and Valuation 55

3.4.5. Cost-benefit 57

3.5. References 58

4 AEROSOL CHEMICAL SPECIATION AND SOURCE IMPACT ANALYSIS NEAR RAIL YARDS 63

4.1. Abstract 63

4.2. Introduction 64

4.3. Experimental Methods 65

4.3.1. Study description 65

4.3.2. Aerosol chemical speciation monitor 67

4.3.3. Positive matrix factorization 67

4.3.4. Aethalometer and black carbon apportionment 68

4.3.5. Multi-angle absorption photometers 69

4.3.6. Tapered element oscillating microbalance 70

4.3.7. Wind sector selective filter based measurements 70

4.4. Results and discussion 72

4.4.1. Organic and elemental carbon and Ions 72

4.4.2. Metals 73

4.4.3. ACSM results validation 74

4.4.4. Organics PMF solution 76

4.4.5. MAAP and 7-wavelength Aethalometer 80

4.4.6. Black carbon speciation 80

4.4.7. Chemical species and wind direction 83

4.5. References 86

5 CONCLUSIONS AND FUTURE RESEARCH 93

5.1. Conclusions 93

5.1.1. Fuel-based fine particulate and black carbon emission factors from a rail yard area in Atlanta 93

5.1.2. Impacts on fine particulate, black carbon and health of converting rail yard locomotives to lower emission technologies 94

5.1.3. Aerosol chemical speciation and source impact analysis near rail yards 95

5.2. Future research 97

APPENDIX A: SUPPORTING INFORMATION FOR CHAPTER 2 100

APPENDIX B: SUPPORTING INFORMATION FOR CHAPTER 3 111

APPENDIX C: DATABASE OF MEASUREMENTS 122

VITA BORIS GALVIS 123

LIST OF TABLES

Page

Table 2.1: Concentrations of PM2.5 and BC for FS, DX, and other Atlanta urban sites in 2011 19

Table 2.2: Downwind/ Upwind concentration differences for DX and FS sites 23

Table 2.3: High-frequency components from wavelet analysis for the DX and FS sites 24

Table 2.4: Emission Factors for the DX and FS sites 25

Table 3.1: Fuel consumption, emission factors and emissions from Inman and Tilford rail yards 43

Table 3.2: Emissions from major on-road mobile sources at the modeling domain 46

Table 3.3: Emissions from major industrial sources at the modeling domain 46

Table 3.4: Annual avoided health incidences 56

Table 3.5: Annual reductions in health costs and premature mortality valuation 57

Table 4.1: Organic and elemental carbon downwind and upwind of the Inman and Tilford rail yard between 06/20/2011 and 11/08/2011 73

Table 4.2: Metals downwind and upwind of the Inman and Tilford rail yard between 06/20/2011 and 11/08/2011 74

Table 4.3: HOA vs. BCf and BBOA vs. BCb regression results 81

Table A.1: Dates of photographic surveillance of Inman rail yard 90

Table A.2: Control emission factors 100

Table B.1: Surface characteristics generated with AERSURFACE 101

Table B.2: Modeling parameters for non-road and on-road mobile sources 102

Table B.3: Modeling parameters for industrial sources 104

Table B.4: Emissions from rail yards 105

Table B.5: Emissions from on-road mobile sources 106

Table B.6: Emissions from industrial sources 107

Table B.7: Concentration-response functions 108

LIST OF FIGURES

Page

Figure 2.1: $PM_{2.5}$ annual arithmetic means at Atlanta urban sites (GAEPD, 2012). 10

Figure 2.2: Schematic of the location of the study 13

Figure 2.3: CO_2 concentration (a) at DX from 12:00 a.m. on September 5, 2011, to 11:59 p.m. on September 6, 2011. The CO_2 concentration signal was separated into spikes and background components by wavelet analysis. (b) Spikes in CO_2 concentration. 17

Figure 2.4: Event associated with a locomotive at the DX site on September 17, 2011. At 2:14 p.m. a train passes by the monitoring site. An event is detected shortly after. The subplot shows the lineal regression of the event detected 19

Figure 2.5: Wind Roses for (a) the DX site and (b) the FS site 20

Figure 2.6: Normalized pollutant concentration roses for (a) BC, (b) $PM_{2.5}$, and (c) CO_2 at the DX and FS monitoring sites. Downwind sectors are marked in gray. 22

Figure 2.7: Events of high BC and corresponding CO_2 concentrations at (a) DX and (b) FS. The minimum concentration measured during each event was taken as baseline. Events were centered at the time when the maximum BC concentration was measured (*t*). Average concentrations 5 min before and 5 min after are shown along with standard deviations (σ) and uncertainties of the mean (σ_x) 27

Figure 2.8: Frequency distributions of emission factors obtained from BC events at the FS and DX sites 28

Figure 3.1: Study location and model domain. Layout of the rail yards in gray. Major industrial sources include A) General Shale Brick Inc plant, B) Georgia Power Company McDonough-Atkinson plant, C) Lafarge Building Materials, Inc, D) Cobb County R.L. Sutton water reclamation facility, E) Atlanta R.M. Clayton water reclamation facility, F) Ennis Paint, Inc., G) Mead Packaging Co. and H) Central Metals Co. Major streets included in the model are shown. Interstate highways are shown for geographic reference. Monitoring sites, denoted (o), are Fire station 8 (FS), Dixie (DX) and Jefferson Street (JS) 39

Figure 3.2: Modeled and measured a) BC and b) $PM_{2.5}$ annual average concentrations 48

Figure 3.3: Modeled and measured a) BC b) $PM_{2.5}$ daily average concentrations at FS 49

Figure 3.4: Modeled to measured ratios of daily average concentrations by percentile for a) BC and b) $PM_{2.5}$. 50

Figure 3.5: Modeled (AERMOD) and measured (MAAP and TEOM) hourly average concentrations for BC at a) FS and b) DX, and $PM_{2.5}$ at c) FS and d) DX 50

Figure 3.6: Source apportionment for BC and $PM_{2.5}$ at FS and DX 52

Figure 3.7: Spatial distribution of annual average concentrations of a) BC, b) $PM_{2.5}$ from all sources in the domain and c) $PM_{2.5}$ from the rail yards. Units of the isolines are $\mu g/m^3$. Industrial sources include (A) General Shale Brick Inc plant, (B) Georgia Power Company McDonough-Atkinson plant, (C) Lafarge Building Materials, Inc, (D) Cobb County R.L. Sutton water reclamation facility, (E) Atlanta R.M. Clayton water reclamation facility, (F) Ennis Paint, Inc., (G) Mead Packaging Co. and (H) Central Metals Co. 53

Figure 3.7: Spatial distribution of annual average $PM_{2.5}$ reduction by retrofitting switcher locomotives with new Gensets. Units of the isolines are µg/m3. Industrial sources include (A) General Shale Brick Inc plant, (B) Georgia Power Company McDonough-Atkinson plant, (C) Lafarge Building Materials, Inc, (D) Cobb County R.L. Sutton water reclamation facility, (E) Atlanta R.M. Clayton water reclamation facility, (F) Ennis Paint, Inc., (G) Mead Packaging Co. and (H) Central Metals Co. 55

Figure 4.1: Study location. Wind sectors for filter sampling are marked red for downwind and green for upwind. 66

Figure 4.2: Time series and regression comparisons of a) 33 minute average concentrations of TEOM $PM_{2.5}$ and BC+NR PM_1 and b) daily averages of TEOM $PM_{2.5}$, FRM $PM_{2.5}$ and BC+NR PM_1 at FS. 75

Figure 4.3: Sulfate and nitrate concentrations reported by ACSM at FS vs. SEARCH at Jefferson street site. 76

Figure 4.4: PMF 3 factor solution mass spectra. Tracers are marked for each factor 77

Figure 4.5: Time series of organic factors 78

Figure 4.6: Organic factors and vs. other observed species near the rail yards. a) BC vs. HOA. b) K vs. BBOA and c) OC vs. OOA. 79

Figure 4.7: BC from MAAP at 670 nm vs. BC from Aethalometer at 660 nm. 80

Figure 4.8: Black carbon apportionment and ACSM results comparison. a) Aethalometer $PM_{2.5}$ BCb vs. ACSM NR PM_1 BBOA and b) Aethalometer $PM_{2.5}$ BCf vs. ACSM NR PM1 HOA. 82

Figure 4.9: Black carbon apportionment during fall and winter 2010-2011 and fall and winter 2011-2012 at FS 83

Figure 4.10: Concentration roses of chemical species at FS during the winter 2011 84

Figure 4.11: Concentration roses of BC speciation results 86

Figure A.1: CO_2, BC and $PM_{2.5}$ time series for FS downwind conditions 94

Figure A.2: CO_2, BC and $PM_{2.5}$ time series for DX downwind conditions 95

Figure A.3: Histograms of CO_2, BC and $PM_{2.5}$ for FS downwind conditions 96

Figure A.4: Histograms of CO_2, BC and $PM_{2.5}$ for DX downwind conditions 97

Figure A.5: Boxplot of BC emission factor by hour of the day at DX site 98

Figure A.6: Boxplot of BC emission factor by hour of the day at FS site 99

Figure A.7: Boxplot of BC emission factor by day of the week at DX site 99

Figure A.8: Boxplot of BC emission factor by day of the week at FS site. 100

Figure B.1: Simulated and measured daily averages of BC and $PM_{2.5}$ at DX 108

SUMMARY

Aerosol emissions from diesel combustion and other activities in rail yards can affect the health of urban populations. Fine particulate ($PM_{2.5}$) concentrations near the Inman and Tilford rail yards in Atlanta, Georgia, are the highest measured in the state. The rail yard complex is surrounded by homes, schools, businesses and other industries. The impact of the aerosol emissions from these rail yards on local concentrations of $PM_{2.5}$ was quantified. Specifically, black carbon and $PM_{2.5}$ fuel-based emission factors from the rail yards were estimated by carbon balance using high time-resolution monitoring, a BC and $PM_{2.5}$ emissions inventory was estimated and dispersion modeling was applied to assess the impact of the rail yard activities on local air quality and the cost and benefits of upgrading locomotive engines with cleaner technologies was assessed. Further, baseline information that will allow a later evaluation of the improvement of local air quality as locomotives operating in the rail yards are upgraded was generated, and a composition profile of the rail yard aerosols was developed using chemical speciation techniques.

These results found that activities from locomotives in the Inman and Tilford Rail yards lead to and an average emission factor of 6.0 ± 0.5 g of $PM_{2.5}$ per gallon of fuel and are responsible for increases in annual average concentrations of approximately 1.3 $\mu g/m^3$ of $PM_{2.5}$ as far as 1 km from the perimeter of the rail yard complex. Approximately 11.7 tons of BC and 26 tons of $PM_{2.5}$ per year were emitted from the rail yards in 2011. The rail yards were found to be important sources of hydrocarbon-like organic aerosols (HOA) and black carbon from fuel (BCf). Upgrading the engines at the rail yards would decrease $PM_{2.5}$ emissions by about 9 t/year, reducing $PM_{2.5}$

concentrations around 0.5±0.1 $\mu g/m^3$ as far as 1 km from the perimeter of the rail yard complex and producing monetized health benefits of approximately 24 million dollars per year.

CHAPTER 1

INTRODUCTION

The rail industry is fundamental to the U.S. economy and is the most energy efficient mode of land transportation. It moves almost half of the nation's freight through a system of 140,000 miles of tracks and generates roughly $265 billion in total annual economic activity (AAR, 2011). The amount of freight transported by rail in the U.S. has followed an increasing trend since the 1960's. In 2008, approximately 1.8 billion ton-miles were carried by the industry (BTS, 2011). Intermodal freight is the fastest growing sector of the railroad industry, accounting for nearly 22 percent of rail revenue in 2010 (DOI, 2011). The rail industry is found in all the major cities in the U.S., concentrating its activities in rail yards.

Rail yards have the potential to significantly influence local fine particulate matter (aerodynamic diameter $\leq$ 2.5 mm; $PM_{2.5}$) concentrations through emissions from diesel-electric locomotives and supporting activities (Cahill et al., 2011;Campbell et al., 2009;Kam et al., 2011;Kim et al., 2004). Emissions from rail yards include black or elemental carbon and organic carbon (Cahill et al., 2011; Sawant et al., 2007), nitrogen oxides (Cahill et al., 2011; Starcrest Consulting Group, 2004), sulfur dioxide, hydrocarbons, carbon monoxide and carbon dioxide, metals and polycyclic aromatic hydrocarbons (Cahill et al., 2011). These emissions are of concern in urban areas where rail yards are in proximity to dwellings, exposing populations to elevated concentrations of these pollutants.

One of the main components of diesel emissions is black carbon (BC). BC is a primary pollutant formed by incomplete combustion and emitted as fine particulate. It affects visibility (Park et al., 2003; Prasad et al., 2010) and is considered the second most important human emission for climate forcing in the industrial-era atmosphere after CO_2

(Bond et al., 2013; Jacobson, 2010; Roberts et al., 2004). The US emits about 640 thousand tons of BC per year. Approximately half of the BC emissions in the U.S. come from mobile sources, and around 90% of BC emissions from mobile sources come from diesel engines (EPA, 2012a, b, c). Other sources of BC are residential heating, industry and biomass burning. Emission estimates indicate that mobile diesel engines, which include non-road diesel-electric locomotives, offer the greatest potential area for BC mitigation applying currently available control technologies (EPA, 2012c).

Diesel emissions have been classified as carcinogenic and are thought to have other suspected negative effects on human health (WHO, 2012). Epidemiological studies of occupational exposure have demonstrated increased risk of death from lung cancer in exposed workers (Attfield et al., 2012; Silverman et al., 2012). Stringent regulations have been put in place to curb diesel emissions in developed nations. New technologies burn diesel fuel more efficiently and reduce emissions through exhaust controls. These new regulations and technologies, along with other measures to reduce BC emissions will need time to have an effect; more so, in developing countries with lax standards, older technologies and more limited resources. Yet, measures to reduce BC emissions from major sources are likely to provide near-term environmental and public health benefits at low relative cost, and implemented in conjunction with substantial methane (CH_4) and CO_2 emissions reductions, could help limit global mean warming below the 2°C threshold during the following 6 decades (Shindell et al., 2012). More research is needed to fully understand what improvements in air quality and in health can be achieved by reductions in diesel emissions (WHO, 2012).

Northwest of Atlanta, Georgia, Inman and Tilford rail yards are located beside residential neighborhoods, industries, and schools. $PM_{2.5}$ concentrations in Atlanta have been decreasing over the past ten years (EPRI, 2012; GAEPD, 2012), but the Fire Station 8 site (FS) near the rail yards has consistently showed the highest annual average $PM_{2.5}$ concentration reported at any of the monitoring sites operated by the state of Georgia

(GAEPD, 2013), suggesting that rail yard associated emissions play an important but still undetermined role in local air quality. This dissertation details a comprehensive research program aimed to quantify the impact of the aerosol emissions from Inman and Tilford railyards on local air quality. The thesis is organized as follows:

Chapter 1: Introduction.

Chapter 2: Fuel-based fine particulate and black carbon emission factors from a rail yard area in Atlanta. The impact on local $PM_{2.5}$ concentrations of the emissions from the Inman and Tilford rail yards in Atlanta was determined. High-time-resolution measurements of BC, $PM_{2.5}$, CO_2, and wind speed and direction were made at two locations, north and south of the rail yards for one year. Emissions factors (i.e., the mass of BC or $PM_{2.5}$ per gallon of fuel burned) were estimated by using the downwind/upwind difference in concentrations, wavelet analysis, and an event-based approach.

Chapter 3: Impacts on fine particulate matter, black carbon and health of converting rail yard locomotives to lower emission technologies. A local emission inventory for northwest Atlanta was estimated and dispersion modeling was used to assess the impact on local $PM_{2.5}$ and BC concentrations coming from the Inman and Tilford rail yard emissions. Modeling results were evaluated against data from two monitoring sites. Potential reductions in $PM_{2.5}$ and BC concentrations that could be accomplished by upgrading traditional switcher locomotives used in this rail yard complex were assessed and the health benefits of these reductions were evaluated. A comparison with costs of upgrades was also made**.**

Chapter 4: Aerosol chemical speciation and source impact analysis near rail yards. Aerosols near the Inman and Tilford rail yard complex in Atlanta were characterized using an aerosol chemical speciation monitor and an Aethalometer. Source apportionment and positive matrix factorization techniques were used to estimate sources and factors for black carbon and organic aerosols respectively. Meteorological information was used to identify locations of sources of different species of pollutants.

Chapter 5: Conclusions and future research. In addition to summarize the results and conclusions from this study, Chapter 5 identifies directions for future research. Such research includes the assessment of changes in air quality after the implementation of cleaner technologies at the rail yard complex, investigating NOx concentrations in the area and accessing or retrieving information on rail yard activity. Also, suggestions for expanding monitoring capacity at low cost for these and other similar sources, broadening the scope of modeling for rail yard impact evaluation and completing the analysis of chemical composition of aerosols emitted by rail yard activities.

1.1 References

Association of American Railroads [AAR]. 2011. Overview of America's Freight Railroads, [accessed May 2013]. Available from https://www.aar.org/keyissues/Documents/Background-Papers/Overview-US-Freight-RRs.pdf.

Attfield, M. D., Schleiff, P. L., Lubin, J. H., Blair, A., Stewart, P. A., Vermeulen, R., Coble, J. B., and Silverman, D. T. 2012. The Diesel Exhaust in Miners Study: A Cohort Mortality Study With Emphasis on Lung Cancer. Journal of the National Cancer Institute. doi: 10.1093/jnci/djs035.

Bond, T. C., Doherty, S. J., Fahey, D. W., Forster, P. M., Berntsen, T., DeAngelo, B. J., Flanner, M. G., Ghan, S., Kärcher, B., Koch, D., Kinne, S., Kondo, Y., Quinn, P. K., Sarofim, M. C., Schultz, M. G., Schulz, M., Venkataraman, C., Zhang, H., Zhang, S., Bellouin, N., Guttikunda, S. K., Hopke, P. K., Jacobson, M. Z., Kaiser, J. W., Klimont, Z., Lohmann, U., Schwarz, J. P., Shindell, D., Storelvmo, T., Warren, S. G., and Zender, C. S. 2013. Bounding the role of black carbon in the climate system: A scientific assessment. Journal of Geophysical Research: Atmospheres:n/a-n/a. doi: 10.1002/jgrd.50171.

Bureau of Transportation Statistics [BTS]. Department of Transportation. 2011. National Transportation Statistics, [accessed May 2013]. Available from http://www.rita.dot.gov/bts/sites/rita.dot.gov.bts/files/NTS_Entire_Q1.pdf.

Cahill, T. A., Cahill, T. M., Barnes, D. E., Spada, N. J., and Miller, R. 2011. Inorganic and Organic Aerosols Downwind of California's Roseville Railyard. Aerosol Science and Technology no. 45 (9):1049-1059. doi: 10.1080/02786826.2011.580796.

Campbell, D., and Fujita, E. M. 2009. Roseville Rail Yard Air Monitoring Project (RRAMP). Final Report Summary of Data QA and Trend Analysis. Desert Research Institute, Reno, NV., [accessed Oct 2012]. Available from http://www.placer.ca.gov/Departments/Air/~/media/apc/documents/UP/2009/December/RRAMPFinalUpdate121009.ashx.

Congestion Mitigation and Air quality Improvement Program [CMAQ]. Department of transportation. 2009. EPD Railroad related emissions reduction project in Atlanta GA20090013, [accessed Apr 2013]. Available from https://fhwaapps.fhwa.dot.gov/cmaq_pub/View/default.aspx?id=GA20090013.

Department of the interior [DOI]. 2011. National Atlas. Overview of U.S. Freight Railroads, [accessed May 2013].

Electric Power Research Institute [EPRI]. 2012. The Southeastern Aerosol Research and Characterization Network: SEARCH, [accessed Oct 2012]. Available from http://www.atmospheric-research.com/studies/search/SEARCHFactSheet.pdf.

Georgia Environmental Protection Division [GAEPD]. 2012. Ambient Monitoring Program Annual Data Reports, [accessed Jan 2013]. Available from http://www.georgiaair.org/amp/report.php.

Georgia Environmental Protection Division [GAEPD]. 2013. Ambient Monitoring Program Air Quality Database, [accessed Feb 2013]. Available from http://www.georgiaair.org/amp/amp_query.html.

Jacobson, M. Z. 2010. Short-term effects of controlling fossil-fuel soot, biofuel soot and gases, and methane on climate, Arctic ice, and air pollution health. Journal of Geophysical Research: Atmospheres no. 115 (D14):D14209. doi: 10.1029/2009JD013795.

Kam, W., Cheung, K., Daher, N., and Sioutas, C. 2011. Particulate matter (PM) concentrations in underground and ground-level rail systems of the Los Angeles Metro. Atmospheric Environment no. 45 (8):1506-1516. doi: 10.1016/j.atmosenv.2010.12.049.

Kim, E., Hopke, P. K., and Edgerton, E. S. 2004. Improving source identification of Atlanta aerosol using temperature resolved carbon fractions in positive matrix factorization. Atmospheric Environment no. 38 (20):3349-3362. doi: 10.1016/j.atmosenv.2004.03.012.

Park, R. J., Jacob, D. J., Chin, M., and Martin, R. V. 2003. Sources of carbonaceous aerosols over the United States and implications for natural visibility. Journal of Geophysical Research-Atmospheres no. 108 (D12). doi: 10.1029/2002jd003190.

Prasad, R., and Bella, V. R. 2010. A Review on Diesel Soot Emission, its Effect and Control. Bulletin of Chemical Reaction Engineering & Catalysis no. 5 (2):69-86.

Roberts, D. L., and Jones, A. 2004. Climate sensitivity to black carbon aerosol from fossil fuel combustion. Journal of Geophysical Research: Atmospheres no. 109 (D16):D16202. doi: 10.1029/2004JD004676.

Sawant, A. A., Nigam, A., Miller, J. W., Johnson, K. C., and Cocker, D. R. 2007. Regulated and Non-Regulated Emissions from In-Use Diesel-Electric Switching Locomotives. Environmental Science & Technology no. 41 (17):6074-6083. doi: 10.1021/es061672d.

Shindell, D., Kuylenstierna, J. C. I., Vignati, E., van Dingenen, R., Amann, M., Klimont, Z., Anenberg, S. C., Muller, N., Janssens-Maenhout, G., Raes, F., Schwartz, J., Faluvegi, G., Pozzoli, L., Kupiainen, K., Höglund-Isaksson, L., Emberson, L., Streets, D., Ramanathan, V., Hicks, K., Oanh, N. T. K., Milly, G., Williams, M., Demkine, V., and Fowler, D. 2012. Simultaneously Mitigating Near-Term Climate Change and Improving Human Health and Food Security. Science no. 335 (6065):183-189. doi: 10.1126/science.1210026.

Silverman, D. T., Samanic, C. M., Lubin, J. H., Blair, A. E., Stewart, P. A., Vermeulen, R., Coble, J. B., Rothman, N., Schleiff, P. L., Travis, W. D., Ziegler, R. G., Wacholder, S., and Attfield, M. D. 2012. The Diesel Exhaust in Miners Study: A Nested Case–Control Study of Lung Cancer and Diesel Exhaust. Journal of the National Cancer Institute. doi: 10.1093/jnci/djs034.

Starcrest Consulting Group, L. L. C. 2004. PORT-WIDE BASELINE AIR EMISSIONS INVENTORY EXECUTIVE SUMMARY, [accessed November 2011]. Available from http://westcoastcollaborative.org/files/sector-marine/Port%20of%20LA%20Emissions%20Inventory.pdf.

U.S. Environmental Protection Agency [EPA]. 2012a. Black Carbon Basic Information, [accessed Jan 2013]. Available from http://www.epa.gov/blackcarbon/basic.html.

U.S. Environmental Protection Agency [EPA]. 2012b. National Emissions Inventory (NEI) Air Pollutant Emissions Trends Data Available from http://www.epa.gov/ttnchie1/trends/.

U.S. Environmental Protection Agency [EPA]. 2012c. Report to Congress on Black Carbon, [accessed Dec 2012]. Available from http://www.epa.gov/blackcarbon/2012report/fullreport.pdf.

World Health Organization [WHO]. 2012. Diesel Engine Exhaust Carcinogenic. Available from http://press.iarc.fr/pr213_E.pdf.

CHAPTER 2

FUEL-BASED FINE PARTICULATE AND BLACK CARBON EMISSION FACTORS FROM A RAIL YARD AREA IN ATLANTA

(Galvis, B. Bergin, M., and Russell A.G. *Journal of the Air & Waste Management Association*, 63(6):648–658, 2013.)

2.1. Abstract

Rail yards have the potential to influence local fine particulate matter (i.e. particles with an aerodynamic diameter ≤ 2.5 mm; $PM_{2.5}$) concentrations through emissions from diesel locomotives and supporting activities. This is of concern in urban regions where rail yards are in proximity to residential areas. Northwest of Atlanta, Georgia, the Inman and Tilford rail yards are located beside residential neighborhoods, industries, and schools. The $PM_{2.5}$ concentrations near the rail yards is the highest measured amongst the state-run monitoring sites (Georgia Environmental Protection Division, 2012; http://www.georgiaair.org/amp/report.php). The authors estimated fuel-based black carbon (BC) and $PM_{2.5}$ emission factors for these rail yards in order to help determine the impact of rail yard activities on $PM_{2.5}$ concentrations, and for assessing the potential benefits of replacing current locomotive engines with cleaner technologies. High-time-resolution measurements of BC, $PM_{2.5}$, CO_2, and wind speed and direction were made at two locations, north and south of the rail yards. Emissions factors (i.e., the mass of BC or $PM_{2.5}$ per gallon of fuel burned) were estimated by using the

downwind/upwind difference in concentrations, wavelet analysis, and an event-based approach. By the authors' estimates, diesel-electric engines used in the rail yards have average emission factors of 2.8 ± 0.2 g of BC and 6.0±0.5 g of $PM_{2.5}$ per gallon of diesel fuel burned. A broader mix of rail yard supporting activities appear to lead to average emission factors of 0.7 ± 0.03 g of BC and 1.5 ± 0.1 g of $PM_{2.5}$ per gallon of diesel fuel burned. Rail yard emissions appear to lead to average enhancements of approximately 1.7 ± 0.1 μg/m^3 of $PM_{2.5}$ and approximately 0.8 ± 0.01 μg/m^3 of BC in neighboring areas on an annual average basis. Uncertainty not quantified in these results could arise mainly from variability in downwind/upwind differences, differences in emissions of the diverse zones within the rail yards, and the influence of on-road mobile source emissions.

2.2. Implications

In-use fuel-based black carbon and fine particulate emission factors for rail yard activities were quantified by novel approaches using near-source high-time-resolution monitoring of ambient concentrations at two sites. Results can reduce the uncertainty in rail yard emission inventories and the approach can be replicated and extended to assess trends and evaluate emission reduction alternatives

2.3. Introduction

Rail yard emissions are thought to originate largely from diesel-electric locomotives called "switchers" that are used to gather cars and assemble them into trains. Switchers are potentially high emitters because they are typically older model locomotives and have low-power duty cycles (U.S. Environmental Protection Agency [EPA], 2011a). Emissions from switchers include primary fine particulate matter (aerodynamic diameter ≤ 2.5 mm; $PM_{2.5}$), elemental and organic carbon (EC/OC),

nitrogen oxides (NOx), sulfur dioxide (SO_2), hydrocarbons, carbon monoxide (CO), and carbon dioxide (CO_2). Diesel emissions have suspected negative effects on human health (World Health Organization [WHO], 2012). Black carbon (BC) from diesel and other fossil fuels absorb solar radiation, affecting visibility (Prasad and Bella, 2010) and climate (Roberts and Jones, 2004). Rail yards have been identified as local sources of particulates (Kam et al., 2011), EC/OC (Sawant et al., 2007; Cahill et al., 2011), NOx (Starcrest Consulting Group, 2004; Cahill et al., 2011), CO_2, SO_2, metals, and polycyclic aromatic hydrocarbons (PAHs) (Cahill et al., 2011).

The contribution of particulate matter from rail yards to U.S. emissions, as estimated in the National Emissions Inventory (NEI), is small compared with on-road mobile sources or power plants (EPA, 2012). Switcher locomotives have been estimated to emit less than 0.1% of the total PM_{10} (PM with an aerodynamic diameter ≤ 10 mm) and $PM_{2.5}$ in the United States EPA, 2008a). Yet, emissions from rail yards located close to residential areas are of new interest because of recent regulations (EPA, 2008b), intensity of operations in limited areas, and the fast growing economic activity of switchyards and intermodal terminals (Laurits R. Christensen Associates, 2009).

In Atlanta, $PM_{2.5}$ concentrations have been decreasing over the past 10 yr (Electric Power Research Institute [EPRI], 2012; Georgia Environmental Protection Division [Georgia EPD], 2012), but near Inman and Tilford rail yards, the Fire Station 8 site (FS) has consistently showed the highest annual average $PM_{2.5}$ concentration reported at any of the Georgia state-run monitoring locations (Figure 2.1.). Georgia EPD (2009) applied the American Meteorological Society/Environmental Protection Agency Regulatory Model (AERMOD) using emission estimates based on NEI methodology, and

found that rail yards contribute approximately 1.9 μg/m^3 to the concentration of $PM_{2.5}$ at FS.

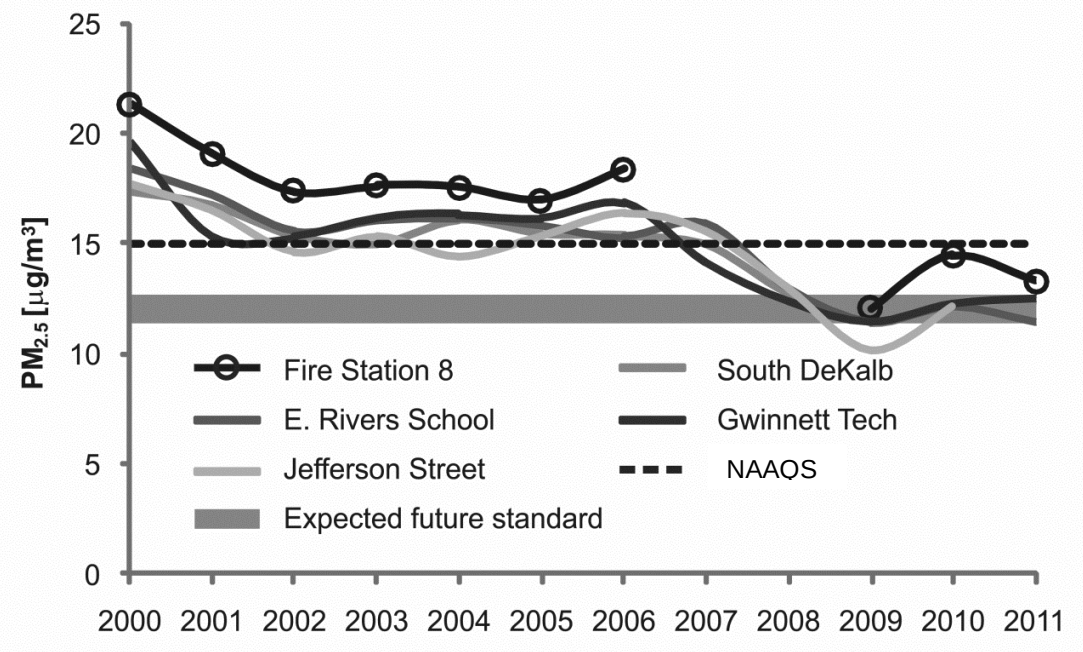

Figure 2.1. $PM_{2.5}$ annual arithmetic means at Atlanta urban sites (Georgia EPD, 2012).

Rail yard emissions are viewed as highly uncertain (Simon et al., 2008). Recently, a 27-state committee called ERTAC Rail developed top-down nationwide rail yard, line-haul, and shortline/regional emission inventories for the years 2007/2008 using confidential information from the railroad companies (Bergin et al., 2012). This inventory was used to update the 2011 EPA - NEI. Previous NEIs used the conventional approach quantify rail yard emissions. Inventories were calculated multiplying state-level yearly average fuel consumption data by nationwide fleet average fuel-based yard emission factors. States currently estimate rail yard emissions using methods based on the same approach (Sierra Research, 2004). Sources of uncertainty are estimated fuel use, distribution of consumption data to each rail category (i.e., switcher vs. Class I

locomotives), allocation of emissions to county level using local activity data (National Cooperative Freight Research Program [NCFRP], 2010), and yard emission factors that don't necessarily represent the variability in engine technologies, specific yard operating conditions, and the yard fleet mix (Simon et al., 2008). Furthermore, the yard emission factors may not adequately account for yard-associated emissions (i.e., emissions from testing and maintenance of locomotives and drayage trucks) (Fritz and Cataldi, 1991). Disaggregated fuel consumption data required to address the fuel related sources of uncertainty are unavailable mainly because companies view fuel consumption as proprietary information (NCFRP, 2010).

Rail yard emission estimates are developed mainly using emission factors for switchers that are an average of engine emissions over a cycle of stationary sequential operation at low and normal idle, and at eight other discrete power levels, called notches, weighted by numerical factors that reflect the time the engine is operated at each notch (CFR-40-92.101-133, 2011). These emissions factors have high reproducibility but may not represent real-world emissions from particular operating conditions (St. Denis et al., 1994; Cocker et al., 2004) and they may not have a quantitative indication of uncertainty. Previous work has been directed to obtain real-word emission factors from small samples of diesel-electric switcher locomotives measuring directly from the stack, varying fuel or type of engine (Fritz and Cataldi, 1991; Honc et al., 2006; Sawant et al., 2007), but little work has been aimed at quantifying their uncertainties, or to estimate emission factors that account for actual activities going on in and around rail yards.

The objective of this work is to advance the understanding of rail yard emissions by estimating $PM_{2.5}$ and BC fuel-based emission factors to reduce uncertainty in emission

inventories. The emission factors will account for the particular operating conditions of the rail yards using near-source high-time-resolution monitoring. This information may be used to improve air quality modeling results, aid in the development of effective air quality management strategies, and, as part of a joint government industry project (Congestion Mitigation and Air Quality Improvement Program, Georgia Environmental Protection Division [CMAQEPD], 2009), to assess the improvement in local air quality as cleaner technologies replace old switcher engines used at Inman and Tilford rail yards.

2.4. Experimental Methods

2.4.1. Monitoring sites

The study was carried out in Atlanta, Georgia, at locations near Inman and Tilford rail yards (Figure 2.2.). CSX's Tilford Yard is a hump terminal that handles approximately 80 trains per week and operates 10 switcher locomotives (Georgia EPD, 2009). Inman Yard is a large Norfolk Southern intermodal facility with 17 switcher locomotives (Georgia EPD, 2009). The yards are adjacent to each other, northwest of downtown Atlanta, inside the perimeter freeway I285 (Figure 2.2.). Other pollution sources in the area include Howells Yard (a small intermodal yard with 15 tracks), Georgia Power Company's McDonough-Atkinson Plant, Ennis Paint, and a Metropolitan Atlanta Rapid Transit Authority (MARTA) garage facility. The McDonough-Atkinson Plant was being converted from coal to natural gas during this study.

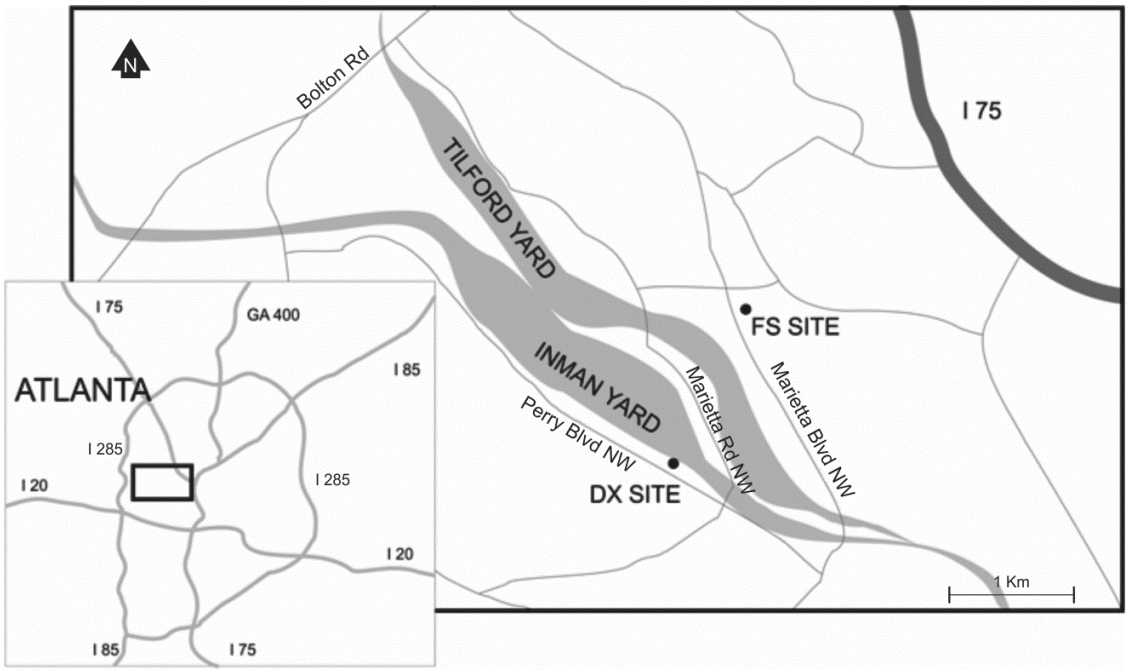

Figure 2.2. Schematic of the location of the study. The two monitoring sites are at the Dixie (DX) and Fire Station 8 (FS) locations.

Two monitoring sites were used: Fire Station 8 (FS) (coordinates: 33.80176˚N, -84.43559˚W) and Dixie (DX) (coordinates: 33.79080˚N,- 84.44026˚W), north and south of the rail yards (Figure 2.2.). Sites are 1.3 km apart. The FS site is part of the Assessment of Spatial Aerosol Composition Network (ASACA) (Butler et al., 2003) and is located at approximately 300 m of the arrival section of Tilford Yard and 30 m of Marietta Boulevard NW(17,000 annual average daily traffic [AADT] approximately), which runs between the FS site and the rail yards. Other roads with less traffic (>2000 AADT), such as Marietta Road, Bolton Road, and Perry Boulevard, surround and run through the rail yards. DX is contiguous to the intermodal terminal at Inman Yard, approximately 80 m from the tracks. The MARTA garage is located southwest of DX.

2.4.2. Air pollutant measurements

BC (multiangle absorption photometer [MAAP]; model 5012; Thermo Scientific, Franklin, MA), $PM_{2.5}$ (1400ab tapered element oscillating microbalance [TEOM]; R & P Thermo Scientific, Franklin, MA; operated at 50˚C), wind speed and wind direction (Young 03002-L wind sentry set; Young-Campbell Scientific, Logan, UT) were measured from December 2010 to December 2011 at both sites. CO_2 (NDIR 41i analyzer; Thermo Scientific, Franklin, MA) was measured from April to December 2011. Coarse particles were removed from the TEOM and the MAAP sample lines by model 2000-30EH 16.7 liters per minute (LPM) 2.5-mm cutoff cyclones (URG, Chapel Hill, NC). Three meters of 1/8 inch outer diameter (OD) Teflon tubing was used to draw 1 LPM to the CO_2 monitors. Samples were taken at a height of approximately 3 m. One-minute averages of all variables were logged as a text file to a field computer and later loaded to a database. CO_2 analyzers were calibrated with a CO_2 certified standard Nexair gas mixture. Rail yard operations were recorded from the DX site using a camera (Hero Gopro 960; Woodman Labs, Inc., Half Moon Bay, CA) to take photos every minute on 42 days between September 15, 2011, and November 14, 2011. A table with the specific dates is available as supplemental material.

The pairs (one for each site) of CO_2 analyzers, TEOMs, and MAAPs were run for 2 weeks side by side at the Georgia Tech campus before deployment. One-minute concentrations measured with CO_2 analyzers and MAAPs were within 5%. Thirty minute $PM_{2.5}$ concentrations reported by the TEOM instruments were within 5%. During monitoring at the rail yards, zero and span checks of the CO_2 analyzers and flow checks

for the TEOMs and MAAPs were carried out on weekly basis and monthly basis, respectively.

2.4.3. Data analysis

We applied the carbon balance method (Singer and Harley, 1996) to calculate fuel-based emission factors, relating the amount of pollutant emitted to the amount of fuel burned (eq 2.1.):

$$EF=Q/(1+Q_{Others})*\omega_c \quad (2.1.)$$

where EF is the emission factor in units of grams of pollutant emitted per gallon of fuel burned, Q is the ratio of the mass of pollutant to mass of carbon from CO_2, and Q_{Others} is the ratio of the mass of carbonaceous species, such as unburned hydrocarbons or CO, to the mass of carbon from CO_2. Three methods were used to calculate Q, including what we refer to as the "delta," the wavelet, and the regression approaches discussed below. It was assumed that CO_2 dominates the carbon balance for the rail yard diesel sources, with carbonaceous species besides CO_2 (e.g., hydrocarbons and CO) playing a minor role in the carbon budget (Yanowitz et al., 2000). Consequently, Q_{Others} is assumed to be significantly less than 1 and is neglected in our calculations. ω_c is the carbon content per gallon of diesel fuel specified by the Code of Federal Regulations (CFR-40-600.113–78) as 2,778 g C/gal. Uncertainties in the properties of the fuel were neglected. All uncertainties reported were calculated as the 95% confidence interval of the mean.

All the approaches to calculate the ratio Q were based on averages from concentration data occurring when wind with velocities greater or equal to 0.5 m/sec and directions between 320˚and 360˚and between 0˚and 90˚at DX and between 170˚and

280˚at FS were measured. These wind sectors comprise approximately the complete area of the rail yards.

The "delta" approach was based on the downwind–upwind difference in pollutant concentrations. The ratio obtained by this method (Q_Δ) is in units of mass of pollutant emitted per mass of C (eq 2.2.):

$$Q_\Delta = \frac{\overline{[P]}_{DW} - \overline{[P]}_{UW}}{(\overline{[CO_2]}_{DW} - \overline{[CO_2]}_{UW}) \times 12/44} \quad (2.2.)$$

where [P] and [CO_2] are the mean pollutant (BC or $PM_{2.5}$) concentration and mean CO_2 concentration respectively in μg/m^3, the subscripts DW and UW indicate when the average is from the downwind or upwind site, respectively. The factor of 12/44 is the atomic mass of carbon over the molecular mass of CO_2. The delta approach is thought to represent emissions from a broad mix of rail yard sources.

A second method used wavelet analysis (Daubechies, 1992) to separate the concentration signals into high- and low frequency components (Figure 2.3). The ratio Qw calculated by this approach is in units of mass of pollutant emitted per mass of C (eq 2.3.).

$$Q_w = \frac{\overline{[P]}}{\overline{[CO_2]} \times 12/44} \quad (2.3.)$$

where [P] and [CO_2] are the mean pollutant (BC or $PM_{2.5}$) concentration and mean CO_2 concentration, respectively, in μg/m^3. The factor of 12/44 is the atomic mass of carbon over the molecular mass of CO_2. It was assumed that the high frequency components extracted by the wavelet-based algorithm are predominantly near-field emissions from a variety of rail yard sources (e.g., drayage trucks, cranes, welding facilities, or switcher locomotives) and from diesel trucks and gasoline vehicles in the surroundings. Low-frequency contributions are assumed to be associated with non-rail yard activities and

represent the background concentrations in the vicinity. A MATLAB (MathWorks, Natick, MA) algorithm was used for this analysis and it is available as supplementary material. Wavelet analysis has been applied previously by Klems et al. (2011) to a similar problem in order to determine the contribution of motor vehicles near a roadway intersection to the ambient ultrafine particle mass by correlating high frequency contributions with fast changes in ultrafine particle chemical composition.

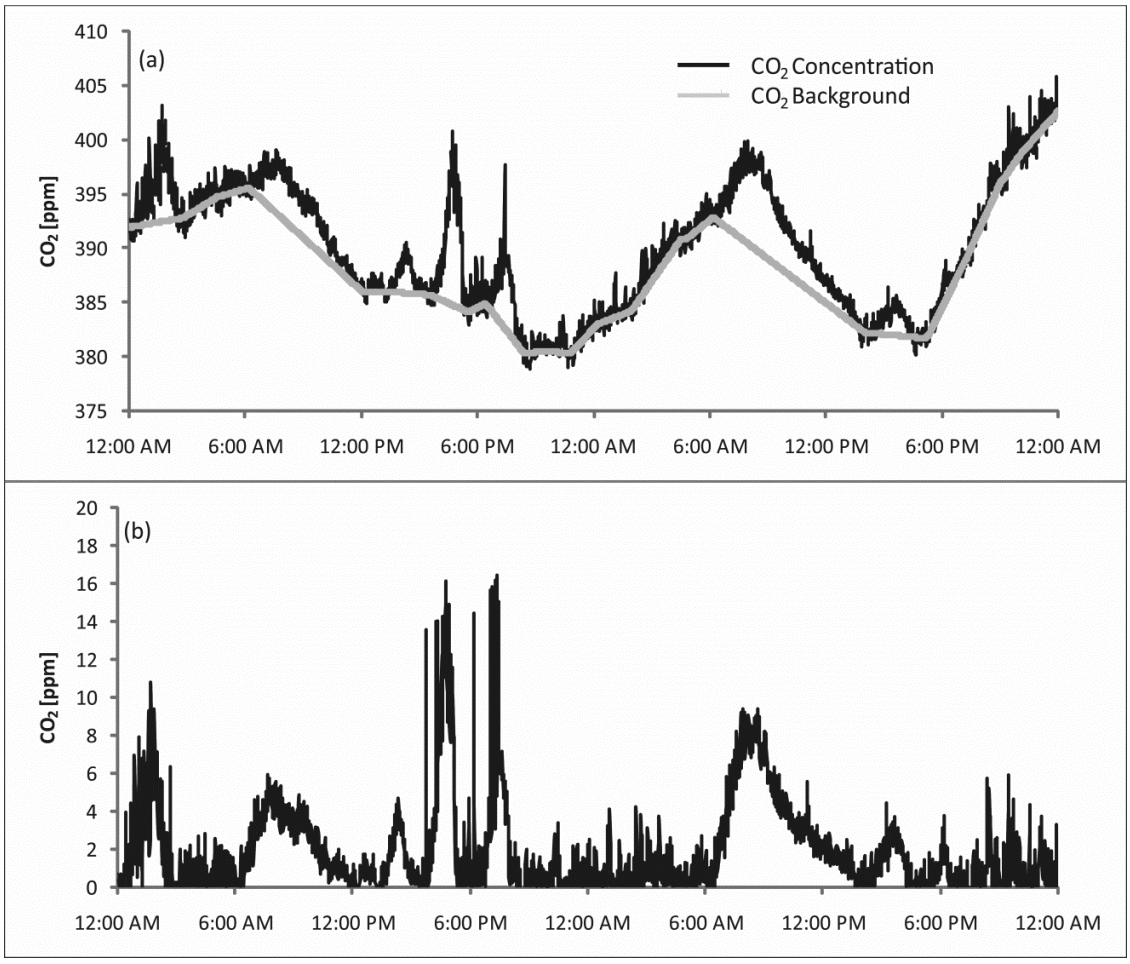

Figure 2.3. CO_2 concentration (a) at DX from 12:00 a.m. on September 5, 2011, to 11:59 p.m. on September 6, 2011. The CO_2 concentration signal was separated into spikes and background components by wavelet analysis. (b) Spikes in CO_2 concentration.

The regression approach, the third technique employed, focused on events of high BC concentrations. Events were identified by selecting groups of 5–20 consecutive-minute data points when the maximum BC concentration of the set was greater than the mean plus 3 times the standard deviation of the BC concentrations occurring in the same hour at the same site and when a linear relationship with a correlation coefficient greater than or equal to 0.90 at a 0.95 confidence level between CO_2 and BC concentrations was obtained (Figure 2.4). Events were selected from data occurring for wind speeds and wind directions with the restrictions described for all the approaches. The ratio, Qr, was calculated as the mean of the slopes of the BC to CO_2 regressions. The ratio of concentrations was converted to a ratio of mass of BC to mass of C from CO_2 by dividing it by the atomic mass of carbon over the molecular mass of CO_2. The minimum concentration measured during the event was taken as the baseline. This approach is likely to represent near-field brief emission events from a subset of rail yard sources (e.g., a passing switcher or line-haul engine). A comparable approach was formulated by Dallmann et al. (2011) to measure BC emission factors from diesel exhaust emissions of trucks used to move containers with in a rail yard and by Hansen and Rosen (1990) to measure BC emission factors from automobiles.

2.5. Results

2.5.1. Concentrations of BC and $PM_{2.5}$

Differences in annual average $PM_{2.5}$ concentrations between Georgia EPD Fire Station 8 and other urban sites have become smaller in recent years (Figure 2.1), due in large part to a combination of factors set in place by the 2008 economic downturn, higher-than-average annual rainfall in 2009 (National Oceanic and Atmospheric Administration

[NOAA], 2012), and air quality policies. In 2011, annual average $PM_{2.5}$ and BC concentrations at DX and FS were comparable (Table 2.1). Annual average $PM_{2.5}$ concentrations are below the current National Ambient Air Quality Standard (NAAQS; 15 µg/m3), but above the proposed level (12 µg/m3)(EPA, 2011b).

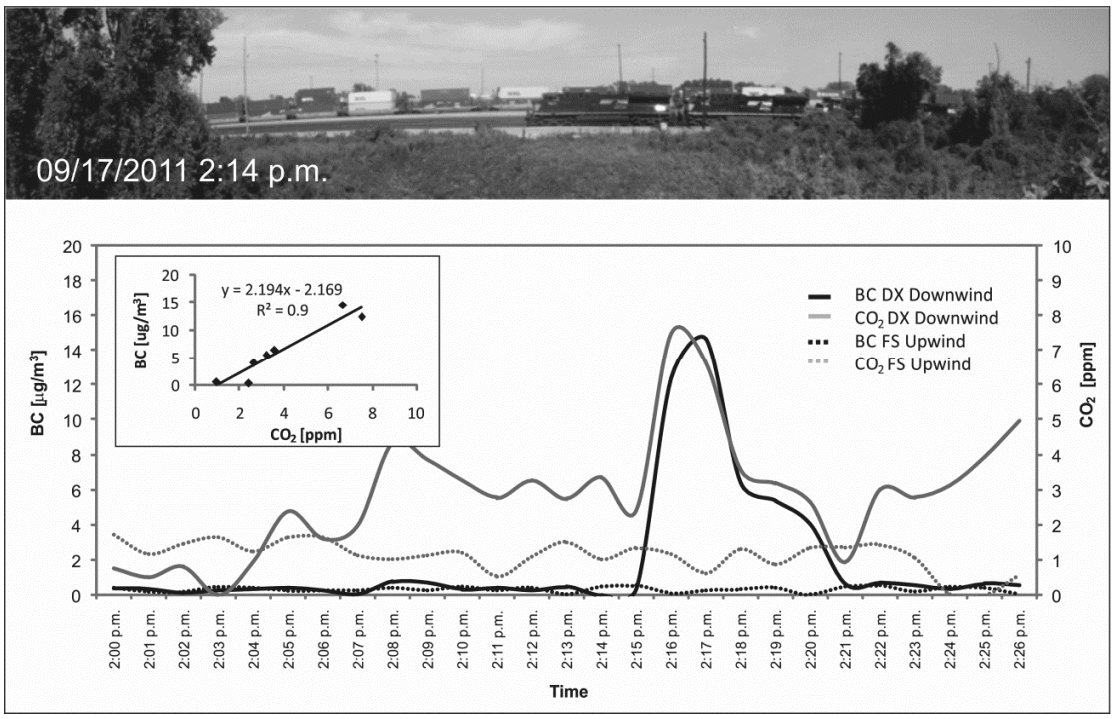

Figure 2.4. Event associated with a locomotive at the DX site on September 17, 2011. At 2:14 p.m. a train passes by the monitoring site. An event is detected shortly after. The subplot shows the lineal regression of the event detected.

Table 2.1. Concentrations of $PM_{2.5}$ and BC for FS, DX, and other Atlanta urban sites in 2011

Site	Method	$PM_{2.5}$ [µg/m^3] †	Method	BC [µg/m^3] †
FS	TEOM	12.3(7.1)	MAAP	1.5(1.4)
DX	TEOM	13.1(8.0)	MAAP	1.3(1.2)
Fire Station 8	FRM [a]	13.3(5.8)		
South DeKalb	FRM [a]	12.4(6.0)	TOR [b]	1.3 (0.9)
Gwinnett Tech	FRM [a]	12.5(6.7)		
E. Rivers School	FRM [a]	11.4(5.0)		

Notes: [a] Federal Reference Method. [b] Thermal/optical reflectance. †Mean (standard deviation).

2.5.2. Wind speed and direction and pollutants

During the study, the predominant wind direction was west southwest at both the DX and FS sites (Figure 2.5.). Average wind speeds of 1.5 m/sec at DX and 1.2 m/sec at FS were measured. The highest speeds were recorded when the wind came from the southeast and southwest quadrants at FS and from the northeast and southeast quadrants at DX. Structures and trees located southwest of DX and northeast of FS could have hindered wind circulation to some extent.

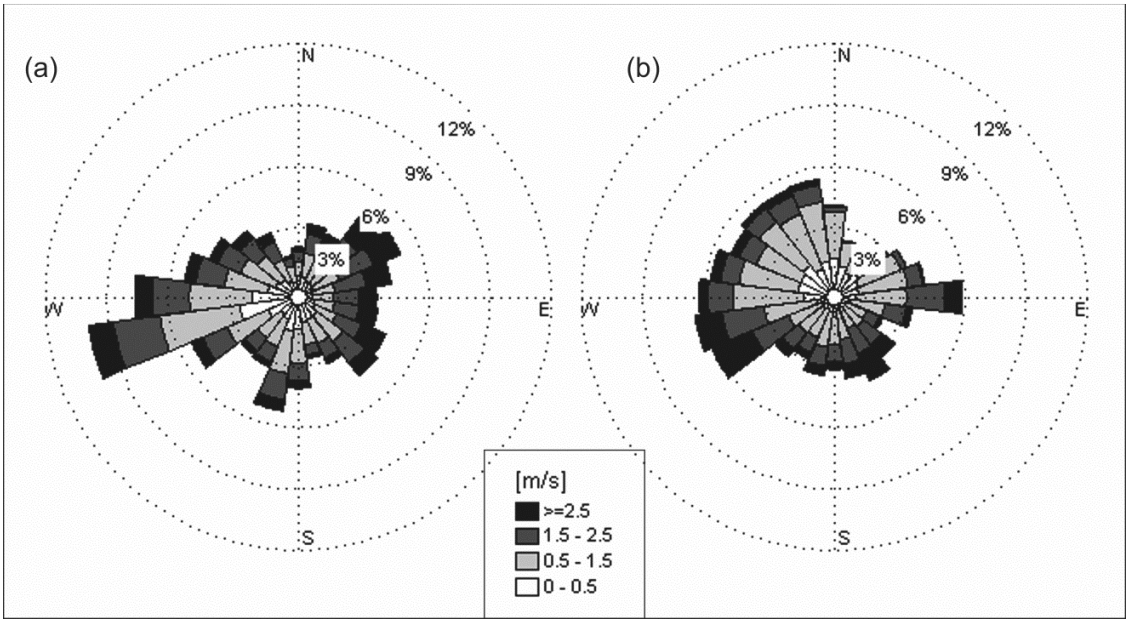

Figure 2.5. Wind Roses for (a) the DX site and (b) the FS site.

We plotted normalized pollutant concentrations to gain insight on the location of the sources that impact DX and FS (Figure 2.6.). Pollutant concentration roses were constructed by normalizing the concentrations subtracting the mean and dividing by the standard deviation and adding one. Normalized pollutant roses show local concentrations

of BC, $PM_{2.5}$, and CO_2 approximately 1.5 times greater than average coming from the direction where the rail yards are located, that is, the northeast quadrant at DX and southeast quadrant at FS, as their main feature (Figure 2.6.). There is a source of BC, $PM_{2.5}$, and CO_2 north of FS. FS could as well be impacted to some degree by BC, CO_2, and $PM_{2.5}$ emissions coming from activities on Marietta Boulevard. The roses suggest that BC is a better tracer for yard activities than $PM_{2.5}$. At both sites, directions of higher than average BC concentrations closely follow the layout of the rail yard. $PM_{2.5}$ and CO_2 concentration roses at DX show sources south and west-southwest, respectively, but no significant BC is associated with those directions.

Somewhat higher concentrations of BC were measured at FS (Table 2.1). FS downwind conditions were measured 44.5% of the time, whereas DX was downwind 32.5 % of the time during the months of this study. Also, wind speed was slightly lower (1.7 m/sec on average) when FS was downwind than when DX was downwind (1.9 m/sec on average). Greater time downwind with lower wind speeds is one reason for the slightly greater BC concentrations at FS. It was much harder to detect $PM_{2.5}$ and CO_2 enhancements from the rail yards due to greater background levels and variability for these contaminants, as well as the variety of their sources.

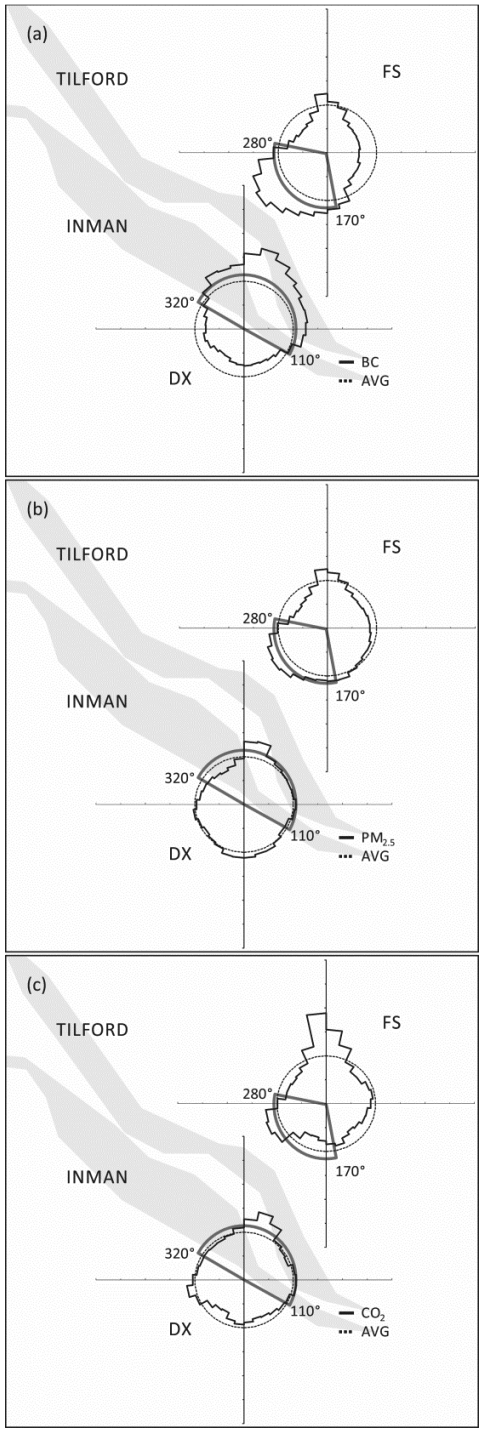

Figure 2.6. Normalized pollutant concentration roses for (a) BC, (b) $PM_{2.5}$, and (c) CO_2 at the DX and FS monitoring sites. Downwind sectors are marked with corresponding angles.

2.5.3. Downwind–upwind differences and high-frequency components

Enhancements in $PM_{2.5}$, BC, and CO_2 concentrations come from the directions where the rail yards are located. $PM_{2.5}$, BC, and CO_2 enhancements are statistically significant (two-sample t tests, with $P < 1E\text{-}10$ in the least satisfactory conditions with 99% confidence). Yet, $PM_{2.5}$, BC, and CO_2 downwind–upwind differences have large variability, showing standard deviations much larger than their means (Table 2.2.). This variability will lead to uncertainty in the emission factors calculated by this method. Histograms of downwind–upwind differences and concentrations time series are presented in the supplemental materials.

Table 2.2. Downwind/ Upwind concentration differences for DX and FS sites.

	Downwind Site	
	DX	FS
$PM_{2.5}$		
Mean [$\mu g/m^3$]	1.5	1.9
Standard deviation [$\mu g/m^3$]	± 8.6	± 10.8
Uncertainty of the mean [$\mu g/m^3$]	± 0.1	± 0.1
Number of observations	25,105	31,123
BC		
Mean [$\mu g/m^3$]	0.7	1.0
Standard deviation [$\mu g/m^3$]	± 1.2	± 1.7
Uncertainty of the mean [$\mu g/m^3$]	± 0.01	± 0.01
Number of observations	27,161	40,998
CO_2		
Mean [ppm]	6.3	5.9
Standard deviation [ppm]	± 28.6	± 33.2
Uncertainty of the mean [ppm]	± 0.3	± 0.3
Number of observations	18,110	33,865

At both sites, means of the high-frequency components of $PM_{2.5}$, BC, and CO_2 concentrations obtained by the wavelet approach are higher when the wind blows from the rail yards than from any other direction. Wavelet analysis helps to rectify the noise and baseline drift of the instruments to a considerable degree, and reduces to some extent the interference of the signals from sources with extremely high frequencies (i.e., fast-

moving gasoline vehicles and diesel trucks). This is apparent in the variability of the results of wavelet approach, which is less than the variability of the results of the delta approach (Table 2.3.). Consequently, the uncertainty derived from this variability could be expected to be smaller in the wavelet approach than in the delta approach. Yet, as mentioned before, spikes could be predominantly near-field emissions from a variety of rail yard sources but also from diesel trucks and gasoline vehicles. This contribution from non-rail yard sources could still confound the results.

Table 2.3. High-frequency components from wavelet analysis for the DX and FS sites.

	Downwind Site	
	DX	FS
$PM_{2.5}$		
Mean [$\mu g/m^3$]	1.8	1.9
Standard deviation [$\mu g/m^3$]	± 3.0	± 4.0
Uncertainty of the mean [$\mu g/m^3$]	± 0.02	± 0.02
Number of observations	57,908	82,223
BC		
Mean [$\mu g/m^3$]	0.7	0.9
Standard deviation [$\mu g/m^3$]	± 1.2	± 1.3
Uncertainty of the mean [$\mu g/m^3$]	± 0.01	± 0.01
Number of observations	53,805	73,134
CO_2		
Mean [ppm]	8.2	6.6
Standard deviation [ppm]	± 19.1	± 11.1
Uncertainty of the mean [ppm]	± 0.1	± 0.1
Number of observations	51,711	50,697

Greater enhancements in $PM_{2.5}$ and BC concentrations were found at FS (Table 2.2). The same result was observed by the wavelet approach. The means of $PM_{2.5}$ spikes and BC spikes were greater when wind blew from the rail yards to FS than when it was blowing from the rail yards to DX (Table 2.3). Results from this part of our analysis are comparable to those obtained by Campbell and Fujita (2009), at the Roseville rail yard in California for 2008 whom measured a downwind–upwind delta of 0.73 ± 0.01 and 1.14 ±

0.01 µg/m^3 of BC and 2.5 ± 0.6 and 2.4 ± 0.7 µg/m^3 of $PM_{2.5}$ at two monitoring sites. Our results support the modeling study by Georgia EPD (2009), which estimated that the rail yard emissions led to an additional 1.9 µg/m^3 of $PM_{2.5}$.

2.5.4. Emission factors

Means of BC and $PM_{2.5}$ emission factors obtained by the delta and the wavelet approaches were similar between both sites (Table 2.4.). For both approaches, FS reported higher emission factors than DX. Results obtained at FS could be confounded by emissions from traffic. There is also uncertainty related to the emissions of the different zones within the rail yards. FS is located near the arrival section of Tilford Yard, where there is also a turntable and fuel storage and repair facilities. The DX site is close to tracks where a mix of locomotives cruise, accelerates, and idle. The intermodal terminal of Inman Yard where there is heavy-duty diesel truck traffic is also close by. Emission factors calculated by the delta approach when the wind is not blowing from the rail yards are presented in the supplemental materials (Table A.1.). As shown, the small values derived (approximately an order of magnitude less than when using concentrations found from the downwind–upwind pairing) support our results.

Table 2.4. Emission Factors for the DX and FS sites

	Downwind Site		Other works
	DX	FS	
EF_{BC} [g of BC /gal fuel]			
Delta approach	0.6±0.04	0.9±0.05	
Wavelet approach	0.5±0.01	0.7±0.01	
Regression approach	3.1±0.2	2.4±0.2	3.8[b]
$EF_{PM_{2.5}}$ [g of $PM_{2.5}$ /gal fuel]			
Delta approach	1.3±0.1	1.8±0.1	
Wavelet approach	1.2±0.02	1.6±0.03	
Regression approach [a]	7.2±0.8	4.8±0.6	4.5[c] , 4.7[d]

Notes: [a] $PM_{2.5}$ emission factor was not calculated directly by the regression approach but estimated from the ratio of BC to PM2.5 and the BC emission factor from the regression approach. [b] Sawant et al. (2007). [c] Expected fleet average PM_{10} emission factor for 2011 (EPA. 2009). [d] Fritz and Cataldi (1991).

BC emission factors from the regression approach are higher than those obtained from the delta and wavelets approaches (Table 2.4.), which is anticipated because the BC events, identified when BC levels rise by 3 standard deviations or more above the mean value during the hour of the event, are likely due to activities with high BC emissions (i.e., switchers or line-haul engines). Results of the regression approach are comparable to elemental carbon emission factors of 3.8 g of BC per gallon of diesel fuel measured directly from the stacks of switcher locomotives (Sawant et al., 2007). The DX site was equipped to photograph rail yard activity to link with pollutant data and investigate the possibility of the recorded events originating from sources other than the rail yards. Photos indicate locomotives, either idling or passing by, shortly (1–3 min) before an event was registered. During the event shown (Figure 2.4), the wind was blowing north-northeast, from the rail yards to DX, with speeds that varied between 1 and 2.5 m/sec. The minimum concentration measured during the corresponding hour was taken as baseline. Overlapping signals of concentrations of BC and CO_2 were registered on the downwind monitoring site, whereas the upwind site showed steady concentrations. Photographs also showed that when no locomotives were present and the wind was blowing from the direction of the rail yards, BC and CO_2 concentrations were poorly correlated. The scenario depicted in Figure 2.4.is an example of the many events used to determine the emissions factors by the regression approach.

Events of high BC concentrations detected at DX were generated inside the rail yards and were less likely to be influenced by other sources. At FS, there is the possibility that some of events were influenced by traffic on Marietta Boulevard. The regression approach yields a smaller average emission factor for FS (Table 2.4). Some events with

higher BC concentrations were detected at DX, but on average BC concentrations during events show an increase of about 3 μg/m^3 of BC at both sites and their respective standard deviations were comparable, as high as 6 μg/m^3 and as low as 1 μg/m^3 above baseline (Figure 2.7.). Differences between FS and DX regression approach results (Table 2.4.) likely derive from the higher variability in CO_2 concentration at FS. Incremental CO_2 concentrations at FS used in the regression approach show an average and standard deviation approximately 2 and 1.4 ppm greater than at DX (Figure 2.7.), leading to lower emissions factors. Given that BC is found to be a good tracer of rail yard activity, and that emission factors calculated by the regression approach show little dependency on the hour of the day or the day of the week (Figures A.5.–A.8.), we infer that most of the events detected at FS were generated inside the rail yards.

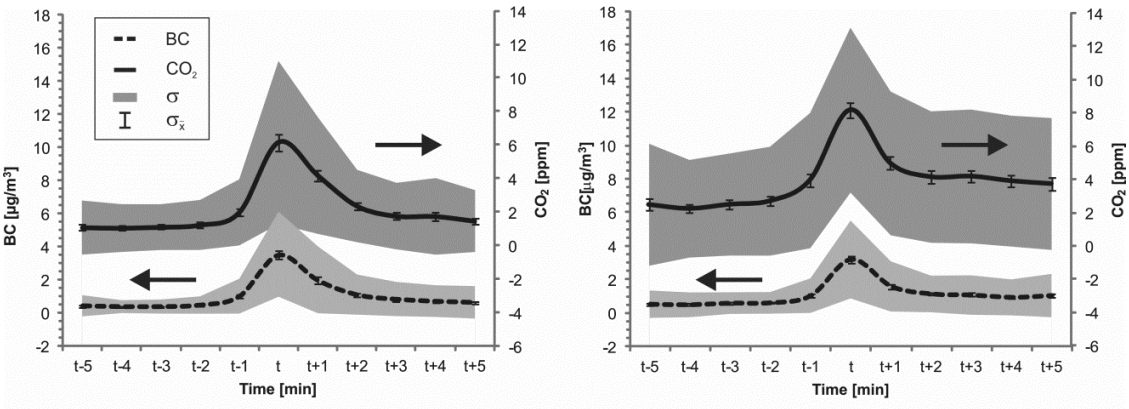

Figure 2.7. Events of high BC and corresponding CO_2 concentrations at (a) DX and (b) FS. The minimum concentration measured during each event was taken as baseline. Events were centered at the time when the maximum BC concentration was measured (*t*). Average concentrations 5 min before and 5 min after are shown along with standard deviations (σ) and uncertainties of the mean (σ_x).

BC emission factors calculated by the regression approach show similar frequency distributions at the two sites (Figure 2.8.), with 423 and 399 events detected at

FS and DX, respectively. Several events, likely coming from high-emitting locomotive engines, produced BC emission factors 1 order of magnitude higher than the PM_{10} emissions standards published by EPA (2009).

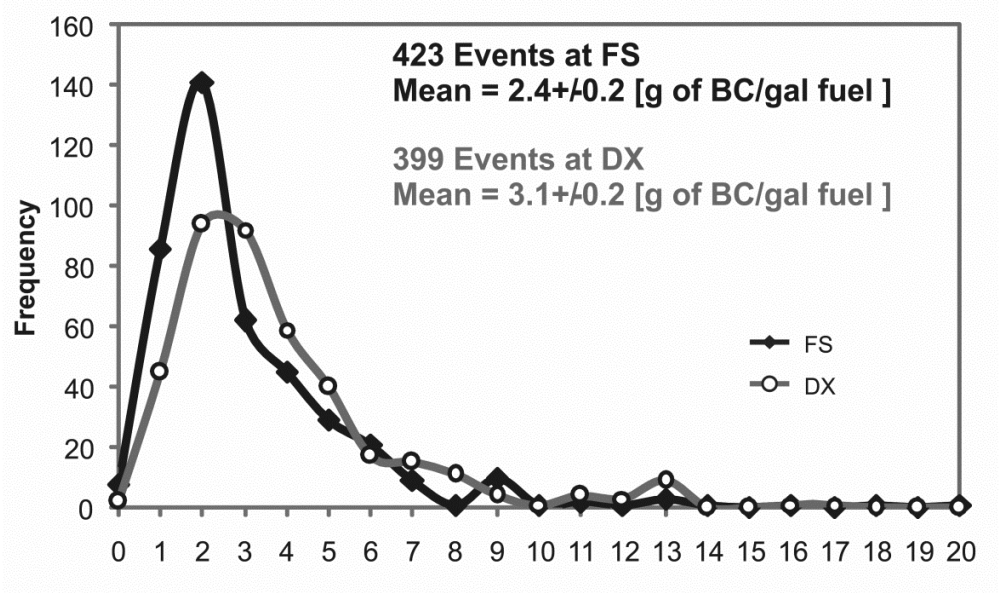

Figure 2.8. Frequency distributions of emission factors obtained from BC events at the FS and DX sites.

Results of the application of the regression approach to estimate $PM_{2.5}$ emission factors were less satisfactory and are not presented. This was expected, given the noise in TEOM data on time scales less than 30 min. However, $PM_{2.5}$ emission factors could be estimated using the ratio of BC to $PM_{2.5}$ obtained from wavelet and delta approaches (0.43 ± 0.02 g BC/g $PM_{2.5}$ at DX and 0.5 ± 0.02 g BC/g $PM_{2.5}$ at FS). Using these ratios, emission factors of 7.2 ± 0.6 g $PM_{2.5}$/gal fuel at DX and 4.8 ± 0.6 g $PM_{2.5}$/gal fuel at FS are obtained.

Total BC and $PM_{2.5}$ emissions can be estimated based on the fuel use at the rail yards and the fuel-based emission factors calculated in this study. Line haul and switching activity at Tilford and Inman rail yards consumed 1.6 and 2.5 million of

gallons of diesel fuel, respectively, during 2011. This was calculated using the method described (Georgia EPD, 2009), which is based on scaling state-level yearly average fuel consumption dividing the gross ton-miles transported in the yard by system-wide fuel combustion efficiency. Gross ton-miles data have been provided in the past for each rail yard by Norfolk Southern and CSX Transportation (Georgia EPD, 2009). System-wide fuel combustion efficiency for 2011 was obtained from data contained in the Class I Railroad Surface Transportation Board R-1 Annual Report from each company (Norfolk Southern, 2011; CSX Transportation, 2011). This estimation does not include the fuel consumed in other activities occurring in the yard. Approximately 11.7 tons of BC and 26 tons of $PM_{2.5}$ per year were emitted from the rail yards in 2011.

2.6. References

Bergin, M. S. , M. Harrell, and M. Janssen. Locomotive emission inventories for the United States from ERTAC Rail. In EPA 2012 International Emission Inventory Conference. Tampa, Florida. August 13–16, 2012. http://www.epa.gov/ttn/chief/conference/ei20/session8/mbergin.pdf (accessed April 2013).

Butler, A., M. Andrew, and A.G. Russell. 2003. Daily sampling of PM2.5 in Atlanta: Results of the first year of the Assessment of Spatial Aerosol Composition in Atlanta study. J. Geophys. Res. 108(D7):8415. doi:10.1029/2002jd002234

Campbell, D., and E. Fujita. 2009. Roseville Rail Yard Air Monitoring Project(RRAMP) Final Report. http://www.placer.ca.gov/Departments/Air/~/media/apc/documents/UP/2009/December/RRAMPFinalUpdate121009.ashx (accessed October 2012).

Cahill, T.A., T.M. Cahill, D.E. Barnes, N.J. Spada, and R. Miller. 2011. Inorganic and organic aerosols downwind of California's Roseville Railyard. Aerosol Sci. Technol. 45:1049–1059. doi:10.1080/02786826.2011.580796

CFR-40-92.101-133. 2011. Control of Air Pollution from Locomotives and Locomotive Engines. In Code of Federal Regulations, Part 40: Protection of Environment, Subpart B.

CFR-40-600.113–78. 2011. Fuel Economy and Carbon-Related Exhaust Emission Regulations for 1978 and Later Model Year Automobiles—Test Procedures. In Code of Federal Regulations, Part 40: Protection of Environment, Subpart B.

Cocker, D.R., S.D. Shah, K. Johnson, J.W. Miller, and J.M. Norbeck. 2004. Development and application of a mobile laboratory for measuring emissions from diesel engines. 1. Regulated gaseous emissions. Environ. Sci. Technol. 38:2182–2189. doi:10.1021/es034888d

Congestion Mitigation and Air Quality Improvement Program, Georgia Environmental Protection Division [CMAQ-EPD]. 2009. EPD railroad related emissions reduction project in Atlanta. Atlanta GA: CMAQ Federal Highway Administration. https://fhwaapps.fhwa.dot.gov/cmaq_pub/View/default.aspx?id=GA20090013 (accessed March 2012).

CSX Transportation. 2011. Class I railroad annual report of CSX transportation, Inc. to the Surface Transportation Board for 2011. http://www.stb.dot.gov/econdata.nsf/f039526076cc0f8e8525660b006870c9/8775aca41ef66efb852579db004c9dee/$FILE/CSXT%202011%20Final%20R1.pdf (accessed December 2012).

Dallmann, T.R., R.A. Harley, and T.W. Kirchstetter. 2011. Effects of diesel particle filter retrofits and accelerated fleet turnover on drayage truck emissions at the Port of Oakland. Environ. Sci. Technol. 45:10773–10779. doi:10.1021/es202609q

Daubechies, I. 1992. Ten Lectures on Wavelets. Philadelphia, PA: Society for Industrial and Applied Mathematics. doi:10.1137/1.9781611970104

Electric Power Research Institute. 2012. The Southeastern Aerosol Research and Characterization Network: SEARCH. http://www.atmosphericresearch.com/studies/search/SEARCH FactSheet.pdf (accessed February 2012).

Fritz, S.G., and G.R. Cataldi. 1991. Gaseous and particulate emissions from diesel locomotive engines. J. Eng. Gas Turbines Power 113:370–376. doi:10.1115/1.2906240

Georgia Environmental Protection Division [GAEPD]. 2009. Dispersion modeling to support the Atlanta PM2.5 SIP local area analysis. Dispersion http://www.gaepd.org/Files_PDF/plans/sip/Appendix_M_PM2.5__Modeling_at_FireSta8.pdf (accessed November 2011).

Georgia Environmental Protection Division [GAEPD]. 2012. Ambient Monitoring Program—Annual data reports. http://www.georgiaair.org/amp/report.php (accessed February 2012).

Hansen, A.D.A., and H. Rosen. 1990. Individual measurements of the emission factor of aerosol black carbon in automobile plumes. J. Air Waste Manage. Assoc. 40:1654–1657. doi:10.1080/10473289.1990.10466812

Honc, R.L., S.G. Fritz, M.B. Schell, A. Tarnow, and A. Bennett. 2006. Fuel consumption and exhaust emissions from a 1,125 kW multiple Genset switcher locomotive. In Proceedings of the the ICEF 2006, ASME Internal Combustion Engine Division 2006, Fall Technical Conference, Sacramento, CA, November 5–8.

Kam, W., K. Cheung, N. Daher, and C. Sioutas. 2011. Particulate matter (PM) concentrations in underground and ground-level rail systems of the Los Angeles Metro. Atmos. Environ. 45:1506–1516. sdoi:10.1016/j.atmosenv.2010.12.049

Kim, E., P.K. Hopke, and E.S. Edgerton. 2004. Improving source identification of Atlanta aerosol using temperature resolved carbon fractions in positive matrix factorization. Atmos. Environ. 38:3349–3362. doi:10.1016/j.atmosenv.2004.03.012

Klems, J., M. Pennington, C. Zordan, L. McFadden, and M. Johnston. 2011. Apportionment of motor vehicle emissions from fast changes in number concentration and chemical composition of ultrafine particles near a roadway intersection. Environ. Sci. Technol. 45:5637–5643. doi:10.1021/es104228q

Laurits R. Christensen Associates, Inc. 2009. Description of the U.S. freight railroad industry. http://www.stb.dot.gov/stb/docs/CompetitionStudy/Volume%201.pdf (accessed February 2012).

Lloyd, A.C., and T.A. Cackette. 2001. Diesel engines: Environmental impact and control. J. Air Waste Manage. Assoc. 51:809–847. doi:10.1080/10473289.2001.10464315

National Cooperative Freight Research Program. 2010. Representing freight in air quality and greenhouse gas models. http://onlinepubs.trb.org/onlinepubs/ncfrp/ncfrp_rpt_004.pdf (accessed November 2011).

National Oceanic and Atmospheric Administration. 2012. National Weather Service Weather Forecast Office. Rainfall scorecard. http://www.srh.noaa.gov/ffc/?n=rainfall_scorecard (accessed June 2012).

Norfolk Southern. 2011. Class I railroad annual report of Norfolk Southern combined railroad subsidiaries to the Surface Transportation Board for 2011. http://www.stb.dot.gov/econdata.nsf/f039526076cc0f8e8525660b006870c9/d945e6d27425d1f6852579db004cfdbd/$FILE/NS%202011%20R-1%20final.pdf (accessed December 2011).

Prasad, R., and Bella R.B. 2010. A review on diesel soot emission, its effect and control. Bull. Chem. React. Eng. Catal. 5:69–86.

Roberts, D.L., and Jones A. 2004. Climate sensitivity to black carbon aerosol from fossil fuel combustion. J. Geophys. Res. 109(D16):D16202. doi:10.1029/2004jd004676

Sawant, A.A., A. Nigam, J.W. Miller, K.C. Johnson, and D.R. Cocker. 2007. Regulated and non-regulated emissions from in-use diesel-electric switching locomotives. Environ. Sci. Technol. 41:6074–6083. doi:10.1021/es061672d

Sierra Research, Inc. 2004. Revised inventory guidance for locomotive emissions. http://www.metro4-sesarm.org/pubs/railroad/FinalGuidance.pdf (accessed November 2011).

Simon, H., D.T. Allen, and A.E. Wittig. 2008. Fine particulate matter emissions inventories: Comparisons of emissions estimates with observations from recent field programs. J. Air Waste Manage. Assoc. 58:320–343.doi:10.3155/1047-3289.58.2.320

Singer, B.C., and R.A. Harley. 1996. A fuel-based motor vehicle emission inventory. J. Air Waste Manage. Assoc. 46:581–593. doi:10.1080/10473289.1996.10467492

St. Denis,M.J., P. Cicero-Fernandez, A.M.Winer, J.W. Butler, and G. Jesion. 1994. Effects of in-use driving conditions and vehicle engine operating parameters on off-cycle events—Comparison with federal test procedure conditions. J. Air Waste Manage. Assoc. 44:31–38. doi:10.1080/1073161X.1994.10467235

Starcrest Consulting Group, L.L.C. 2004. Port-wide baseline air emissions inventory. Executive summary. http://westcoastcollaborative.org/files/sector-marine/Port%20of%20LA%20Emissions%20Inventory.pdf (accessed November 2011).

U.S. Environmental Protection Agency [EPA]. 2008a. Regulatory impact analysis: Control of emissions of air pollution from locomotive engines and marine compression ignition engines less than 30 liters per cylinder. http://www.epa.gov/otaq/regs/nonroad/420d07001chp3.pdf (accessed November 2011).

U.S. Environmental Protection Agency [EPA]. 2008b. EPA finalizes more stringent emissions standards for locomotives and marine compression—Ignition engines. http://www.epa.gov/otaq/regs/nonroad/420f08004.pdf (accessed November 2011).

U.S. Environmental Protection Agency [EPA]. 2009. Emission factors for locomotives. http://www.epa.gov/otaq/regs/nonroad/locomotv/420f09025.pdf (accessed December 2012).

U.S. Environmental Protection Agency [EPA]. 2011a. Rail and locomotives. http://www.epa.gov/diesel/ports/rail.htm (accessed November 2011).

U.S. Environmental Protection Agency. 2011b. Policy assessment for the review of the particulate matter National Ambient Air Quality Standards. http://www.epa.gov/ttnnaaqs/standards/pm/data/20110419pmpafinal.pdf (accessed June 2012).

U.S. Environmental Protection Agency [EPA]. 2012. National Emissions Inventory (NEI) air pollutant emissions trends data. http://www.epa.gov/ttnchie1/trends/ (accessed February 2012).

World Health Organization [WHO]. 2012. Diesel engine exhaust carcinogenic. http://press.iarc.fr/pr213_E.pdf (accessed June 2012).

Yanowitz, J., R.L. McCormick, and M.S. Graboski. 2000. In-use emissions from heavy-duty diesel vehicles. Environ. Sci. Technol. 34:729–740. doi:10.1021/es990903w

CHAPTER 3

IMPACTS ON FINE PARTICULATE MATTER, BLACK CARBON AND HEALTH OF CONVERTING RAIL YARD LOCOMOTIVES TO LOWER EMISSION TECHNOLOGIES

(Galvis, B. Bergin, M., Huang Y., Boylan J., and Russell A.G. *Atmospheric Environment*. Submitted)

3.1. Abstract

Reductions in emissions from major sources of fine particulate matter ($PM_{2.5}$) and black carbon (BC) that affect densely populated regions such as the surrounding area of a major rail yard complex in Atlanta, Georgia can provide near-term environmental and public health benefits at low relative cost. We estimated the potential reductions in $PM_{2.5}$ and BC concentrations that could be accomplished by upgrading traditional switcher locomotives used in this rail yard complex and evaluated the health benefits of these reductions for comparison with upgrade costs.

Analysis indicates that the line-haul and switcher activities at the Tilford and Inman rail yards are responsible for increases in annual average concentrations of 0.5 $\mu g/m^3$ (39%) and 0.7 $\mu g/m^3$ (56%) of BC, and for 1.0 $\mu g/m^3$ (7%) and 1.6 $\mu g/m^3$ (14%) of $PM_{2.5}$ at two monitoring sites located north and south of the rail yards, respectively. Upgrading the engines of the switcher locomotives used at the rail yards with lower emitting technologies would decrease $PM_{2.5}$ and BC emissions by about 9 and 3 t/year respectively, reducing $PM_{2.5}$ concentrations between 0.3±0.1 $\mu g/m^3$ and 0.6±0.1 $\mu g/m^3$ and BC concentrations between 0.1 ±0.02 $\mu g/m^3$ and 0.2±0.03 $\mu g/m^3$ at the monitoring

sites north and south of the rail yards respectively. This measure would facilitate $PM_{2.5}$ NAAQS attainment in the area. We estimate that health benefits of approximately 24 million dollars per year could be gained.

3.2. Introduction

The rail industry is reducing emissions from rail yards across the nation, with the support of the US Department of Transportation's Congestion Mitigation and Air Quality Improvement Program (CMAQ) and other federal, state and private funding. Some of the measures taken to reduce emissions involve rail yard switcher locomotives typically regarded as high emitters (EPA, 2011). Switcher locomotives can be retrofitted with new generator set (Genset) technologies. A Genset is a computer controlled electric generator coupled to an array of two or three off–road EPA Tier II/III diesel engines. Gensets have low emissions and would reduce fuel consumption by about 25% (Honc et al., 2006). Switcher locomotives could also be replaced with "mother-slug sets". In a mother-slug set a conventional diesel locomotive called "mother" transmits the excess power generated by its diesel electric engine at low speeds to a "slug" which is a locomotive with only traction motors but no engine nor electric generator. The slug contains a large block of ballast to provide sufficient weight for traction. A mother-slug set replaces 2 switcher locomotives, can save approximately 33% of the fuel consumed and can meet EPA tier II/III emissions standards (NS, 2011).

The Georgia Environmental Protection Division (GAEPD) along with the rail industry is currently pressing forward with a project to replace older switcher locomotives operating in the 'urban core' of Atlanta. This area is currently in non-attainment of the $PM_{2.5}$ National Ambient Air Quality Standard (NAAQS). Funding has

been awarded by the Georgia Department of Transportation to the GAEPD through the CMAQ Program (CMAQ, 2009) as part of this effort. Initially using Gensets was favored but recently the mother-slug alternative is also being considered.

Changes of $PM_{2.5}$ and BC concentrations from the implementation of rail yard emission reduction measures have seldom been quantified. The same is true for the associated health benefits. A few prior studies assessed impacts from rail yard emissions using Gaussian dispersion models. However, estimates of emissions from rail yards are typically highly uncertain due to inadequacies in emission factors and activity indicators, and there can be sources around rail yards that confound or are not captured in modeling results. Generic emission factors normally used may fail to effectively represent operating conditions, technologies and yard fleet mix (Galvis et al., 2013), and often, construction of activity indicators is not suited to a specific rail yard because it does not describe the particular freight services and geographic characteristics (Gould et al., 2009). These factors lead to significant uncertainties in modeling rail yard impacts and raise the need for thorough model evaluation. However, insufficient spatial and temporal coverage of monitoring data around rail yard areas often hinders this task.

Previous work carried out by Sierra Research (2011) compared modeled diesel particulate matter (DPM) and nitrogen oxides (NOx) ground-level concentrations to measured upwind-downwind concentration differences of BC, elemental carbon (EC), organic carbon (OC), $PM_{2.5}$ and NOx measured at 4 monitoring stations operated during the Roseville Rail yard Air Monitoring Project (RRAMP) in California. Gaussian dispersion models were used to assess the impact of rail yard emissions on local air quality. Models were run with rural and urban dispersion coefficients and two different

meteorological data sets. In all cases, both measurements and models, found reductions in DPM and NOx impacts over the four-year period of the RRAMP study. Reductions observed were mostly attributed to the decrease of emissions at the rail yard over that period. Comparisons of the measured $PM_{2.5}$ and NOx concentrations with simulated DPM and NOx concentrations predicted by the models did not show good agreement (Campbell et al., 2009).

Feinberg et al. (2011) estimated impacts on local air quality of the CSXT Rougemere rail yard in Dearborn, Michigan using a Gaussian atmospheric dispersion model, though did not include a model evaluation. They developed a bottom-up temporally and spatially allocated $PM_{2.5}$ emissions inventory before and after a Genset retrofit of the switchers in the yard. Results of the inventory estimated a reduction in $PM_{2.5}$ emissions from 2007 to 2008, attributed to Genset retrofits and reductions in the sulfur content of the diesel fuel.

Health risk assessments for several rail yards have been carried out by the California Air Resources Board (CARB, 2011).They used emissions inventories and air quality modeling results previously prepared for the rail yards, to characterize potential cancer and non-cancer risks associated with exposure to DPM. They estimated impacted areas and exposed population associated with different cancer risk levels for different exposure durations. They also reported near-source cancer risks.

GAEPD (2006) assessed benefits of avoided mortality and morbidity of several emissions control strategies including reducing 10% of emissions of ground level anthropogenic primary carbon $PM_{2.5}$ (EC and OC) throughout the state of Georgia. EC is one of the main emissions from rail yard areas. They used the Community Multiscale Air

Quality Modeling System to estimate changes in ambient air pollution levels and the Environmental Benefits Mapping and Analysis Program (BenMAP) (ABT, 2012) to assess the health benefits of the changes. They concluded that ground level controls of primary carbon significantly reduced exposure and have the highest health benefits of all the strategies evaluated saving 223 million dollars annually.

The objectives of this research are to estimate the impact on local air quality of $PM_{2.5}$ and BC emissions from Tilford and Inman rail yards in Atlanta, GA, and to assess the reduction on the $PM_{2.5}$ and BC concentrations that could be accomplished by converting the switcher locomotives at the rail yards to low emission technologies. Emissions from the rail yards are estimated using available fuel consumption data and emission factors measured for the rail yards (Galvis et al., 2013). First a 2011 base case is simulated, and results are compared to measurements of BC and $PM_{2.5}$ made at monitoring sites near the rail yards over the same period. Two scenarios are simulated; the first one simulates all the switcher locomotives at both yards are retrofitted with Gensets. The second one simulates all the switcher locomotives at both yards are substituted by mother-slug sets. The change in local PM2.5 concentrations between the base and controlled scenarios are used to determine health benefits by using BenMAP.

3.3. Material and Methods

3.3.1. Study location

The Inman and Tilford rail yard complex is located in Norwest Atlanta, Georgia inside the I-285 perimeter freeway (Figure 3.1.). Inman is operated by Norfolk Southern (NS) and Tilford by CSX Transportation (CSXT). Descriptions of the rail yard complex can be found in previous works (Galvis et al., 2013;GAEPD, 2009a). Marietta Blvd NW

(~15,000 annual average daily traffic [AADT]) and Bolton Rd (~ 18,000 AADT) run alongside northwest and northeast of the rail yards, respectively. Marietta Rd NW (~ 2,000 AADT) separates the Inman intermodal section from the arrival section of Tilford yard.

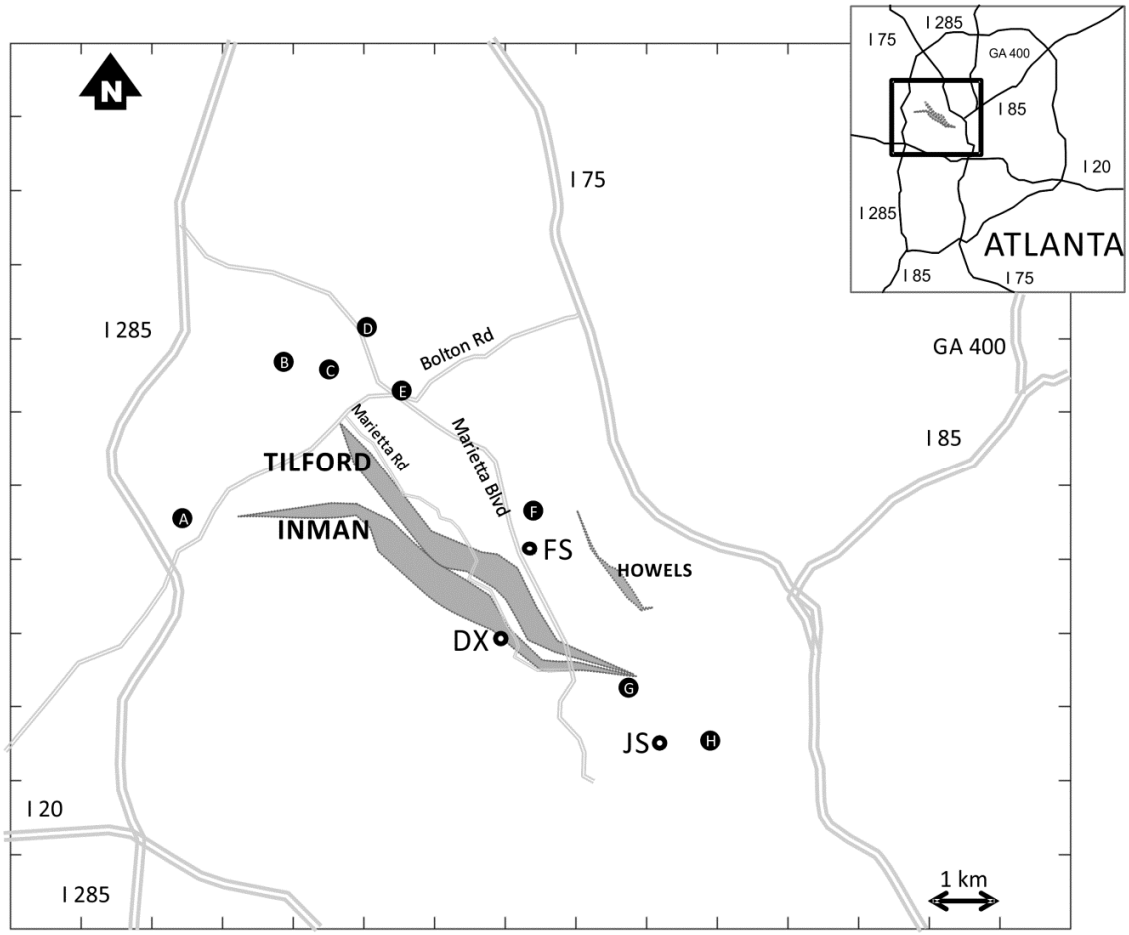

Figure 3.1. Study location and model domain. Layout of the rail yards in gray. Major industrial sources include A) General Shale Brick Inc plant, B) Georgia Power Company McDonough-Atkinson plant, C) Lafarge Building Materials, Inc, D) Cobb County R.L. Sutton water reclamation facility, E) Atlanta R.M. Clayton water reclamation facility, F) Ennis Paint, Inc., G) Mead Packaging Co. and H) Central Metals Co. Major streets included in the model are shown. Interstate highways are shown for geographic reference. Monitoring sites, denoted (o), are Fire station 8 (FS), Dixie (DX) and Jefferson Street (JS).

During 2011, BC and $PM_{2.5}$ concentrations were monitored at the Fire Station 8 (FS) (33.80176 N,-84.43559 W) ASACA network site (Butler et al., 2003), and at the Dixie Driveline & Spring Co. (DX) (33.79080 N,-84.44026 W) (Figure 3.1.). $PM_{2.5}$ measurements were made with Tapered Elements Oscillating Microbalances [TEOMs] (model 1400ab; R&P Thermo Scientific, Franklin, MA). BC measurements were made with Multi Angle Absorption Photometers [MAAPs] (model 5012; Thermo Scientific, Franklin, MA). A full description of the monitoring sites and measurements can be found elsewhere (Galvis et al., 2013). These monitoring data, along with $PM_{2.5}$ concentrations measured by GAEPD (2013) using a Federal Reference Method sampler (FRM) at FS, were used to evaluate modeling results.

3.3.2. Dispersion modeling

Emission impacts from Inman and Tilford rail yards, the nearby smaller Howells yard, major surface streets and 8 industrial sources were assessed using an atmospheric Gaussian dispersion model, the American Meteorological Society/Environmental Protection Agency Regulatory Model (AERMOD) (EPA version 12345) (EPA, 2012b). The model domain was set to cover a 15km by 12 km area centered at FS (Figure 3.1.). A 500-meter spaced gridded receptor network was defined in the model and discrete receptors were set at FS and DX sites. Gridded and discrete receptors were assigned terrain elevations using Digital Elevation Model data (USGS, 2012). AERMOD was applied using the urban option to account for the urban heat island effect. A population of 156,000 was used for the simulations. The population was calculated by multiplying the population density of the Atlanta census county division (Census, 2010), 869 inhabitants/km^2 by the domain area of 180 km^2. AERMET (EPA version 12345) was

used to preprocess 2011 meteorological upper air data at 12Z GMT from the Peachtree City, GA NWS station and from hourly surface observations at the Atlanta Hartsfield Airport, GA NWS station. AERSURFACE (EPA version 13016) with the NCLD92 dataset was used to estimate land use characteristics and micrometeorological parameters (i.e., albedo, Bowen ratio and surface roughness) (Table B1).

3.3.3. Sources

3.3.3.1. Mobile Sources

The Inman and Tilford rail yard complex, the Howells Yard, and the on-road mobile sources on Marietta Blvd, Marietta Rd, and Bolton Rd (Figure 3.1.) were defined in the model as multiple volume sources. Inman and Tilford yards were defined each as two volume sources (Inman-A, Inman-B, Tilford-A, and Tilford-B) while Howells was treated as a single volume source. Emissions from line haul and switcher operations were split, but used the same source parameters (Table B2). The release height and initial vertical coordinate for rail yard sources was set to 4.6 m, which is an estimated average height of the diesel locomotive engines in the rail yards (Table B2). The initial lateral coordinates (Table B2) were estimated from the rail yards' width and length (GAEPD, 2012a; EPA, 1995). Bolton Rd and Marietta Rd are represented in the model as three volume sources each. Marietta Blvd is represented as a total of 27 volume sources, corresponding to eleven 50 m, ten 120 m, four 300 m, and two ~ 1500 m segments. Relatively fine segments are defined close to FS and coarse further away. On-road emission release heights and initial vertical coordinates are set to 2.44 m, an estimated average height of vehicles in the area. The initial lateral coordinates were calculated from each segment width and length (Table B2). Perry Blvd NW runs next to DX. This is a

minor road (~1000 AADT) though it does serve a Metropolitan Atlanta Rapid Transit Authority (MARTA) garage. Emissions from this and the rest of the roads in the domain were not included.

3.3.3.2. Industrial Sources

Emissions from the major industrial sources in the domain were modeled. Seven facilities are modeled as point sources, and the stack information was obtained from Integrated Air Information Platform (IAIP) or from Aeromatic Information Retrieval System (AIRS) (Table B3). Ennis Paint was modeled as a volume source, with parameters estimated following GAEPD (2012a) and EPA (1995). Central Metals Co is simulated as three point sources with 2/6, 1/2 and 1/6 of total emissions, respectively.

3.3.4. Emissions

Emissions from the rail yards (Table 3.1) were calculated by multiplying $PM_{2.5}$ and BC rail yard specific emissions factors (R_{EF}) measured in a previous study (Galvis et al., 2013) by the 2011 fuel consumption in the modeling domain. The fuel consumption in the domain was calculated separately for switchers (SFC_D) and line-haul locomotives (LH_{FCD}).

SFC_D for the yards was obtained from GAEPD (2012b).We used the result of the adjusted tonnage method, which is based on link-level line-haul tonnage data and yard and fleet specific information provided by NS. Fuel usage for switcher locomotives retrofitted with Gensets was calculated as 75% of 2011 SFC_D. Fuel consumption for mother-slug sets was obtained from a personal communication with Michelle Bergin.

Table 3.1. Fuel consumption, emission factors and emissions from Inman and Tilford rail yards.

	Unit	TILFORD	INMAN
Base Case. Traditional Switcher Locomotives			
Switchers Fuel Usage [a]	gal/year	600,000	1,007,000
	(m^3/year)	(2,270)	(3,810)
BC Emission Factor [b]	g/gal	2.4±0.2	3.1±0.2
	(g/m^3)	(634±53)	(819±53)
$PM_{2.5}$ Emission Factor [b]	g/gal	4.8±0.6	7.2±0.8
	(g/m^3)	(1,268±159)	(1,9024±211)
Line-haul + Switcher BC Emissions	t/year	3.3±0.3	7.8±0.5
Line-haul + Switcher $PM_{2.5}$ Emissions	t/year	6.6±1.0	18.1±2.0
Scenario 1. New Gensets			
Gensets Fuel Usage [c]	gal/year	450,000	490,000
	(m^3/year)	(1,700)	(1,850)
Gensets $PM_{2.5}$ and BC	g/gal	0.8±0.4	0.8±0.4
Emission Factor [c]	(g/m^3)	(211±106)	(211±106)
Line-haul + Gensets BC Emission	t/year	2.2±0.3	5.0±0.5
Line-haul + Gensets $PM_{2.5}$ Emission	t/year	4.1±0.6	11.2±1.4
Scenario 2. Mother-slug sets			
Mother-slug Fuel Usage [c]	gal/year	475,000	560 ,000
	(m^3/year)	(1,800)	(2,220)
Mother-slug $PM_{2.5}$ and BC	g/gal	2.9±0.4	1.6±0.4
Emission Factor [c]	(g/m^3)	(766±106)	(423±106)
Line-haul + Mother-slug BC Emission	t/year	3.2±0.3	5.5±0.5
Line-haul + Mother-slug $PM_{2.5}$ Emission	t/year	5.14±0.6	11.8.±1.4

[a] (GAEPD, 2012b)
[b] (Galvis et al., 2013)
[c] (GAEPD, 2009b;EPA, 2010a;Honc et al., 2006)
[d] Personal communication with Michelle Bergin.

$LHFC_D$ was obtained for each rail yard by dividing the gross ton miles (GTM) transported in the modeling domain (G_D) by the system-wide fuel combustion efficiency (η) as follows:

$$LHFC_D[gal] = \frac{G_D[GTM]}{\eta\,[\mathrm{GTM/gal}]} \quad (3.1.)$$

where G_D was calculated as the GTM transported in the county (G_C) times the ratio of the track miles in the modeling domain (T_D) to the track miles in the county (T_C) as follows:

$$G_D[GTM] = G_C[GTM] \times \frac{T_D[miles]}{T_C[miles]} \quad (3.2.)$$

η was calculated by dividing the GTM transported system-wide (G_S) by the system-wide fuel consumption (FC_S), as follows:

$$\eta\,[\mathrm{GTM/gal}] = \frac{G_S[GTM]}{FC_s[gal]} \quad (3.3.)$$

G_C, T_D and T_C were provided for each rail yard by NS and CSXT companies GAEPD (2009a). G_S and FC_S are data contained in NS (2012) and CSXT (2012) Class I Railroad R-1 Annual Report to the Surface Transportation Board (Table B4). Line-haul fuel usage was 779,000 gal/year (2950 m^3/year) and 1,500,000 gal/year (5680 m^3/year) for Tilford and Inman respectively. These values were used in all scenarios simulated, to calculate total rail yard emissions.

Two types of emission factors were reported by (Galvis et al., 2013), one for the mix of sources inside the rail yards, (i.e. trucks, cranes and locomotives) and another for switcher and line haul locomotives. A specific emission factor was reported for each of the rail yards. In this work we applied the emission factor for switcher and line haul locomotives to estimate rail yard emissions, given that fuel consumption from trucks and other sources inside the intermodal rail yards was not available, and the focus is on

controlling switcher emissions. This could lead to an underestimate of rail yard emissions.

Emissions from rail yard sources were split in proportion to their size. Both Inman-A and Inman-B are assumed to each produce half of the switcher and line-haul emissions from the Inman yard, while Tilford-A and Tilford-B are assumed to produce two-thirds and one-third of the of the switcher and line-haul emissions of the Tilford yard respectively, based on approximate physical size of each. Emissions of switcher locomotives retrofitted with Gensets or replaced by mother-slug sets were calculated using $PM_{2.5}$ estimates of fuel consumption and emission factors reported previously (GAEPD, 2009b; EPA, 2010a; Honc et al., 2006) and obtained by personal communication with Michelle Bergin. Uncertainties in emission factors were considered in our emission inventory, but no information on uncertainties of fuel consumption was available.

The on-road mobile emissions from Bolton Road (between James Jackson Parkway and Marietta Blvd), Marietta Rd, and Marietta Blvd (Table 3.2) were obtained from Atlanta Regional Commission link-based Vehicle Miles Traveled (VMT) database for 2010 (ARC, 2011). Marietta Blvd is a four-lane arterial road with high volume of heavy-duty trucks transporting goods to and from the rail yard; therefore, its emissions are considerably larger than Bolton Rd and Marietta Rd which are two-lane minor collector roads. The emissions for each segment of the roads were set to be proportional to its length relative to the total length of the road (Table B5). BC emissions are a proportion to $PM_{2.5}$ emissions calculated using ratios reported by EPA (2012a) and traffic splits between diesel and gasoline vehicles (ARCADIS, 2005) (Table B5).

Table 3.2. Emissions from major on-road mobile sources at the modeling domain.

	$PM_{2.5}$ Emissions* [t/year]	BC Emissions** [t/year]
Bolton Rd	0.3	0.1
Marietta Blvd	1.2	0.4
Marietta Rd	0.4	0.1

*(ARC, 2011).
** BC emissions are a proportion to $PM_{2.5}$ emissions calculated using ratios reported by EPA (2012a).

For industrial sources, $PM_{2.5}$ emission rates (Table 3.3) were estimated based on information contained in the CERR emission inventory and the GAEPD permitting database. Whenever $PM_{2.5}$ emissions were not available, PM_{10} emissions or PM emissions were modeled (Table B6). As a result, $PM_{2.5}$ impacts from industrial sources are likely overestimated. BC emissions are found from $PM_{2.5}$ emissions using ratios reported for each type of industrial activity by EPA (2012a).

Table 3.3. Emissions from major industrial sources at the modeling domain.

	$PM_{2.5}$ Emissions* [t/year]	Ratio BC to $PM_{2.5}$** [g BC]/ [g $PM_{2.5}$]	BC Emissions [t/year]
Georgia Power Company McDonough-Atkinson plant	132.4	0.38	50.3
Lafarge Building Materials, Inc.	40.8	0.02	0.8
General Shale Brick Inc. plant	24.9	0.02	0.5
Cobb County R.L. Sutton water reclamation facility	36.6	0.02	0.7
Atlanta R.M. Clayton water reclamation facility	9.5	0.02	0.2
Mead Packaging Co.	19.1	0.02	0.4
Central Metals Co.	7.3	0.02	0.1

* CERR emission inventory and the GAEPD permitting database
**BC emissions are a proportion to $PM_{2.5}$ emissions calculated using ratios reported by EPA (2012a) for similar industrial activities.

3.3.5. Background concentrations

Background concentrations were obtained from monitoring data reported by the Southeastern Aerosol Research and Characterization Network (EPRI, 2012) at Jefferson Street (JS) (33.777627 N,-84.416672 W) , which is situated well away from the rail yards and the other major sources being modeled (Figure 3.1.). They measure $PM_{2.5}$ with a TEOM and BC with an Aethalometer. Wavelet analysis (Daubechies, 1992) was used to separate the low frequency components of five minute average $PM_{2.5}$ and BC concentrations. A linear regression between local minima of the low frequency components produced five-minute background concentrations that were averaged by hour, by day of the week and by month. Background annual average concentrations in 2011 were approximately 9.9 $\mu g/m^3$ of $PM^{2.5}$ and 0.52 $\mu g/m^3$ of BC.

3.3.6. Health impacts

BenMAP was used to assess the avoided health impacts brought about by the conversion to lower emitting switcher locomotives and to estimate their associated economic value. The reduction in PM2.5 concentrations accomplished by changes to switcher locomotives at both rail yards along with population calculated for the model domain using data from the Atlanta census county division (Census, 2010) were used as main inputs. BenMAP calculates health related benefits using concentration-response (C-R) functions. C-R functions (Table S7) relate a change in the concentration of a pollutant with a relative change in the incidence of a health endpoint. Next BenMAP calculates the economic value of avoided health effects multiplying the incidence in health effects by a monetary value of the health effect. We used the current EPA-default options for PM health impact assessments to obtain incidence and valuation results (EPA, 2010b). We used the value of

statistical life (VSL) recommended by the EPA Science Advisory Board (EPA, 2010b) to calculate the health benefits of avoided mortality.

3.4. Results and Discussion

3.4.1. Model evaluation

Annual average concentrations estimated with AERMOD at FS and DX are within 8% and 20% of measured $PM_{2.5}$ and BC concentrations, respectively (Figure 3.2). Simulated $PM_{2.5}$ concentrations at FS agree with TEOM measurements and BC measurements at the same site are found to be 0.3 $\mu g/m^3$ higher than the model result (Figure 3.2a). Simulated concentrations at DX underestimate $PM_{2.5}$ annual average concentrations by about 1.1 $\mu g/m^3$ and slightly overestimate BC (Figure 3.2b). Discrepancies at DX could be attributed to AERMOD limitations when reproducing concentrations close to the sources (Holmes et al., 2006) and at FS to uncertainty in on-road mobile sources emissions, as well as other modeling uncertainties.

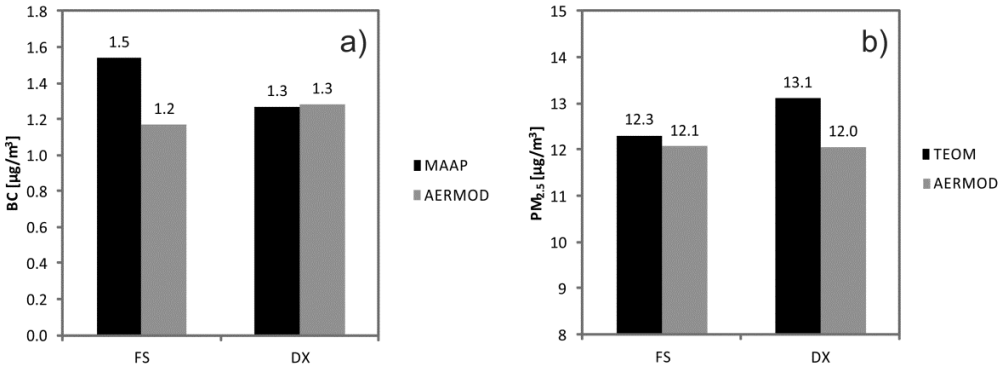

Figure 3.2. Modeled and measured a) BC and b) $PM_{2.5}$ annual average concentrations.

Simulated daily averages of BC at FS compared well with MAAP measurements. Model results explained about 50% of the variability in the measurements at this site

(Figure 3.3a.).The BC measured concentrations at DX showed more variability than modeled. $PM_{2.5}$ concentrations at both sites produced by the model agreed well (Figure 3.3b. and Fig B1). The model falls short to a slight extent when trying to reproduce the variability of the daily average $PM_{2.5}$ measurements. Modeled $PM_{2.5}$ daily averages closely follow TEOM and FRM measurements trend during winter and spring. Summer and fall daily averages are underestimated and overestimated respectively. Further investigation of the fall overestimate found that there was a major change at Plant McDonough that lowered its emissions (EPA, 2013).

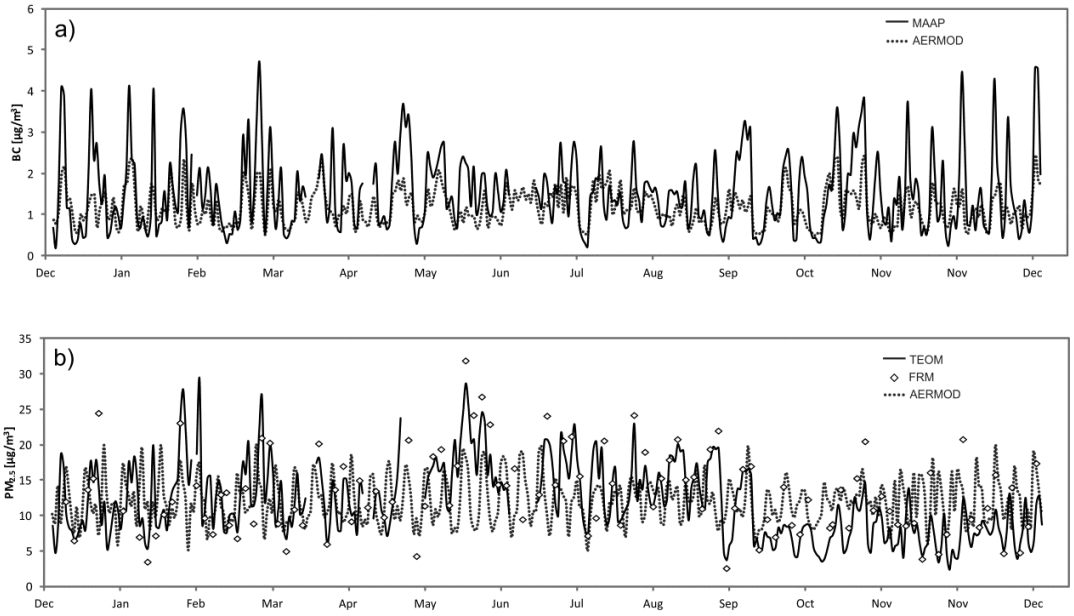

Figure 3.3. Modeled and measured a) BC b) $PM_{2.5}$ daily average concentrations at FS.

Modeled daily averages overestimate low concentrations and underestimate high concentrations by up to 50% in the worst case (Figure 3.4.). Estimates of BC daily averages at DX show an opposite behavior, underestimating low concentrations by around 20% and overestimating concentrations between the 90th and 98th percentile by around 30% (Figure 3.4a.). Given that BC emissions at DX come mainly from the rail

yards and that the site is 80m from the tracks this is a demanding situation for accurate modeling.

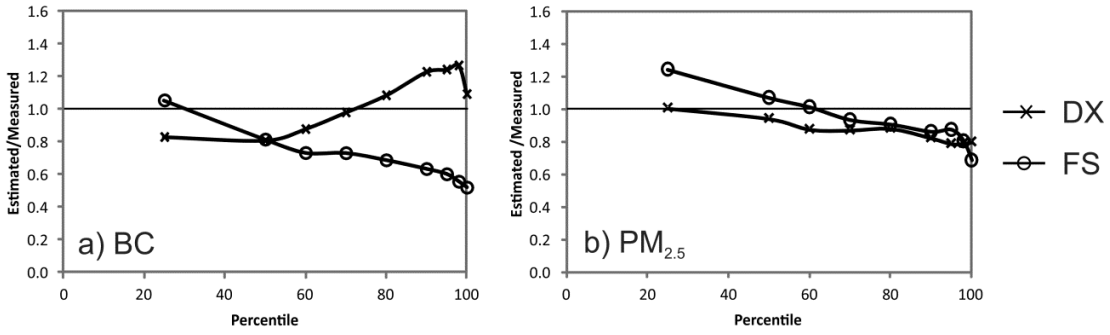

Figure 3.4. Modeled to measured ratios of daily average concentrations by percentile for a) BC and b) $PM_{2.5}$.

Comparisons between measured hourly average concentrations and model results indicate that the model exhibits slight under dispersion in the early morning and evening, and over dispersion in the afternoon. Results do not fully capture morning rush hour peaks for both contaminants and other short-term features (Figure 3.5.).

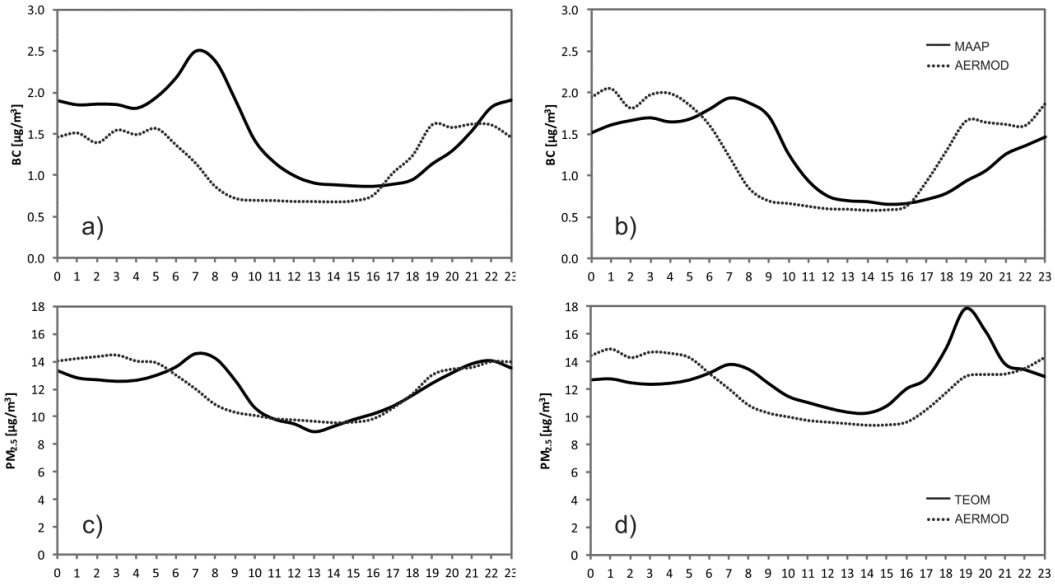

Figure 3.5. Modeled (AERMOD) and measured (MAAP and TEOM) hourly average concentrations for BC at a) FS and b) DX, and PM2.5 at c) FS and d) DX.

3.4.2. Source apportionment

Apportionment of BC and $PM_{2.5}$ from AERMOD results indicates that the line-haul and switcher activities in the rail yards are the most important source of BC in the domain, accounting for approximately 0.5±0.03 $\mu g/m^3$ (39%) and 0.7±0.04 $\mu g/m^3$ (56%) of BC at FS and DX respectively, and for approximately 1±0.1 $\mu g/m^3$ (7%) and 1.6±0.2 $\mu g/m^3$ (14%) of $PM_{2.5}$ at FS and DX respectively (Figure 3.6.). Calculations indicate a greater impact on $PM_{2.5}$ at DX and FS came from the Inman yard. Approximately 5% and 13% of $PM_{2.5}$ at FS and DX respectively are apportioned to Inman yard, whereas 2% and 1.5% of $PM_{2.5}$ at FS and DX respectively are attributed to Tilford yard. Line-haul activities at both yards were found to have slightly higher impacts than switchers, accounting for roughly 4% and 9 % of $PM_{2.5}$ at FS and DX respectively. Switchers at both yards were responsible for roughly 4% and 5.5% of $PM_{2.5}$ at FS and DX respectively.

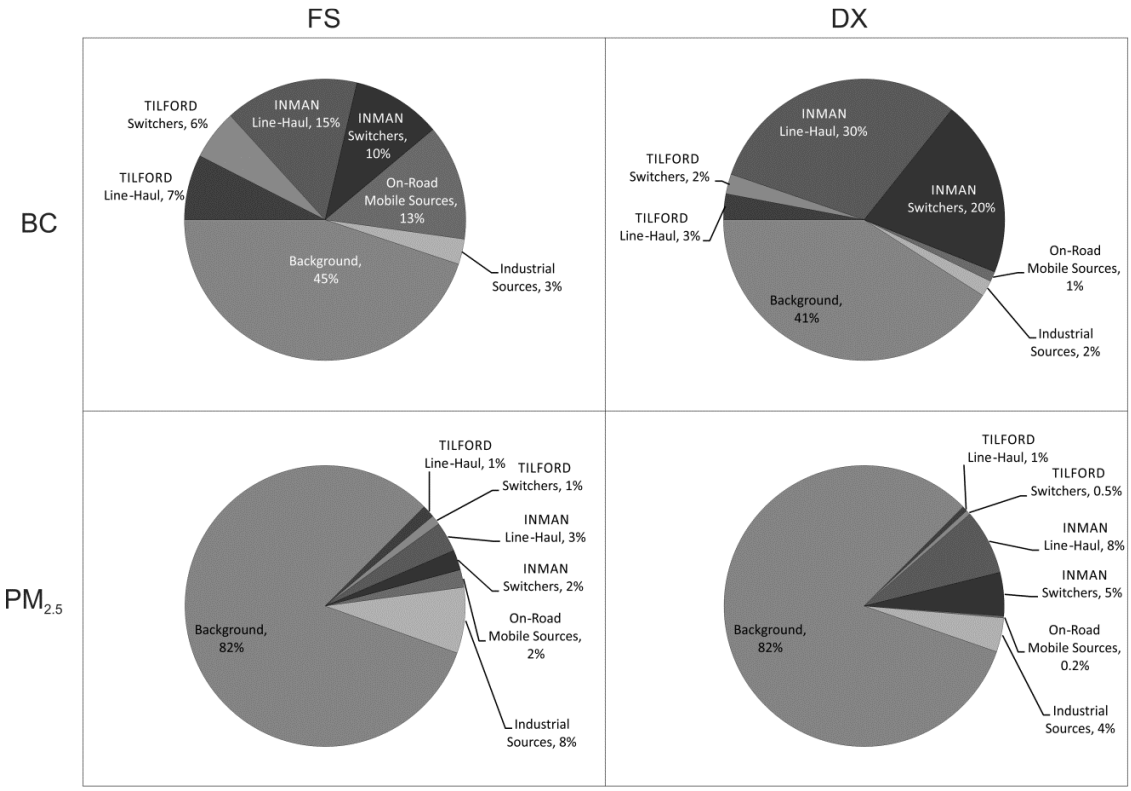

Figure 3.6. Source apportionment for BC and $PM_{2.5}$ at FS and DX.

3.4.3. Air quality impact evaluation

The spatial distributions of BC correspond to the rail yard layout whereas distributions of $PM_{2.5}$ also correspond to the location of the industrial sources (Figure 3.7a. and 3.7b.). BC concentrations of approximately 1 $\mu g/m^3$ outline the rail yards up to 2 km from the center of the complex (Figure 3.7a.).

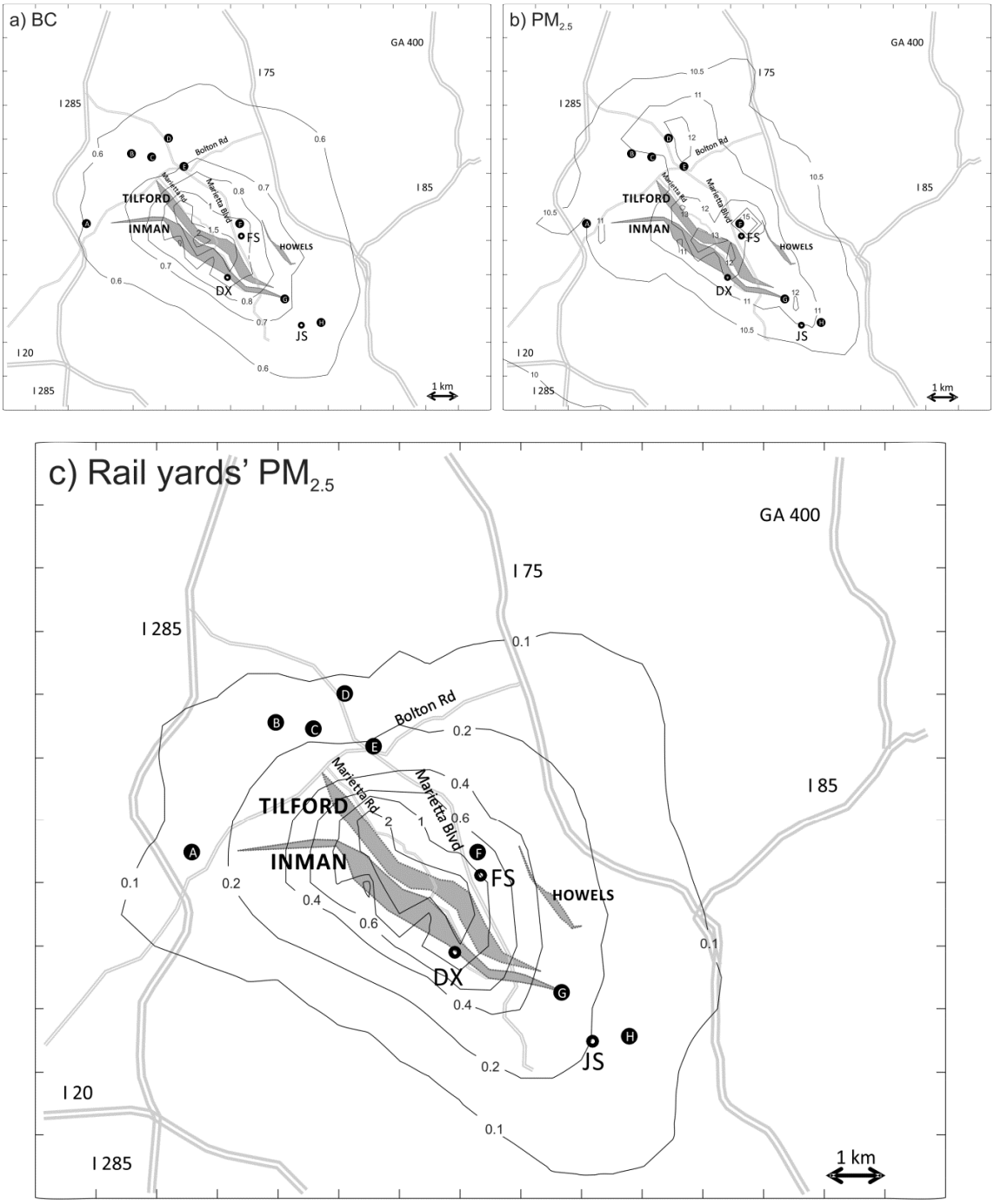

Figure 3.7. Spatial distribution of annual average concentrations of a) BC, b) $PM_{2.5}$ from all sources in the domain and c) $PM_{2.5}$ from the rail yards. Units of the isolines are $\mu g/m^3$. Industrial sources include (A) General Shale Brick Inc plant, (B) Georgia Power Company McDonough-Atkinson plant, (C) Lafarge Building Materials, Inc, (D) Cobb County R.L. Sutton water reclamation facility, (E) Atlanta R.M. Clayton water reclamation facility, (F) Ennis Paint, Inc., (G) Mead Packaging Co. and (H) Central Metals Co.

The spatial distribution of $PM_{2.5}$ annual average concentrations over the domain indicates hot spots, 5 to 2 $\mu g/m^3$ above background, at the center of the rail yard complex and east of D trough G (Figure 3.7b.). Higher impacts of $PM_{2.5}$ from the rail yards are located to the northeast of the domain. Annual average $PM_{2.5}$ concentrations from the rail yards are about 1 $\mu g/m^3$ up to 1 km northeast from the center of the complex (Figure 3.7c.).

Reductions of $PM_{2.5}$ concentrations by retrofitting switchers with new Genset units (Figure 3.8.) are 0.4±0.1 $\mu g/m^3$ and 0.6±0.1 $\mu g/m^3$ at FS and DX respectively (i.e. 3% and 5% of total $PM_{2.5}$ concentration at each site). Conversion to mother-slug sets could gain reductions of about 0.3±0.1 $\mu g/m^3$ and 0.6±0.1 $\mu g/m^3$ at FS and DX respectively. In both scenarios, $PM_{2.5}$ reductions of about 1 $\mu g/m^3$ are located over the rail yards and extend mostly toward the northeast of the domain. $PM_{2.5}$ impacts from the switcher locomotives at the rail yards are reduced on average by 35%.

BC from the rail yards would be reduced by approximately 23% if mother-slug sets are implemented and by 35% retrofitting with new Gensets. BC concentrations will be diminished by 0.1 ±0.02 $\mu g/m^3$ and 0.2±0.03 $\mu g/m^3$ at FS and DX respectively, when the conversions take effect.

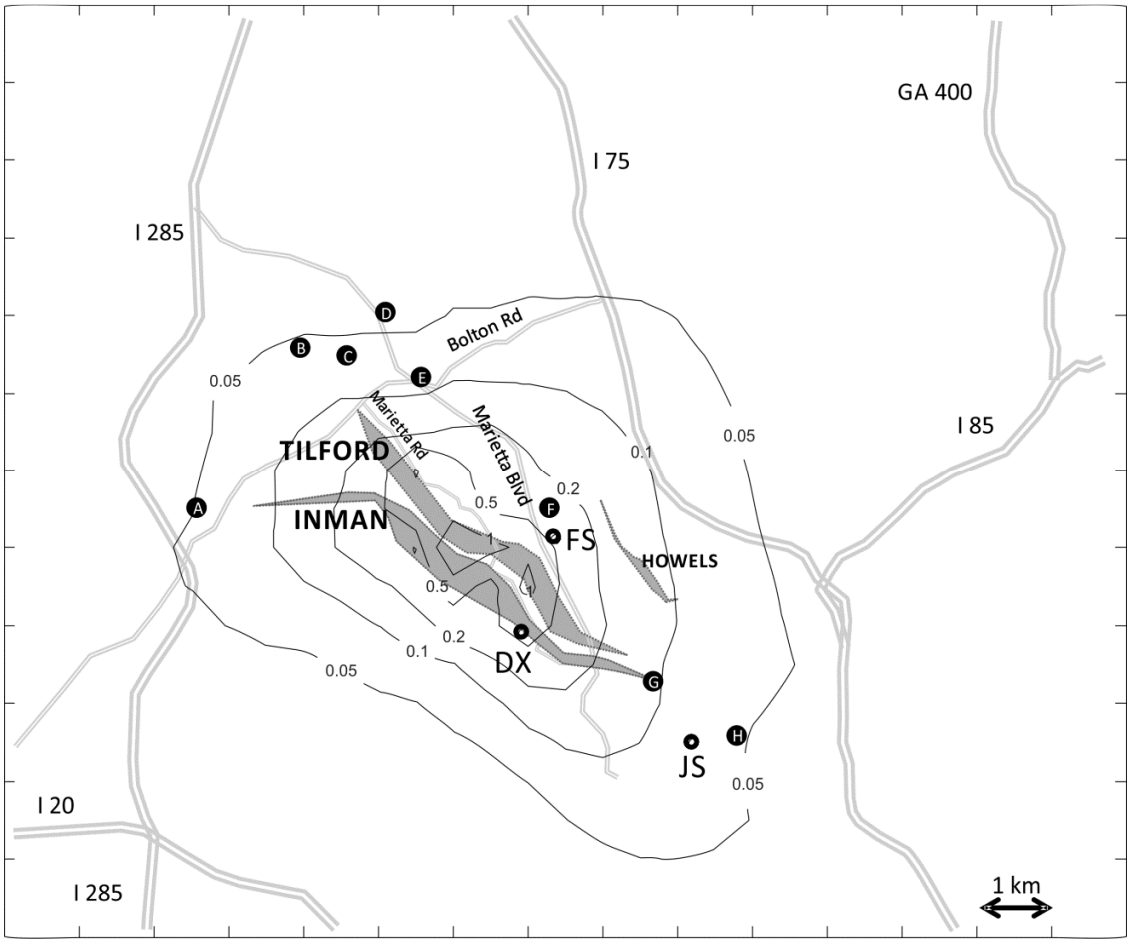

Figure 3.8. Spatial distribution of annual average $PM_{2.5}$ reduction by retrofitting switcher locomotives with new Gensets. Units of the isolines are $\mu g/m^3$. Industrial sources include (A) General Shale Brick Inc plant, (B) Georgia Power Company McDonough-Atkinson plant, (C) Lafarge Building Materials, Inc, (D) Cobb County R.L. Sutton water reclamation facility, (E) Atlanta R.M. Clayton water reclamation facility, (F) Ennis Paint, Inc., (G) Mead Packaging Co. and (H) Central Metals Co.

3.4.4. Health incidence and valuation

We used BenMAP to calculate the avoided incidence in health impacts and the economic value saved by the reduction in primary $PM_{2.5}$ concentrations. Annual avoided incidence results (Table 3.4.) are based on estimates of reduced exposure to $PM_{2.5}$ of the population in the model domain. Results show approximately 3 avoided cases of premature mortality in the 25-99 age group per year and less than one avoided case for

infants. Minor restricted activity days have the highest incidence with approximately 1200 cases. Reductions in asthma exacerbation and work loss days are also important.

Table 3.4. Annual avoided health incidences.

Health endpoint | Age group	Mean reduction in incidence ± standard deviation	
	Scenario 1 Gensets retrofit	Scenario 2 Conversion to mother-slug sets
Mortality, All Cause | 30-99	1.1±0.2	1±0.1
Mortality, All Cause | 25-99	2.5±0.6	2.1±0.5
Mortality, All Cause | infants	0.01±0.01	0.01±0.01
Emergency Room Visits, Asthma | 0-99	0.8±0.3	0.7±0.2
HA, All Respiratory |65-99	0.3±0.1	0.2±0.03
HA, Asthma |0-17	0.03±0.01	0.02±0.01
HA, Chronic Lung Disease | 18-64	0.1±0. 02	0.08±0.01
HA, All Cardiovascular (less Myocardial Infarctions) | 65-99	0.3±0.03	0.3±0.03
HA, All Cardiovascular (less Myocardial Infarctions) | 18-64	0.2±0.04	0.2±0.03
Work Loss Days | 18-64	201±15	166±12
Minor Restricted Activity Days | 18-64	1168±103	966±85
Acute Bronchitis | 8-12	2±1	1.4±0.8
Lower Respiratory Symptoms | 7-14	21±6	18±5
Upper Respiratory Symptoms | 9-11	31±12	25±10
Asthma Exacerbation, Cough | 6-18	412±198	340±164
Asthma Exacerbation, Shortness of Breath | 6-18	146±155	121±128
Asthma Exacerbation, Wheeze | 6-18	49±19	40±16

HA: Hospital Admissions.

Economic value is assigned by BenMAP (ABT, 2012). based on specific cost factors for each health endpoint. Cost factors correspond to research compiled in BenMAP. Reductions in primary $PM_{2.5}$ concentrations due to retrofitting switcher locomotives at Inman and Tilford rail yards save approximately $20 to $24 million in annual avoided health costs (Table 3.5). Converting switchers at the yards to mother-slug sets produces $4 million less savings that retrofitting them with new Gensets. Avoided mortality accounts for 99% of the savings in both scenarios.

Table 3.5. Annual reductions in health costs and premature mortality valuation.

Endpoint | Valuation Method | Age Group	Mean yearly benefits ± Standard deviation [$]					
	Scenario 1 Gensets retrofit			Scenario 2 Conversion to mother-slug sets		
Mortality | VSL, based on 26 value of life studies. | 0-99	24,100,000	±	17,300,000	19,900,000	±	14,400,000
Hospital Admissions, Respiratory | COI: med costs + wage loss | 65-99	5,600	±	4,000	4,700	±	3,300
Hospital Admissions, Respiratory | COI: med costs + wage loss | 0-64	600	±	200	500	±	150
Hospital Admissions, Cardiovascular | COI: med costs + wage loss | 65-99	7,500	±	3,400	6,200	±	3,100
Hospital Admissions, Cardiovascular | COI: med costs + wage loss | 18-64	9,300	±	2,100	7,700	±	1,800
Acute Respiratory Symptoms | WTP: 1 day, CV studies | 18-99	80,000	±	20,000	66,000	±	17,000
Lower Respiratory Symptoms | WTP: 1 day, CV studies | 0-17	450	±	200	370	±	170
Upper Respiratory Symptoms | WTP: 1 day, CV studies | 0-17	1,000	±	600	800	±	500
Work Loss Days | Median daily wage, county-specific | 18-65	38,000	±	2,800	31,500	±	2,300
Asthma Exacerbation | WTP: bad asthma day | 18-99	4,700	±	7,700	4,900	±	6,400
Emergency Room Visits, Respiratory | COI | 0-99	300	±	180	240	±	150
Acute Bronchitis | WTP: 6 day illness, CV studies | 0-17	800	±	800	670	±	500
Total	**24,200,000**	**±**	**17,000,000**	**20,000,000**	**±**	**14,400,000**

VSL: Value of statistical life, COI: Cost of illness, WTP: Willingness to pay, CV: cardiovascular

3.3.5. Cost - benefit

Funding for retrofitting switcher locomotives awarded through CMAQ and matched by industry are expected to amount to 3 annual disbursements, each of 17

million (GAEPD, 2009b). The retrofitted switcher locomotives will remain in service for at least 10 years. With a discount rate of 0.75% (Federal discount rate for April 2013), the resulting positive net present value (NPV) of retrofitting switcher locomotives at Inman and Tilford yards with new genset or replacing them with mother slugs sets is $ 179 million and $ 140 million respectively. This result doesn't take in to account additional pollutants or other factors such as fuel savings or maintenance costs that could affect the cash flows of the project.

3.4. References

ABT Associates. 2012. BenMAP environmental benefits mapping and analysis program - user's manual, [accessed Jan 2013]. Available from http://www.epa.gov/air/benmap/models/BenMAPManualOct2012.pdf.

Atlanta Regional Commission [ARC]. 2011. Atlanta Regional Commission link-based vehicle miles traveled data., [accessed Nov 2012]. Available from http://www.atlantaregional.com/.

ARCADIS. 2005. Bolton / Moores Mill Transportation and Circulation Study, [accessed May 2013]. Available from https://dl.dropboxusercontent.com/u/18763207/bmt%20final%20report.pdf.

Butler, A. J., Andrew, M. S., and Russell, A. G. 2003. Daily sampling of PM2.5 in Atlanta: Results of the first year of the Assessment of Spatial Aerosol Composition in Atlanta study. Journal of Geophysical Research: Atmospheres no. 108 (D7):8415. doi: 10.1029/2002JD002234.

Campbell, D., and Fujita, E. M. 2009. Roseville Rail Yard Air Monitoring Project (RRAMP). Final Report Summary of Data QA and Trend Analysis. Desert Research Institute, Reno, NV., [accessed Oct 2012]. Available from http://www.placer.ca.gov/Departments/Air/~/media/apc/documents/UP/2009/December/RRAMPFinalUpdate121009.ashx.

California Air Resources Board [CARB]. 2011. Railyard Health Risk Assessments and Mitigation Measures, [accessed Apr 2013]. Available from http://www.arb.ca.gov/railyard/hra/hra.htm.

Census Bureau. 2010. Population and Housing Census [accessed Apr 2013]. Available from http://www.census.gov/popfinder/.

Congestion Mitigation and Air quality Improvement Program [CMAQ]. Department of transportation. 2009. EPD Railroad related emissions reduction project in Atlanta GA20090013, [accessed Apr 2013]. Available from https://fhwaapps.fhwa.dot.gov/cmaq_pub/View/default.aspx?id=GA20090013.

CSXT. 2012. Class I Railroad Annual Report, [accessed Dec 2012]. Available from http://www.stb.dot.gov/econdata.nsf/f039526076cc0f8e8525660b006870c9/8775aca41ef66efb852579db004c9dee?OpenDocument.

Daubechies, I. 1992. Ten Lectures on Wavelets. Edited by Society for Industrial and Applied Mathematics, CBMS-NSF Regional Conference Series in Applied Mathematics.

Electric Power Research Institute [EPRI]. 2012. The Southeastern Aerosol Research and Characterization Network: SEARCH, [accessed Oct 2012]. Available from http://www.atmospheric-research.com/studies/search/SEARCHFactSheet.pdf.

Feinberg, S., Yadav, V., Heiken, J., and Turner, J. 2011. Midwest Rail Study: Modeled Near-Field Impacts of Emissions of Fine Particulate Matter from Railyard Activities. Transportation Research Record: Journal of the Transportation Research Board no. 2261 (-1):106-114. doi: 10.3141/2261-12.

Georgia Environmental Protection Division [GAEPD]. 2006. CMAQ/BenMAP-based health-benefits analysis in support of the Georgia SIPs for O3 and PM2.5. In Community Modeling and Analisys System - CMAS. Chapel Hill, NC.

Georgia Environmental Protection Division [GAEPD]. 2009a. Dispersion Modeling to Support the Atlanta PM2.5 SIP Local Area Analysis, [accessed Aug 2012]. Available from http://www.gaepd.org/Files_PDF/plans/sip/Appendix_M_PM2.5_Dispersion_Modeling_at_FireSta8.pdf.

Georgia Environmental Protection Division [GAEPD]. 2009b. Voluntary Reduction of Emissions from Railyards in Metro Atlanta Region, [accessed Oct 2012]. Available from http://www.georgiaair.org/airpermit/downloads/planningsupport/regdev/sips_and_revisions/atlanta_8hr_ozone/appendixt.pdf.

Georgia Environmental Protection Division [GAEPD]. 2012a. Guideline for Modeling PM10 Ambient Concentration In Areas Impacted by Quarry Operation Producing Crushed Stone, [accessed Feb 2013]. Available from http://www.georgiaair.org/airpermit/downloads/sspp/modeling/quarryguideline_august2012.pdf.

Georgia Environmental Protection Division [GAEPD]. 2012b. Railroad Emission Inventories. Locomotive Emission Inventories for the United States from ERTAC Rail., [accessed Mar 2013]. Available from http://www.georgiaair.org/airpermit/downloads/planningsupport/regdev/locomotives/railyard_switcher_semap.xls.

Georgia Environmental Protection Division [GAEPD]. 2013. Ambient Monitoring Program Air Quality Database, [accessed Feb 2013]. Available from http://www.georgiaair.org/amp/amp_query.html.

Galvis, B., Bergin, M., and Russell, A. G. 2013. Fuel-based fine particulate and black carbon emission factors from a railyard area in Atlanta. Journal of the Air & Waste Management Association (63):618–628.

Gould, G., and Niemeier, D. A. 2009. Review of Regional Locomotive Emission Modeling and the Constraints Posed by Activity Data, [accessed Jan 2013]. Available from http://www.escholarship.org/uc/item/3gn498w6.

Holmes, N. S., and Morawska, L. 2006. A review of dispersion modelling and its application to the dispersion of particles: An overview of different dispersion models available. Atmospheric Environment no. 40 (30):5902-5928. doi: http://dx.doi.org/10.1016/j.atmosenv.2006.06.003.

Honc, R. L., Fritz, S. G., Schell, M. B., Tarnow, A., and Bennett, A. 2006. Fuel Consumption and Exhaust Emissions From a 1,125 kW Multiple Genset Switcher Locomotive. ASME Conference Proceedings no. 2006 (42606):1-8. doi: 10.1115/ICEF2006-1515.

Norfolk Southern [NS]. 2011. Biz NS Continuing A Railroad Tradition, [accessed May 2013]. Available from http://www.nscorp.com/nscorphtml/bizns/bzns1211/NovDecBizNS_WEB.pdf.

Norfolk Southern [NS]. 2012. Class I Railroad Annual Report, [accessed Nov 2012]. Available from http://www.stb.dot.gov/econdata.nsf/f039526076cc0f8e8525660b006870c9/d945e6d27425d1f6852579db004cfdbd?OpenDocument.

Sierra Research, I. 2011. Modeling Evaluation Study for the Union Pacific J.R. Davis (Roseville) Rail Yard, [accessed Jan 2013]. Available from http://www.placer.ca.gov/departments/air/~/media/apc/documents/UP/2011/RailYardMonitoringReport101311.ashx.

U. S. Environmental Protection Agency [EPA]. 1995. USER'S GUIDE FOR THE INDUSTRIAL SOURCE COMPLEX (ISC3) DISPERSION MODELS VOL1, [accessed Oct 2012]. Available from http://www.epa.gov/scram001/userg/regmod/isc3v1.pdf.

U. S. Environmental Protection Agency [EPA]. 2010a. Exhaust and Crankcase Emission Factors for Nonroad Engine Modeling Compression Ignition [accessed Jan 2013]. Available from http://www.epa.gov/otaq/models/nonrdmdl/nonrdmdl2010/420r10018.pdf.

U. S. Environmental Protection Agency [EPA]. 2010b. Valuing Mortality Risk Reductions for Environmental Policy, [accessed Mar 2013]. Available from http://yosemite.epa.gov/ee/epa/eerm.nsf/vwAN/EE-0563-1.pdf/$file/EE-0563-1.pdf.

U. S. Environmental Protection Agency [EPA]. 2011. Rail and Locomotives | Clean Ports USA | US EPA. Available from http://www.epa.gov/diesel/ports/rail.htm.

U. S. Environmental Protection Agency [EPA]. 2012a. Report to Congress on Black Carbon, [accessed Dec 2012]. Available from http://www.epa.gov/blackcarbon/2012report/fullreport.pdf.

U. S. Environmental Protection Agency [EPA]. 2012b. USER'S GUIDE FOR THE AMS/EPA REGULATORY MODEL - AERMOD, [accessed Dec 2012]. Available from http://www.epa.gov/ttn/scram/dispersion_prefrec.htm#aermod.

U. S. Environmental Protection Agency [EPA]. 2013. Air Markets Program Data, [accessed May 2013]. Available from http://ampd.epa.gov/ampd/.

U.S. Geological Survey [USGS]. 2012. The National Map Viewer and Download Platform, [accessed Oct 2012]. Available from http://nationalmap.gov/viewer.html.

CHAPTER 4

AEROSOL CHEMICAL SPECIATION AND SOURCE IMPACT ANALYSIS NEAR RAIL YARDS

(Galvis, B. Bergin, M., Ng. N. L., Kollman, M.S. and Russell A.G. In preparation)

4.1. Abstract

Chemical speciation of aerosols near the Inman and Tilford rail yard complex in Atlanta, GA indicates that the rail yards are an important source of hydrocarbon like organic aerosols (HOA) and black carbon from fuel (BCf). The rail yard complex contributed to about 1.2 and 1 $\mu g/m^3$ of HOA and BCf respectively, during a monitoring campaign in 2011. Elemental carbon (EC) concentrations from wind sector selective filter based measurements confirm downwind upwind continuous measurements and dispersion modeling results for $PM_{2.5}$ BC. A ratio of BCf/HOA of 1.0±0.5 at FS from ACSM and Aethalometer measurements and a downwind upwind EC/OC ratio of 1.0±1.9 from wind sector selective filter based measurements might was found in concentrations coming from the direction where the rail yard complex was located. Wind sector selective filter based measurements also indicate that the rail yards is a source of Lead, Antimony and Barium likely from a welding facility located inside the complex. Trajectory analysis founds that oxidized organic aerosols (OOA), biomass burning organic aerosols (BBOA), sulfates, nitrates and ammonia were associated with air masses from directions other than the location of the rail yard complex.

4.2. Introduction

The importance of rail yard activities for air quality and climate change (NCFRP, 2010) and the serious health effects of diesel fuel combustion fumes (WHO, 2012), which are their most important emissions, compel extensive work to improve the chemical characterization of atmospheric aerosols around rail yards. Current understanding of emissions from rail yards has identified black carbon (BC) and oxygenated carbonaceous species as their main components. Cahill et al. (2011) carried out a characterization of the inorganic and organic constituents of aerosols from the Roseville rail yard and repair facility in California. They found that rail yard emissions consisted of ultra-fine and very fine aerosols associated with diesel exhaust. They identified species such as black carbon (BC), organic matter, polycyclic aromatic hydrocarbons (PAHs) (particularly, high concentrations of benzo[a]pyrene), phosphorus, zinc, and sulfur. They also found coarse soil aerosols contaminated with anthropogenic metals and petroleum-derived n-alkanes. Sawant et al. (2007), analyzed emissions from three in-use diesel-electric switching locomotives and also found PAHs (predominantly, naphthalene and its derivatives) and n-alkanes.

Organic aerosols (OA) are a mix of thousands of compounds with extremely different properties that can change its composition in the atmosphere and has diverse primary and secondary sources (Zhang et al., 2007). OA can be one of the main components of fine particulate (Kanakidou et al., 2005; Zhang et al., 2007). In Atlanta, OA dominates atmospheric aerosols composition (Budisulistiorini et al., 2013; Lin et al., 2013; Xu et al., 2013). Investigating OA concentrations near rail yards is essential to advance the chemical characterization of emissions from these sources, improve their

representation in models and develop efficient strategies to control their impact on air quality.

The objective of this work is to advance the understanding of the impact of emissions from rail yards by performing a chemical characterization of OA, metals and BC near the Inman and Tilford rail yard complex in Atlanta, GA. And provide a composition profile of aerosol rail yard emissions that can be used to improve air quality modeling.

4.3. Experimental Methods

4.3.1. Study description

Two monitoring sites were used to perform measurements of concentrations of aerosol species near the Inman and Tilford rail yard complex in Atlanta, GA (Figure 4.1.). Fire Station 8 (FS) (33.80176˚N,-84.43559˚W) and Dixie (DX) (coordinates: 33.79080˚N,-84.44026˚W), north and south of the rail yard complex. FS site is part of the Assessment of Spatial Aerosol Composition Network (ASACA) (Butler et al., 2003). Analyses of concentrations of non-refractory (NR) species in PM_1 (particulate matter with an aerodynamic diameter ≤ 1 μm) were performed with an Aerosol Chemical Speciation Monitor (ACSM) (Aerodyne, Billerica, MA, US) (Ng et al., 2011) during a winter 2011 monitoring campaign at FS. At the same site, black carbon concentrations in fine particulate ($PM_{2.5}$ BC) were measured with a 7-wavelengt Aethalometer (model AE30 Magee Scientific Corporation, Berkeley, CA, US) from November 2010 until April 2011 and from December 2012 until March 2012. $PM_{2.5}$ BC was also measured at DX and FS with a multi-angle absorption photometer (MAAP) (Thermo Scientific Model 5012) (Petzold et al., 2004; Petzold et al., 2002). MAAP measurements were made from

November 2010 until March 2012. Analysis of MAAP $PM_{2.5}$ BC concentrations was published previously (Galvis et al., 2013) and results at FS are used here for validation of Aethalometer findings. Other long standing measurements at FS include $PM_{2.5}$ mass (particulate matter with aerodynamic diameter less than 2.5 μm) as part of the ASACA project. Filter based measurements of metals, elemental and organic carbon (EC/OC) and ions were carried out during summer and fall 2011 at FS and at DX. Descriptions of the rail yard complex and the monitoring sites can be found in previous works (Galvis et al., 2013). Marietta Blvd NW (17.000 AADT approximately), a road with heavy duty diesel traffic, runs between FS and the rail yard complex.

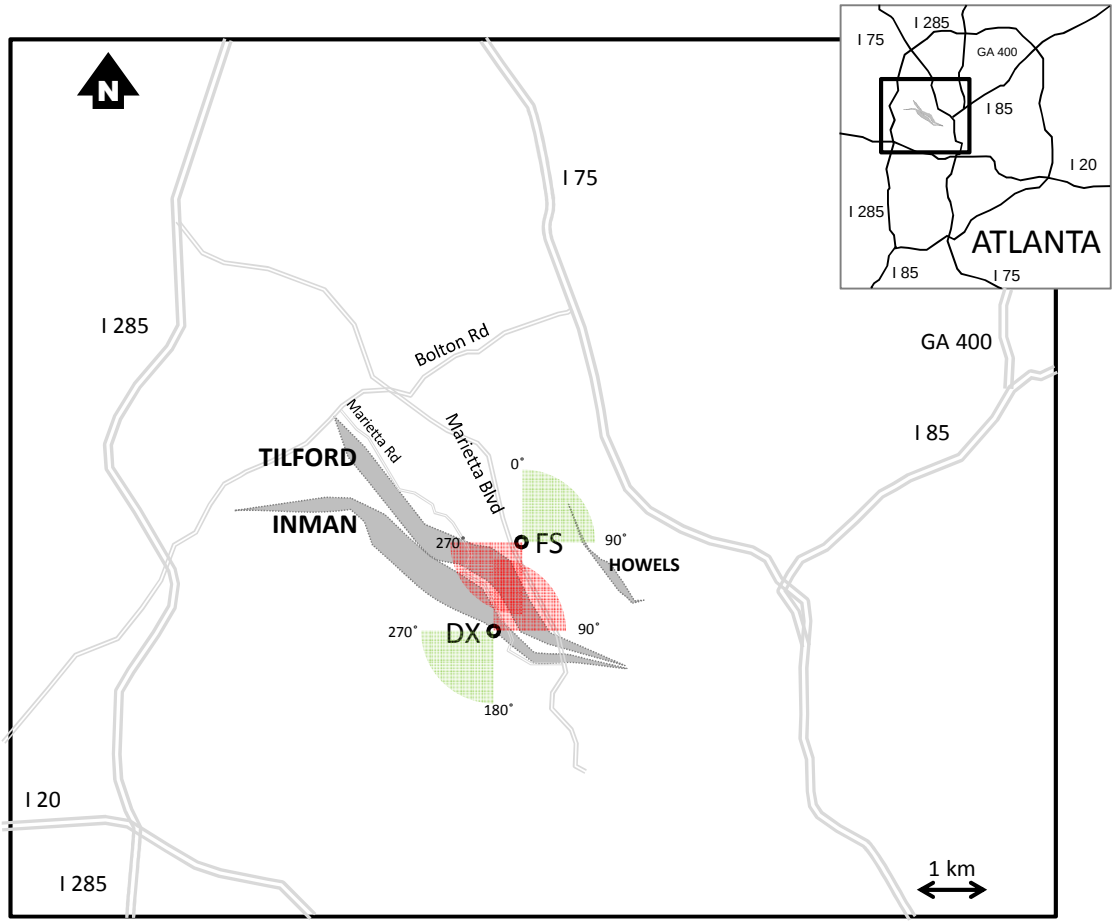

Figure 4.1. Study location. Wind sectors for filter sampling are marked red for downwind and green for upwind.

4.3.2. Aerosol chemical speciation monitor

An ACSM was used between 11/22/2011 and 12/12/2011 to measure quantitative mass spectra of the NR species with aerodynamic diameters between 30 and 700 nm (~PM_1) where NR species are operationally defined as those that flash vaporize at 600 °C and 10−5 torr (Ng et al., 2011). These NR species include organics, sulfates, nitrates, ammonia and chlorides and exclude black carbon, metals, mineral dust, and sea salt. Measurements were carried out during three weeks, from November 22 to December 12 of 2011. The ACSM samples aerosols through an aerodynamic lens at 0.1 L min^{-1}, which focuses particles into a narrow beam and carries them in to a high vacuum detection chamber; there the NR components flash vaporize on impact with a heated surface. The resulting gas molecules are detected and chemically characterized by 70eV electron impact quadrupole mass spectrometry. A detailed description of these instruments can be found in Ng et al. (2011). ACSM spectra were recorded with a time resolution of 33 min. The aerosol sampling inlet (2.5 µm URG cyclone with 3L min^{-1} flow, Chapel Hill, NC) was located 3m above the ground. The aerosol was dried and the enclosure at FS was maintained at approximately 20°C. ACSM spectra were analyzed using the toolkit provided by Aerodyne for the IGOR Pro software package (Wavemetrics, Inc., Portland, OR, US). The collection efficiency due to particle bounce (CE) was estimated at 0.5. A response factor for ammonium ($RIENH_4$) was set to 4.

4.3.3. Positive matrix factorization

Many approaches have been taken to analyze organics contribution to atmospheric aerosols. A comprehensive review of these approaches (Ulbrich et al., 2009) found that the recently developed real-time aerosol chemical speciation instruments based

on mass spectrometry, such as the ACSM, combined with Positive Matrix Factorization (PMF) has become the most commonly used technique for OA source apportioning. Briefly, PMF is an unmixing model in which a dataset is presumed to be the result of the linear combination of factors with constant profiles that have variable contributions (Paatero et al., 1994). All of the values in the profiles and contributions are constrained to be positive (Paatero, 1997). PMF is based on mass conservation and does not require information about factor profiles. The drawback of the method is that the number of factors for the model must be selected by the user, aiming to obtain a solution that in his eyes best explains the data (Ulbrich et al., 2009). This leads to subjective results (Engel-Cox et al., 2007; Reff et al., 2007). Further, multiple solutions can be obtained from distinct linear transformations or "rotations" of the factors during the matrix unmixing operation. Ulbrich et al. (2009) developed a procedure and computational tools to interpret the PMF analysis of organics spectra from aerosol mass spectrometers. This work follows their recommendations to choose a number of factors and a particular rotation and uses PMF2 v4.2 and PMF Evaluation Tool (PET) developed by them to execute the analysis and interpret the results. The ambiguities associated with choosing the number of factors and their best rotations are reported.

4.3.4. Aethalometer and black carbon apportionment

A 7-wavelentght Aethalometer was used to measure $PM_{2.5}$ BC concentrations. BC mass loadings reported by the Aethalometer are based on the optical absorption of aerosol deposited on a quartz fiber filter. The instrument measures the attenuation of 370, 470, 520, 590, 660, 880, and 950 nm wavelength radiation. The BC mass concentrations reported are estimated from the absorption coefficient calculated using the factory

defined mass absorption efficiencies for each wavelength. Data was recorded with a 2-min time resolution. The aerosol was sampled using a URG 2.5 µm cyclone with 3 L min^{-1} flow. The instrument was operated without the filter saver option to avoid high loadings in the filter tape. Possible artifacts in the attenuation measurements reported by the Aethalometer were corrected applying a previously published algorithm (Weingartner et al., 2003). A linear regression model, developed by Sandradewi et al. (2008), apportioned BC in ambient air using light absorption measurements made with 7-wavelength Aethalometers and provides information on the amount of BC from biomass burning and fossil fuel combustion. Briefly, the aerosol absorption coefficient (b_{abs}) is equal to $\lambda^{-\alpha}$, where λ is the wavelength and α is the source-specific wavelength dependence of BC light absorption, called the Angstrom exponent. The model uses b_{abs}, measured by the Aethalometer and, α to apportion biomass burning and fuel sources of BC. Values of α for biomass burning BC vary between 1.9 and 2.2 (Sandradewi et al., 2008). For fuel emissions, a value of 1±0.1 has been reported (Bond et al., 2006; Bond et al., 2004). We selected α values of 1 and 2 for fuel and biomass burning, respectively, and the measurements reported by the 7 - wavelength Aethalometer at 470 and 880 nm as recommended by Crippa et al. (2013), to apply the Sandradewi et al.,(2008) model to obtain BC apportionment to biomass burning and fuel.

4.3.5. Multi-angle absorption photometer

A multi-angle absorption photometer (MAAP) (Thermo Scientific Model 5012) (Petzold et al., 2004; Petzold et al., 2002) was used to measure $PM_{2.5}$ BC concentrations. MAAP measurements were made from November 2010 until March 2012 at FS and DX. Data was recorded with a 1 min time resolution. The MAAP determines BC mass

loadings based on aerosol optical absorption at 670 nm. It simultaneously measures radiation scattered back from and passing through a particle-loaded filter. It measures the scattered back radiation at three angles to account for its angular distribution created by the light-scattering properties of the aerosol components. The optical absorption coefficient of the aerosol is determined by a radiative transfer algorithm (Petzold et al., 2004; Petzold et al., 2002), which account for multiple scattering effects and absorption enhancement due to reflections from the filter. The aerosol measured with the MAAP was sampled using a URG 2.5 µm cyclone with 16.7L min^{-1} flow.

4.3.6. Tapered element oscillating microbalance

$PM_{2.5}$ mass concentrations were measured using a1400ab tapered element oscillating microbalance [TEOM] (R & P Thermo Scientific, Franklin, MA, US), operated at 50°C with a Nafion dryer (Permapure Inc. Toms River, NJ) and reporting data every minute.

4.3.7. Wind sector selective filter based measurements

Upwind and downwind wind sector selective filter based measurements of $PM_{2.5}$ metals, elemental and organic carbon (EC/OC) and ions were performed at FS and DX. The sector selective technique is based on controlling a vacuum pump to draw air in to the aerosol sampling system only when wind from a given sector is detected. Wind sectors where set between 0 and 90 degrees at FS and 180 and 270 at DX for upwind samples, and between 180 and 270 at FS and 0 and 90 degrees at DX for downwind samples (Figure 4.1). Sample periods varied between 8 at 42 hours and took up to 5 days to complete. Sample periods were recorded with an electronic timer that kept count of the time when the pump was operating. 42 samples were collected between June and

November 2011 (Appendix C). Two un-denuded particle composition monitors (PMCs) were constructed for this task. The systems drew 16.7 liters per minute (LPM) of air through 2.5 μm cutoff cyclones (URG, Chapel Hill, NC) on to Teflon (2 μm PP ring supported, Whatman Inc., Florham Park, NJ), Nylon (2 μm Nylasorb, Pall Corporation, Ann Arbor, MI) and quartz (AQFA4700, EMD Millipore Billerica, MA) 47 mm filters. The flow through each filter was controlled using three identical critical orifices (O'Keeffe Controls Co, Monroe, CT), set to guarantee that each filter collected a third of the flow. Aluminum filter holders were used for quartz filters and acrylic filter holders for Nylon and Teflon filters. Acetal copolymer 3/8" three way splitters and fittings (John Guest USA Inc., Fairfield, NJ) were used to secure the filter holders and the cyclones. Pieces of less than 2.5 cm of Tygon tubing were used to connect the three way splitter to the cyclone and to the aluminum filter holder and to the two acrylic filter holders. The flow was checked with a Bios DryCcal Defender 520 volumetric primary flow standard (Mesa Labs, Butler, NJ) at the beginning of each sampling period each time a filter was changed. Filter holders were washed with 17.8 megohm-cm deionized water between each use. Nitric acid washed Teflon filters were provided by the Wisconsin State Laboratory of Hygiene at the University of Wisconsin-Madison, where the metals were analyzed by inductively coupled plasma mass spectrometry (ICPMS). Filters were transported to the ASACA laboratory in Atlanta and back to Madison in Petri dishes sealed with Teflon tape. Filter holders were loaded with quartz, Teflon and Nylon filters at the ASACA laboratory and transported to and from the field in portable coolers, where they were kept refrigerated at 4℃ until analysis. Carbonaceous and ionic species analysis was made at the ASACA laboratory. Analysis of EC/OC was made using a thermal-

optical transmission carbon aerosol analyzer (Sunset labs, Tigard, OR) (Birch et al., 1996) following the NIOSH Method. Ionic species were analyzed using ion chromatography (IC) (Baumann et al., 2003). 4 lab blanks and 8 field transport blanks where collected. Lab blanks were kept in the lab with at same storage conditions than the samples. Field transport blanks were taken to the monitoring sites, placed in the PCMs for one hour and returned. Volume of air filtered was calculated by multiplying the flow in each filter (5.67 LPM) by the sampled time. Concentrations were obtained from mass data from analysis and volume data. Metals concentration data were disregarded if it was less than the average blanks concentration plus 2 standard deviations of the blanks. Uncertainties reported by analysis instruments were propagated to downwind upwind differences.

4.4. Results and Discussion

4.4.1. Organic and elemental carbon and Ions

OC species dominate aerosols composition north and south the rail yards (Table 4.1.and Appendix C). Concentrations found at both sites are consistent with previous measurements in and around Atlanta (Blanchard et al., 2011; Weber et al., 2007). The contribution of rail yards to EC concentrations as found by downwind upwind differences from filter based analysis confirms previous results from continuous measurements (Galvis et al., 2013). Rail yards were found responsible for an enhancement of about 0.6 $\mu g/m^3$ of EC concentrations during the filter based measurement campaign and for an annual average enhancement of 0.7 to 1 $\mu g/m^3$ of $PM_{2.5}$ BC concentrations during 2011. Similar enhancements in concentrations due to rail yard activity were reported by Cahill

et al. (2011), who observed a nighttime downwind upwind enhancement of 0.7 $\mu g/m^3$ of BC from the Roseville yard in California. A downwind upwind EC/OC ratio of 1.1 found from downwind – upwind concentrations is similar to ratios found in aerosols from combustion of diesel fuel in locomotives at different power levels with an average of 1.7 and a standard deviation of 1.8 (Sawant et al., 2007). However, uncertainty of OC and EC downwind upwind differences, derived from propagation of error, is high (68% and 217%). This is expected given the great variability in concentrations of these species, especially of OC. Uncertainties of downwind upwind differences were not reported in the previous work by Cahill et al. (2011).

Table 4.1. Organic and elemental carbon downwind and upwind of the Inman and Tilford rail yard between 06/20/2011 and 11/08/2011.

	OC* ($\mu g/m^3$)	EC* ($\mu g/m^3$)	EC/OC**
AVG DW	6.4 ± 0.9	1.3 ± 0.3	0.2±0.1
AVG UW	5.8 ± 0.9	0.7 ± 0.3	0.1±0.1
DW-UW	0.6 ± 1.3	0.6 ± 0.4	1.0±1.9

* Average ± uncertainty of samples.

** DW-UW EC/OC ratio was calculated as the fraction of the DW-UW EC over the DW-UW OC.

Concentrations of ions from wind sector selective filter based measurements indicated no evident differences between downwind and upwind locations and will not be discussed further. A table with these measurements can be found in Appendix C.

4.4.2. Metals

Average measured concentrations of metals at DX and FS (Appendix C) are comparable to measurements done during 2011 by the SEARCH network at Jefferson Street site near the rail yards (EPRI, 2012). Of the 49 metals analyzed, Sulfur (S), Vanadium (V), Antimony (Sb), Lead (Pb) and Arsenic(As) and Barium (Ba) have more

than 50% of the samples with signals greater than the average blank concentration minus twice the standard deviation of the blanks. Ba, Sb and Pb are commonly emitted in welding processes (EPA, 1994; NSRP, 2002) and likely are coming from Norfolk Southern's rail flash welding and track assembly facility at Inman yard.

Table 4.2. Metals downwind and upwind of the Inman and Tilford rail yard between 06/20/2011 and 11/08/2011.

	S* (ng/m^3)		V* (ng/m^3)		Sb* (ng/m^3)		Pb* (ng/m^3)		As* (ng/m^3)		Ba* (ng/m^3)	
AVG DW	420.84	±42.8	0.42	±0.06	0.47	±0.03	1.11	±0.10	0.44	±0.22	2.61	±0.28
AVG UW	392.16	±39.2	0.37	±0.07	0.38	±0.04	0.60	±0.06	0.40	±0.16	1.76	±0.23
DW-UW	28.7	±58.0	0.05	±0.09	0.09	±0.07	0.51	±0.15	0.04	±0.35	0.85	±0.35

*Average ± uncertainty of samples.

4.4.3. ACSM results validation

Average aerosol concentrations during the period measured were 7.4 µg/m^3, 1.25 µg/m^3, 6.45 µg/m^3 for NR PM_1 ACSM, MAAP BC and TEOM $PM_{2.5}$ respectively. Given that NR PM_1 excludes aerosols with aerodynamic diameters greater than 1 µm, BC and other species, NR PM1 concentration should be less than $PM_{2.5}$ concentration, though TEOM operation at 50˚C causes the loss of volatile species such as ammonium nitrate and some organics (Eatough et al., 2003; Hering et al., 2004) which can partially account for the difference between the measurements. Average nitrate concentration measured by the ASACA network between 11/22/2011 and 12/12/2011 were 0.6 µg/m^3. Average nitrate concentration measured by the SEARCH network at the Jefferson Street site near the rail yard complex between 11/22/2011 and 12/12/2011 was 0.7 µg/m^3. The correlation coefficient between NR PM_1+ BC vs. TEOM $PM_{2.5}$ is 0.42 (Figure 2a). Bias is within the expected amount for the ACSM (Ng et al., 2011) and the MAAP (Petzold et

al., 2002; Petzold et al., 2004). There are several periods of time in which the ACSM reports higher loadings than the TEOM. There are also a few short periods of time with high loadings recorded by the TEOM, but not the ACSM or the MAAP (Figure 2a).Vibration, humidity and temperature changes can cause noise in the TEOM measurements. Comparing $PM_{2.5}$ daily averages reported by the TEOM and BC+NR PM_1 averages reported by the MAAP and the ACSM to daily $PM_{2.5}$ FRM measured by GAEPD (2013) and SEARCH (2012) is evident that TEOM measurements are biased low whereas MAAP+ACSM measurements agree with FS $PM_{2.5}$ FRM (R^2=0.96) and JS $PM_{2.5}$ FRM (R^2=0.93) and (Figure 2b).

a)

b)

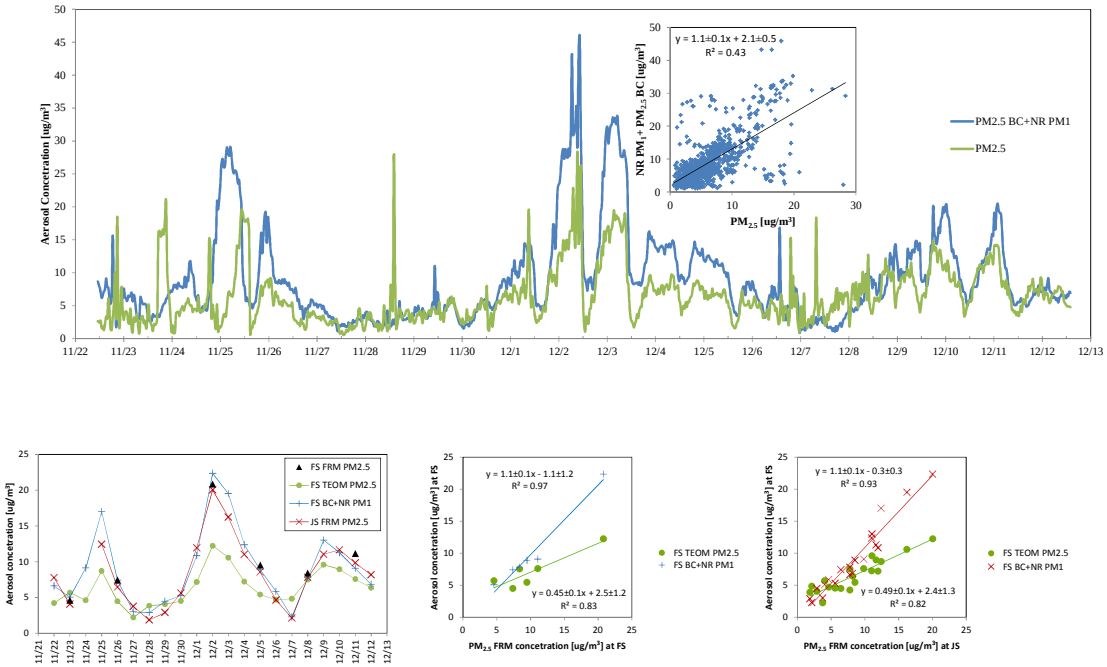

Figure 4.2. Time series and regression comparisons of a) 33 minute average concentrations of TEOM $PM_{2.5}$ and BC+NR PM_1 and b) daily averages of TEOM $PM_{2.5}$, FRM $PM_{2.5}$ and $PM_{2.5}$ BC+NR PM_1 at FS and FRM $PM_{2.5}$ at JS.

Sulfate and nitrate concentrations reported for the SEARCH network at the Jefferson Street site (EPRI, 2012) agree well (R^2 = 0.81 and R^2 = 0.88 respectively) with

ACSM measurements at FS, but they are biased low, approximately %35 and 20% respectively (Figure 4.3.). As expected NR PM_1 ACSM sulfate and nitrate measurements are slightly lower than filter based $PM_{2.5}$ sulfate and nitrate.

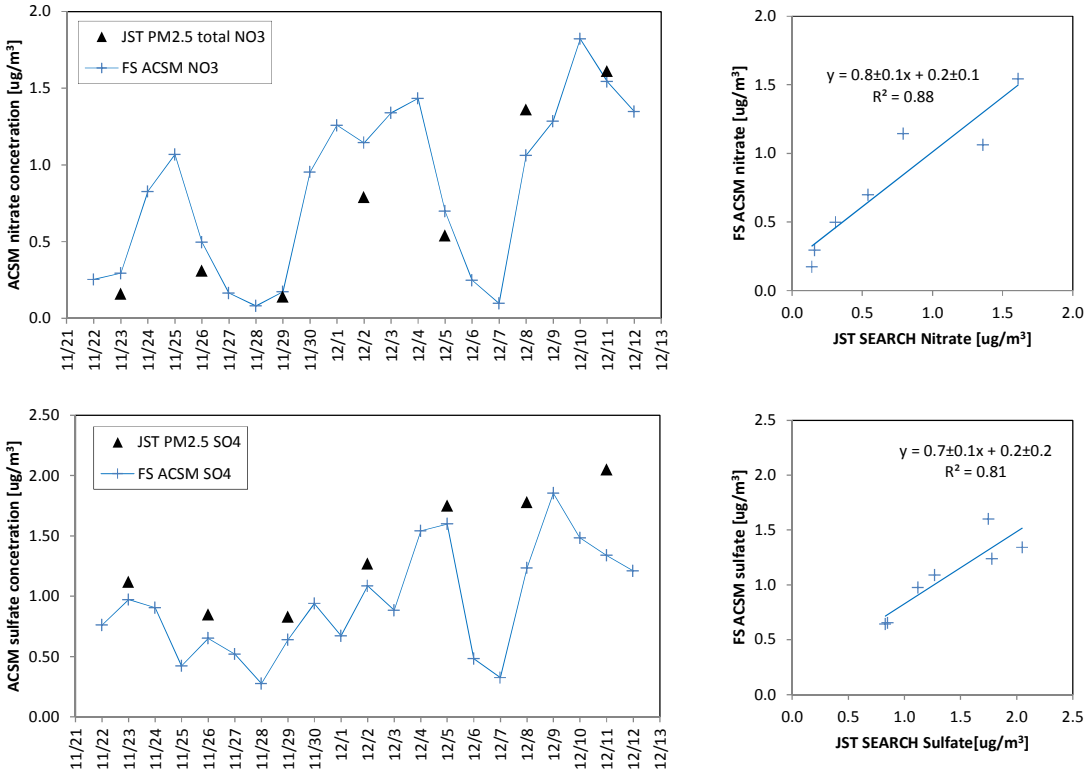

Figure 4.3. Daily average sulfate and nitrate concentrations reported by ACSM at FS vs. SEARCH at Jefferson street site.

4.4.4. Organics PMF solution

Organics ACSM spectra were further deconvoluted using PMF. A three 3 factor solution (Figure 4.4) was chosen based on the fraction of the signal represented by tracers at specific mass-to-charge (m/z) ratios compared to reference mass spectra, the change in residuals and the comparison of the time series of the factors and of other observed species. Uncertainty of the selected factor solution was investigated using a seed parameter equal to 1 and no bootstrapping was run. Different rotational forcing (FPEAK)

parameters were tested but no evidence was found that a FPEAK value different from 0 was needed. The criteria listed by Zhang et al. (2012) were followed to choose the solution presented in this work. The sum of the weighed squared residuals (*Q*) for a 2 factor solution, a 3 factor solution and a 4 factor solution were 2.095%, 1.3% and 0.05 % respectively. No new information was gained from the mass spectra when considering more than three factors and the split of factors was evident. The residual was significantly smaller when considering 3 factors instead of 2. Marginal diminishing of the residual was gained when including a fourth factor and above.

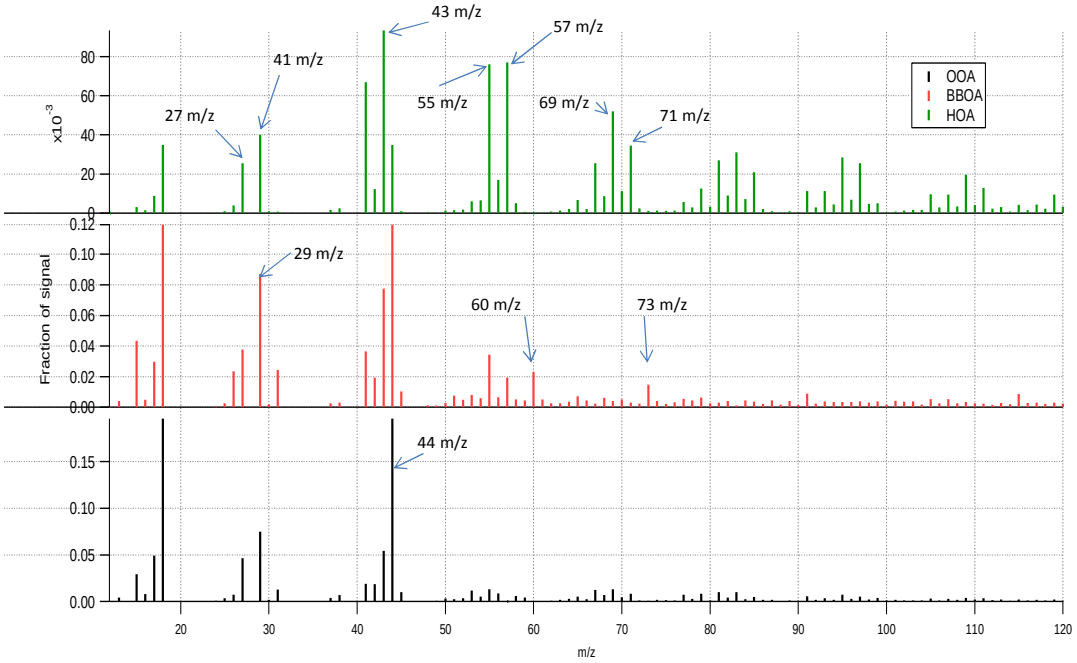

Figure 4.4. PMF 3 factor solution mass spectra. Tracers are marked for each factor.

A first factor was identified as hydrocarbon like organic aerosols (HOA). It showed specific tracers at 27, 41, 43, 55, 57, 69, 71 m/z and other aliphatic hydrocarbon fragments (Canagaratna et al., 2004; Aiken et al., 2010; Ng et al., 2010). A second factor was identified as primary biomass burning organic aerosol (BBOA). It showed specific tracers at 29, 60 and 73 m/z, which are associated to fragments of sugars such as

levoglucosan (Alfarra et al., 2007; Ng et al., 2010). The last factor was identified as oxidized organic aerosol (OOA), a highly oxygenated factor indicated by the peak associated with the tracer CO_2^+ at 44 m/z (Aiken et al., 2010; Ng et al., 2010).

4.4.2.1. Organic factors time series

The HOA time series shows concentration spikes that occur in short periods of time. Some of these spikes are seen in HOA time series, but not in BBOA or OOA time series, suggesting they could come from fresh emissions from mobiles sources (Figure 4.5. marked in blue). Some peaks are simultaneously present in both BBOA and HOA time series, suggesting a fresh biomass burning source in the vicinity (Figure 4.5. marked in orange). Features shared by HOA, BBOA and OOA time series (Figure 4.5. marked in light green) suggest distant burn sources, far enough for oxidized organic aerosols to be important. One interesting feature of the time series is how some of the peaks look like the top has been cut off; the loading will increase and then remain at that level for some time. These plateau shapes seem to begin and end in mid-afternoon and could indicate impact from and specific nearby source, but further research is needed to investigate the cause of this feature in the time series.

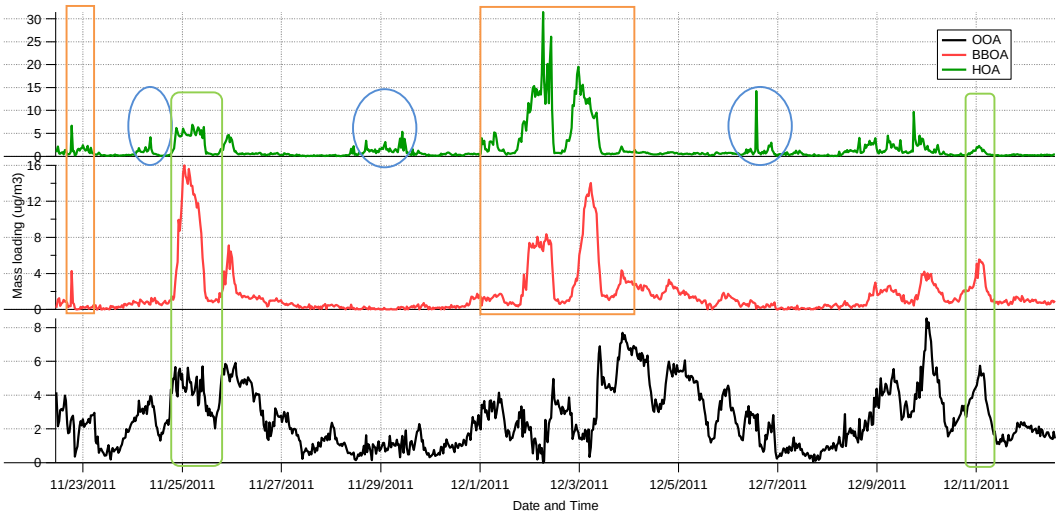

Figure 4.5. Time series of organic factors.

FS ACSM HOA correlate with FS MAAP $PM_{2.5}$ BC (R^2= 0.94) (Figure 4.6a), which is expected given that both relate to primary emissions. Analysis supporting their rail yard origin is discussed later. FS ACSM BBOA correlate (R^2= 0.97) with potassium $PM_{2.5}$ filter based measurements (Figure 4.6b) at the Jefferson Street SEARCH site (EPRI, 2012). Potassium is regarded as a tracer for biomass burning (Watson et al., 2001). ACSM OOA correlate well (R^2= 0.82) with $PM_{2.5}$ TOR OC filter based measurements (Figure 4.6c) at the Jefferson Street SEARCH site (EPRI, 2012). Most of organic carbon in Atlanta is secondary in origin (Lin et al., 2013). Correlation between ACSM OOA and $PM_{2.5}$ TOR OC suggests a secondary origin for OOA . FS ACSM OOA correlates with FS ACSM sulfates and nitrates (R^2= 0.3 and 0.6 respectively). Given that NO_3 is more volatile than SO_4, this suggests that part of the OOA is semi-volatile (SV-OOA), as opposed to low-volatile (LV-OOA), or may be formed from sources that also emit nitrate precursors (NOx).

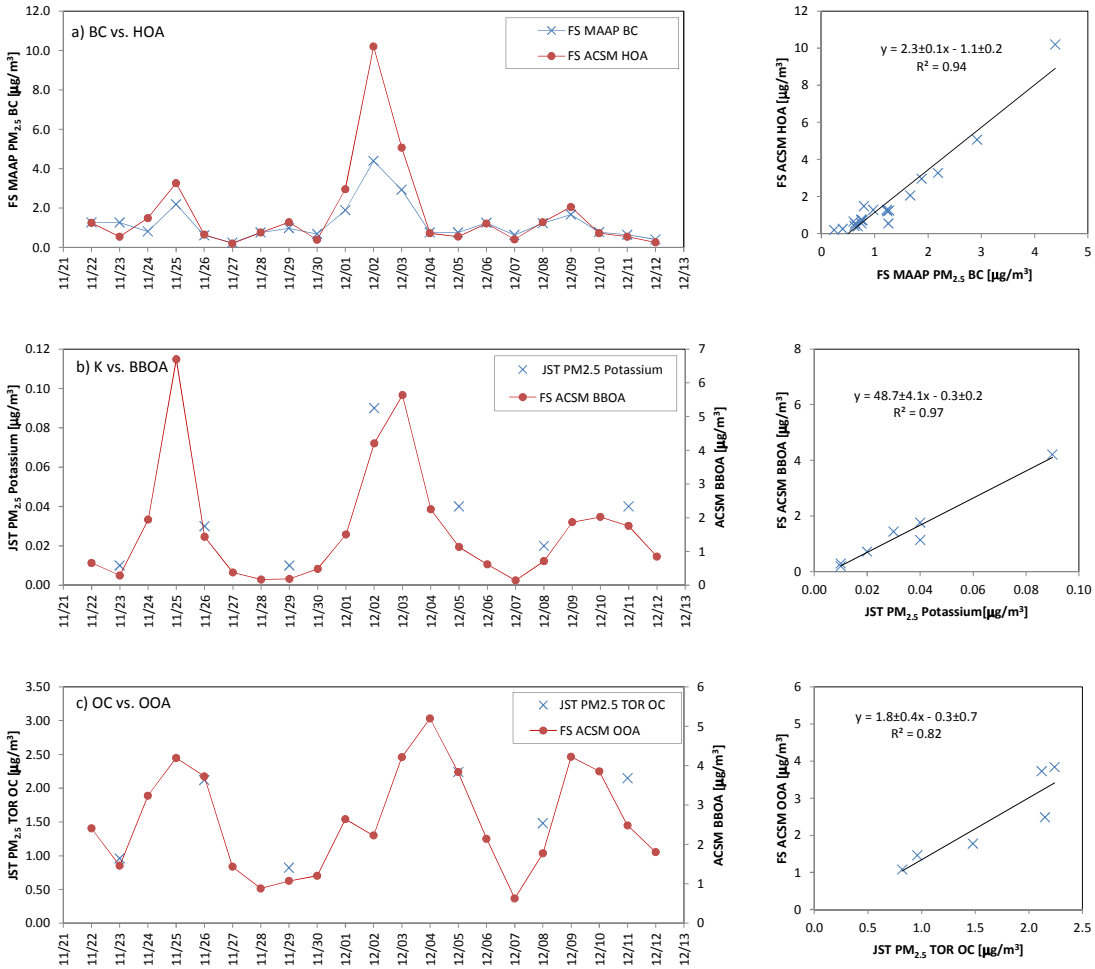

Figure 4.6. Daily averages of organic factor concentrations vs. other observed species near the rail yards. a) BC vs. HOA. b) K vs. BBOA and c) OC vs. OOA.

4.4.5. MAAP and 7-wavelength Aethalometer

We compared BC measurements made with the MAAP and the Aethalometer between 12/6/2011 and 12/12/2011. The MAAP measures BC concentration by determining aerosol optical absorption at 670 nm. The MAAP was designed to avoid shadowing and scattering artifacts (Petzold et al., 2004; Petzold et al., 2002). Hourly averages of BC concentrations measured at 670 nm by the MAAP and at 660 nm by the Aethalometer correlated well (R^2=0.64), with a small bias (Figure 4.7.).

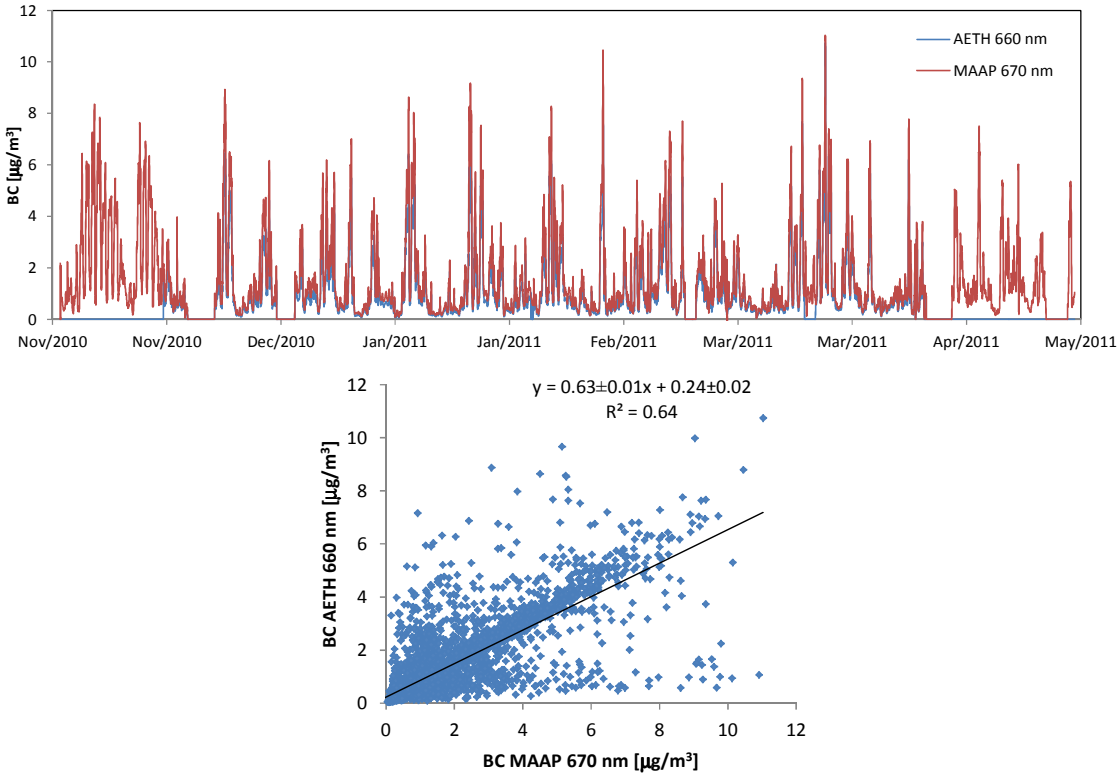

Figure 4.7. BC from MAAP at 670 nm vs. BC from Aethalometer at 660 nm.

4.4.6. Black carbon speciation

Attenuation measurements done with the Aethalometer are thought to have artifacts produced by the shadowing effect of impacted particles at high mass accumulation and by scattering from the filter fibers. Corrections for these artifacts were implemented applying a previously published algorithm (Weingartner et al., 2003). With the corrected attenuation data, $PM_{2.5}$ BC mass was apportioned using the model proposed by Sandradewi et al. (2008) and applied by Crippa et al. (2013). The model resolves the contribution of biomass burning (BCb) and fuel combustion (BCf) to BC, using the dissimilarity in the wavelength-dependent light absorption of these two sources. $PM_{2.5}$ BC apportionment obtained from Aethalometer measurements was compared with PM_1 OA factors from ACSM measurements. Agreement of BCb with BBOA and of BCf with

HOA respectively was found (Figure 4.8. and Table 4.3.). Correlation between NR PM_1 OA factors and $PM_{2.5}$ BC optical apportionment results is comparable to results obtained by Crippa et al. (2013), for the metropolitan area of Paris during winter 2010. The ratio of HOA to BCf (Table 4.1) is also similar to the ratio reported by Crippa et al. (2013). The average HOA to BCf and BBOA to BCb observed ratios are comparable to average organic matter (OM) to BC ratios from smog chamber experiments for diesel vehicle emissions (0.28±0.15)(Chirico et al., 2011) and for a modern log wood burners (0.12±0.04) (Heringa et al., 2011), respectively.

Table 4.3. HOA vs. BCf and BBOA vs. BCb regression results.

	ACSM NR PM_1 HOA vs. Aethalometer $PM_{2.5}$ BCf			ACSM NR PM_1 BBOA vs. Aethalometer $PM_{2.5}$ BCb		
This Study	Slope	0.3±0.02		Slope	0.10±0.004	
	Intercept	0.2±0.03		Intercept	0.02±0.01	
	R^2	0.50		R^2	0.71	
Crippa et al. (2013)	Slope	0.37	0.61	Slope	3.16	3.62
	Intercept	0.33	-0.12	Intercept	0.11	-0.12
	R^2	0.48	0.77	R^2	0.73	0.59

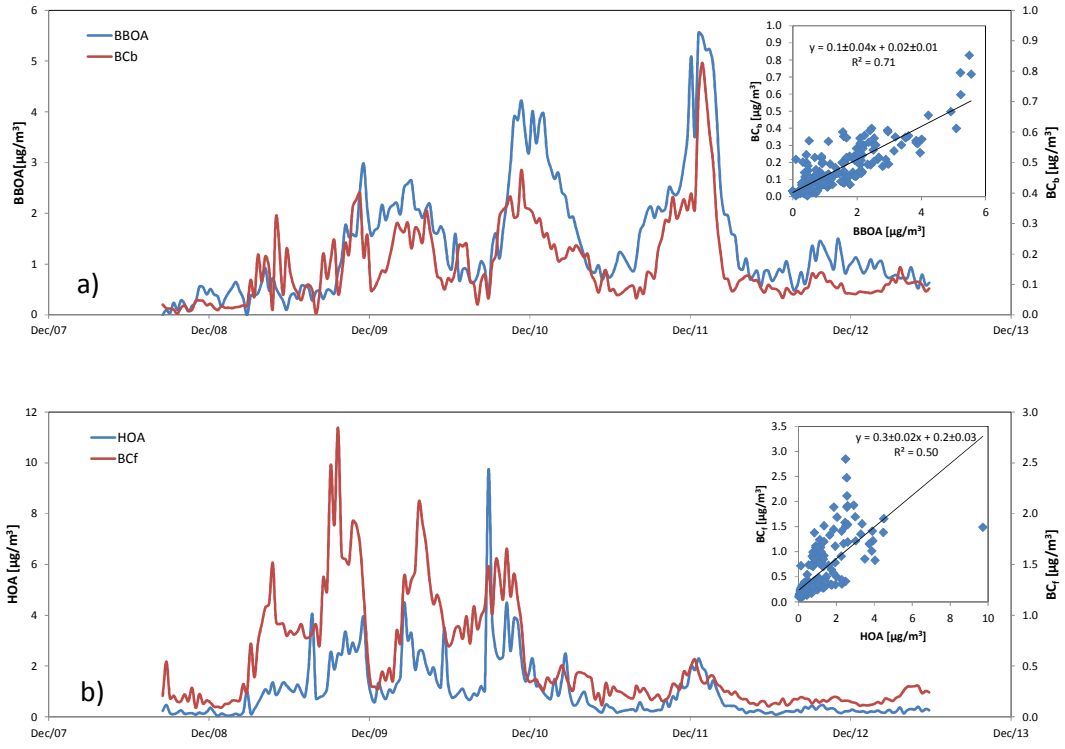

Figure 4.8. Black carbon apportionment and ACSM results comparison. a) Aethalometer $PM_{2.5}$ BCb vs. ACSM NR PM_1 BBOA and b) Aethalometer $PM_{2.5}$ BCf vs. ACSM NR PM_1 HOA.

Measurements indicate that during the period when the ACSM and the Aethalometer were simultaneously measuring (December 7 to 12, 2011), FS was significantly impacted by biomass burning aerosols. BCb and BCf accounted for 28% and 72% of the black carbon mass respectively. Longer term measurements during fall and winter 2010-2011 and fall and winter 2011-2012 (Figure 4.9.) indicate that the site is impacted 82% by BCf and 18% by BCb with average ± standard deviation of 0.9±0.7 µg/m^3 BCf and 0.2±0.1 µg/m^3 BCb, respectively.

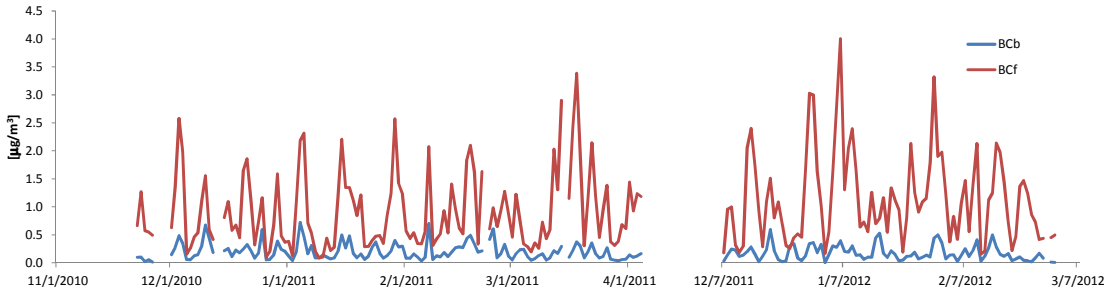

Figure 4.9. Black carbon apportionment during fall and winter 2010-2011 and fall and winter 2011-2012 at FS.

4.4.7. Chemical species and wind direction.

From November 22 to December 12, the mass NR PM_1 aerosols at FS was mostly organic (72%), with few nitrates (11%) , sulfates (12%) and ammonia (5%). Organics were composed of 31% OOA, 20% HOA and 21 % BBOA. A majority of NR PM_1 mass being organics has also has been observed at other Atlanta sites during different seasons (Budisulistiorini et al., 2013; Lin et al., 2013; Xu et al., 2013).

Concentration roses were plotted to identify the direction from which the different chemical species of the aerosols originated (Figure 4.10.). Temporal resolution of data plotted was 33 minutes. Roses show the direction from where the wind was blowing and the average pollutant concentration from that direction during the monitoring campaign. The $PM_{2.5}$ rose is slightly skewed to the northeast and northwest quadrants but without sharply defined directions suggesting a diverse set of sources. The highest contribution to $PM_{2.5}$ came from the north (up to 9 $\mu g/m^3$average). The BC rose shows two defined lobes, one from the southwest quadrant with average concentrations impacts up to 2 $\mu g/m^3$, where the rail yards and Marietta street are located, and another from the north and north northeast quadrants with average concentrations impact up to 1.5 $\mu g/m^3$. NR PM_1 Organics come mainly from the northeast quadrant with average concentration

impacts up to 10 µg/m^3. NR PM_1 OOA dominates the organics and shares their northeast quadrant origin with up to 6 µg/m^{3}of average concentration. NR PM_1 HOA concentrations have main features southwest (up to 2 µg/m^3 on average) and north northeast (up to 1.5 µg/m^3 on average), similar to what was observed in $PM_{2.5}$ BC, which is expected given that those two components are strongly correlated (Figure 4.6a). Emissions from the rail yards and from Marietta Blvd are likely the source of the $PM_{2.5}$ BC and NR PM_1 HOA southwest concentrations. NR PM_1BBOA concentrations come from the northeast quadrant (up to 2.5 µg/m^3 average concentration). Nitrates show a defined lobe north northeast with average concentrations up to 3 µg/m^3. Sulfates and ammonia impact the FS mainly from the north, sulfate being more uniformly distributed in all directions.

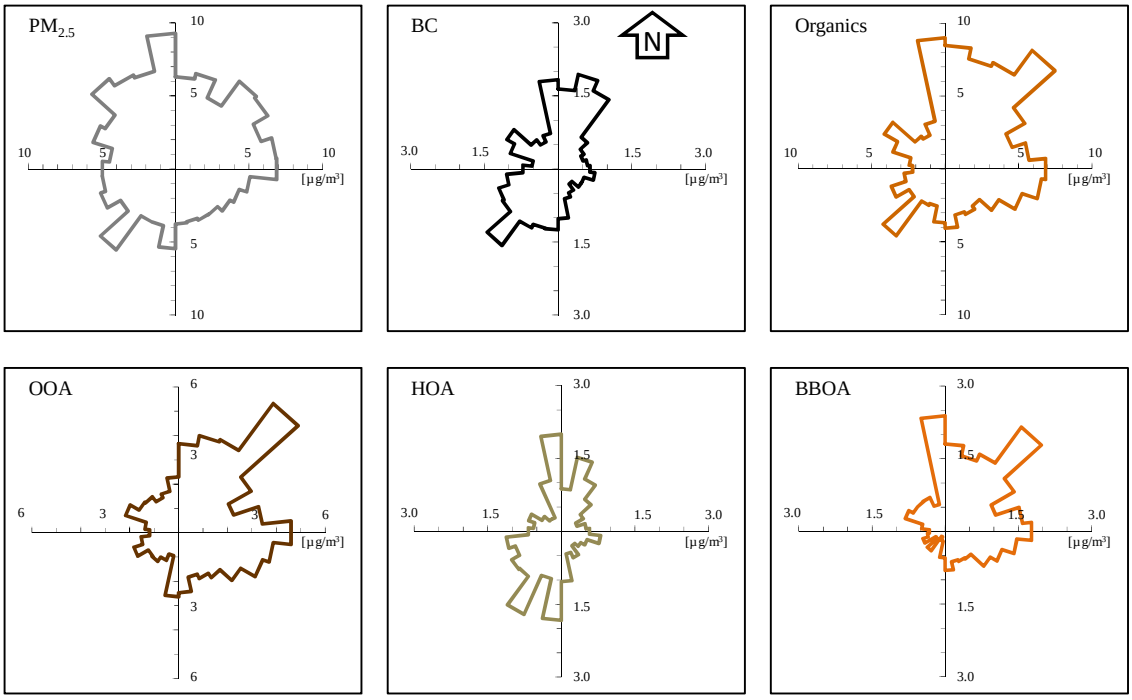

Figure 4.10. Concentration roses of chemical species at FS during the winter 2011

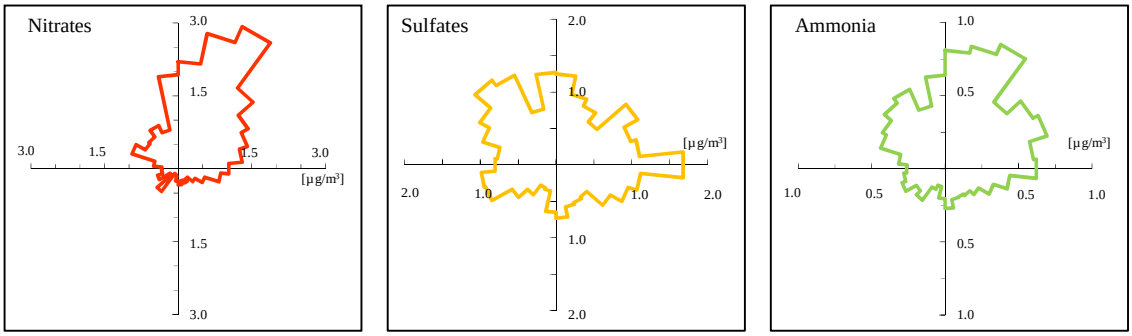

Figure 4.10. (continued). Concentration roses of chemical species.

The rose of $PM_{2.5}$ BCf speciation results, obtained with monitoring data from the fall and winter 2010-2011 and the fall and winter 2011-2012 indicate that $PM_{2.5}$ BCf comes from the direction where the rail yards and Marietta Blvd are located (Figure 4.11). $PM_{2.5}$ BCf rose is similar to annual average $PM_{2.5}$ BC rose found previously at FS, and together with annual average $PM_{2.5}$ BC rose at DX point in the direction of the rail yards (Galvis et al., 2013). Average BCf concentrations from the southwest quadrant are 1.2 µg/m^3, 60 % greater than the average over all directions. This result parallels annual average $PM_{2.5}$ BC downwind upwind concentration differences obtained previously, 1.0 µg/m^3 at FS and 0.7 µg/m^3 at DX (Galvis et al., 2013) and are similar to annual average impact of $PM_{2.5}$ BC concentrations coming from the rail yards and on road mobile sources estimated by dispersion modeling, 0.6 and 0.7 µg/m^3 at FS and DX respectively (Chapter 3). BCb optical apportionment results indicate biomass burning impacts distributed evenly from the east and southwest quadrants.

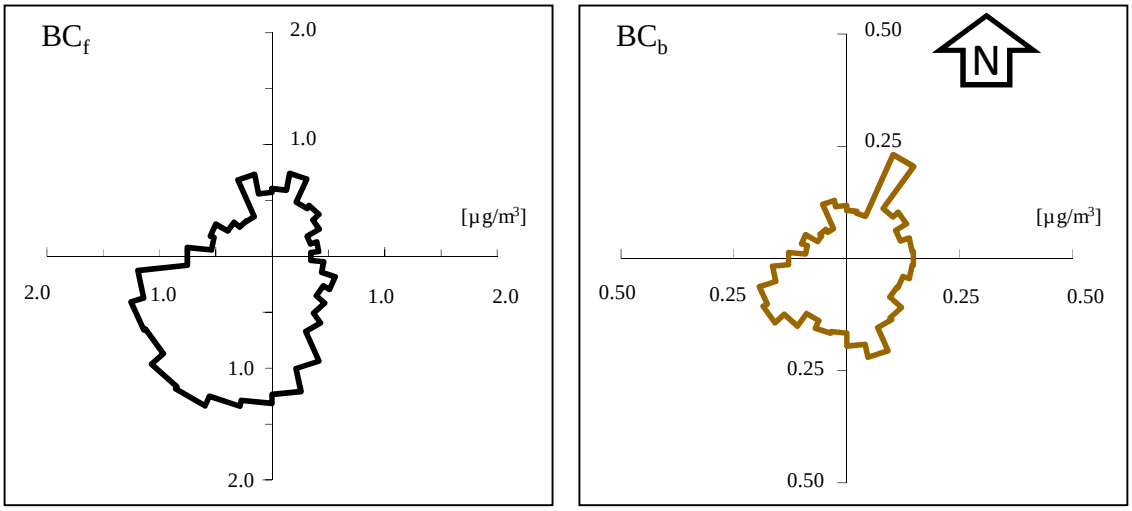

Figure 4.11. Concentration roses of BC speciation results

4.5.References

Aiken, A. C., de Foy, B., Wiedinmyer, C., DeCarlo, P. F., Ulbrich, I. M., Wehrli, M. N., Szidat, S., Prevot, A. S. H., Noda, J., Wacker, L., Volkamer, R., Fortner, E., Wang, J., Laskin, A., Shutthanandan, V., Zheng, J., Zhang, R., Paredes-Miranda, G., Arnott, W. P., Molina, L. T., Sosa, G., Querol, X., and Jimenez, J. L. 2010. Mexico city aerosol analysis during MILAGRO using high resolution aerosol mass spectrometry at the urban supersite (T0) – Part 2: Analysis of the biomass burning contribution and the non-fossil carbon fraction. Atmos. Chem. Phys. no. 10 (12):5315-5341. doi: 10.5194/acp-10-5315-2010.

Alfarra, M. R., Prevot, A. S. H., Szidat, S., Sandradewi, J., Weimer, S., Lanz, V. A., Schreiber, D., Mohr, M., and Baltensperger, U. 2007. Identification of the Mass Spectral Signature of Organic Aerosols from Wood Burning Emissions. Environmental Science & Technology no. 41 (16):5770-5777. doi: 10.1021/es062289b.

Baumann, K., Ift, F., Zhao, J. Z., and Chameides, W. L. 2003. Discrete measurements of reactive gases and fine particle mass and composition during the 1999 Atlanta Supersite Experiment. Journal of Geophysical Research: Atmospheres no. 108 (D7):8416. doi: 10.1029/2001JD001210.

Birch, M. E., and Cary, R. A. 1996. Elemental carbon-based method for occupational monitoring of particulate diesel exhaust: methodology and exposure issues. Analyst no. 121 (9):1183-90.

Blanchard, C. L., Hidy, G. M., Tanenbaum, S., and Edgerton, E. S. 2011. NMOC, ozone, and organic aerosol in the southeastern United States, 1999–2007: 3. Origins of

organic aerosol in Atlanta, Georgia, and surrounding areas. Atmospheric Environment no. 45 (6):1291-1302. doi: http://dx.doi.org/10.1016/j.atmosenv.2010.12.004.

Bond, T., and Bergstrom, R. 2006. Light Absorption by Carbonaceous Particles: An Investigative Review. Aerosol Science and Technology no. 40 (1):27-67. doi: citeulike-article-id:438043.doi: 10.1080/02786820500421521.

Bond, T. C., Streets, D. G., Yarber, K. F., Nelson, S. M., Woo, J.-H., and Klimont, Z. 2004. A technology-based global inventory of black and organic carbon emissions from combustion. Journal of Geophysical Research: Atmospheres no. 109 (D14):D14203. doi: 10.1029/2003JD003697.

Butler, A. J., Andrew, M. S., and Russell, A. G. 2003. Daily sampling of PM2.5 in Atlanta: Results of the first year of the Assessment of Spatial Aerosol Composition in Atlanta study. Journal of Geophysical Research: Atmospheres no. 108 (D7):8415. doi: 10.1029/2002JD002234.

Budisulistiorini, S. H., Canagaratna, M. R., Croteau, P. L., Marth, W. J., Baumann, K., Edgerton, E. S., Shaw, S. L., Knipping, E. M., Worsnop, D. R., Jayne, J. T., Gold, A., and Surratt, J. D. 2013. Real-time continuous characterization of secondary organic aerosol derived from isoprene epoxydiols in downtown atlanta, georgia, using the aerodyne aerosol chemical speciation monitor. Environ Sci Technol no. 47 (11):5686-94. doi: 10.1021/es400023n.

Cahill, T. A., Cahill, T. M., Barnes, D. E., Spada, N. J., and Miller, R. 2011. Inorganic and Organic Aerosols Downwind of California's Roseville Railyard. Aerosol Science and Technology no. 45 (9):1049-1059. doi: 10.1080/02786826.2011.580796.

Canagaratna, M. R., Jayne, J. T., Ghertner, D. A., Herndon, S., Shi, Q., Jimenez, J. L., Silva, P. J., Williams, P., Lanni, T., Drewnick, F., Demerjian, K. L., Kolb, C. E., and Worsnop, D. R. 2004. Chase Studies of Particulate Emissions from in-use New York City Vehicles. Aerosol Science and Technology no. 38 (6):555-573. doi: 10.1080/02786820490465504.

Chirico, R., Prevot, A. S. H., DeCarlo, P. F., Heringa, M. F., Richter, R., Weingartner, E., and Baltensperger, U. 2011. Aerosol and trace gas vehicle emission factors measured in a tunnel using an Aerosol Mass Spectrometer and other on-line instrumentation. Atmospheric Environment no. 45 (13):2182-2192. doi: http://dx.doi.org/10.1016/j.atmosenv.2011.01.069.

Crippa, M., DeCarlo, P. F., Slowik, J. G., Mohr, C., Heringa, M. F., Chirico, R., Poulain, L., Freutel, F., Sciare, J., Cozic, J., Di Marco, C. F., Elsasser, M., Nicolas, J. B., Marchand, N., Abidi, E., Wiedensohler, A., Drewnick, F., Schneider, J., Borrmann, S., Nemitz, E., Zimmermann, R., Jaffrezo, J. L., Prévôt, A. S. H., and Baltensperger, U. 2013. Wintertime aerosol chemical composition and source apportionment of the organic fraction in the metropolitan area of Paris. Atmos. Chem. Phys. no. 13 (2):961-981. doi: 10.5194/acp-13-961-2013.

Eatough, D. J., Long, R. W., Modey, W. K., and Eatough, N. L. 2003. Semi-volatile secondary organic aerosol in urban atmospheres: meeting a measurement challenge. Atmospheric Environment no. 37 (9–10):1277-1292. doi: http://dx.doi.org/10.1016/S1352-2310(02)01020-8.

Electric Power Research Institute [EPRI]. 2012. The Southeastern Aerosol Research and Characterization Network: SEARCH, [accessed Oct 2012]. Available from http://www.atmospheric-research.com/studies/search/SEARCHFactSheet.pdf.

Engel-Cox, J. A., and Weber, S. A. 2007. Compilation and assessment of recent positive matrix factorization and UNMIX receptor model studies on fine particulate matter source apportionment for the eastern United States. J Air Waste Manag Assoc no. 57 (11):1307-16.

Galvis, B., Bergin, M., and Russell, A. G. 2013. Fuel-based fine particulate and black carbon emission factors from a railyard area in Atlanta. Journal of the Air & Waste Management Association (63):618–628.

Georgia Environmental Protection Division [GAEPD]. 2013. Ambient Monitoring Program Air Quality Database, [accessed Feb 2013]. Available from http://www.georgiaair.org/amp/amp_query.html.

Hering, S., Fine, P. M., Sioutas, C., Jaques, P. A., Ambs, J. L., Hogrefe, O., and Demerjian, K. L. 2004. Field assessment of the dynamics of particulate nitrate vaporization using differential TEOM® and automated nitrate monitors. Atmospheric Environment no. 38 (31):5183-5192. doi: http://dx.doi.org/10.1016/j.atmosenv.2004.02.066.

Heringa, M. F., DeCarlo, P. F., Chirico, R., Tritscher, T., Dommen, J., Weingartner, E., Richter, R., Wehrle, G., Prévôt, A. S. H., and Baltensperger, U. 2011. Investigations of primary and secondary particulate matter of different wood combustion appliances with a high-resolution time-of-flight aerosol mass

spectrometer. Atmos. Chem. Phys. no. 11 (12):5945-5957. doi: 10.5194/acp-11-5945-2011.

Kanakidou, M., Seinfeld, J. H., Pandis, S. N., Barnes, I., Dentener, F. J., Facchini, M. C., Van Dingenen, R., Ervens, B., Nenes, A., Nielsen, C. J., Swietlicki, E., Putaud, J. P., Balkanski, Y., Fuzzi, S., Horth, J., Moortgat, G. K., Winterhalter, R., Myhre, C. E. L., Tsigaridis, K., Vignati, E., Stephanou, E. G., and Wilson, J. 2005. Organic aerosol and global climate modelling: a review. Atmos. Chem. Phys. no. 5 (4):1053-1123. doi: 10.5194/acp-5-1053-2005.

Lin, Y. H., Knipping, E. M., Edgerton, E. S., Shaw, S. L., and Surratt, J. D. 2013. Investigating the influences of SO2 and NH3 levels on isoprene-derived secondary organic aerosol formation using conditional sampling approaches. Atmos. Chem. Phys. Discuss. no. 13 (2):3095-3134. doi: 10.5194/acpd-13-3095-2013.

National Cooperative Freight Research Program [NCFRP]. 2010. Representing Freight in Air Quality and Greenhouse Gas Models, [accessed Novemeber 2011]. Available from http://onlinepubs.trb.org/onlinepubs/ncfrp/ncfrp_rpt_004.pdf.

Ng, N. L., Canagaratna, M. R., Zhang, Q., Jimenez, J. L., Tian, J., Ulbrich, I. M., Kroll, J. H., Docherty, K. S., Chhabra, P. S., Bahreini, R., Murphy, S. M., Seinfeld, J. H., Hildebrandt, L., Donahue, N. M., DeCarlo, P. F., Lanz, V. A., Prévôt, A. S. H., Dinar, E., Rudich, Y., and Worsnop, D. R. 2010. Organic aerosol components observed in Northern Hemispheric datasets from Aerosol Mass Spectrometry. Atmos. Chem. Phys. no. 10 (10):4625-4641. doi: 10.5194/acp-10-4625-2010.

Ng, N. L., Herndon, S. C., Trimborn, A., Canagaratna, M. R., Croteau, P. L., Onasch, T. B., Sueper, D., Worsnop, D. R., Zhang, Q., Sun, Y. L., and Jayne, J. T. 2011. An Aerosol Chemical Speciation Monitor (ACSM) for Routine Monitoring of the Composition and Mass Concentrations of Ambient Aerosol. Aerosol Science and Technology no. 45 (7):780-794. doi: 10.1080/02786826.2011.560211.

National Shipbuilding Research Program [NSRP]. 2002. Characterization of welding emissions at naval shipbuilding support activities, [accessed November 2012]. Available from http://www.nsrp.org/3-Key_Deliverables/FY00_Welding_Emissions/FY00_Welding_Emissions-Mgmt-Appilicable.pdf.

Paatero, P., and Tapper, U. 1994. Positive matrix factorization: A non-negative factor model with optimal utilization of error estimates of data values. Environmetrics no. 5 (2):111-126. doi: 10.1002/env.3170050203.

Paatero, P. 1997. Least squares formulation of robust non-negative factor analysis. Chemometrics and Intelligent Laboratory Systems no. 37 (1):23-35. doi: http://dx.doi.org/10.1016/S0169-7439(96)00044-5.

Petzold, A., Hansgerd, K., and Schönlinner, M. 2002. Continuous Measurement of Atmospheric Black Carbon Using a Multi-angle Absorption Photometer. Environmental Science & Pollution Research (Special Issue 4):78-82.

Petzold, A., and Schönlinner, M. 2004. Multi-angle absorption photometry—a new method for the measurement of aerosol light absorption and atmospheric black carbon. Journal of Aerosol Science no. 35 (4):421-441. doi: http://dx.doi.org/10.1016/j.jaerosci.2003.09.005.

Reff, A., Eberly, S. I., and Bhave, P. V. 2007. Receptor modeling of ambient particulate matter data using positive matrix factorization: review of existing methods. J Air Waste Manag Assoc no. 57 (2):146-54.

Sandradewi, J., Prévôt, A. S. H., Szidat, S., Perron, N., Alfarra, M. R., Lanz, V. A., Weingartner, E., and Baltensperger, U. 2008. Using Aerosol Light Absorption Measurements for the Quantitative Determination of Wood Burning and Traffic Emission Contributions to Particulate Matter. Environmental Science & Technology no. 42 (9):3316-3323.

Sawant, A. A., Nigam, A., Miller, J. W., Johnson, K. C., and Cocker, D. R. 2007. Regulated and Non-Regulated Emissions from In-Use Diesel-Electric Switching Locomotives. Environmental Science & Technology no. 41 (17):6074-6083. doi: 10.1021/es061672d.

Ulbrich, I. M., Canagaratna, M. R., Zhang, Q., Worsnop, D. R., and Jimenez, J. L. 2009. Interpretation of organic components from Positive Matrix Factorization of aerosol mass spectrometric data. Atmos. Chem. Phys. no. 9 (9):2891-2918. doi: 10.5194/acp-9-2891-2009.

U.S. Environmental Protection Agency [EPA]. 1994. Development of Particulate and Hazardous Emission Factors for Electric Arc Welding (AP-42, Section 12.19) Revised Final Report, [accessed December 2012]. Available from http://www.epa.gov/ttn/chief/ap42/ch12/bgdocs/b12s19.pdf.

U.S. Environmental Protection Agency [EPA]. 2009. Dispersion Modeling to Support the Atlanta PM2.5 SIP Local Area Analysis, [accessed Aug 2012]. Available from http://www.gaepd.org/Files_PDF/plans/sip/Appendix_M_PM2.5_Dispersion_Modeling_at_FireSta8.pdf.

U.S. Environmental Protection Agency [EPA]. 2012. Report to Congress on Black Carbon, [accessed Dec 2012]. Available from http://www.epa.gov/blackcarbon/2012report/fullreport.pdf.

U.S. Environmental Protection Agency [EPA]. 2013. Technology Transfer Network (TTN) Air Quality System (AQS) Data Mart.

Watson, J. G., Chow, J. C., and Houck, J. E. 2001. PM2.5 chemical source profiles for vehicle exhaust, vegetative burning, geological material, and coal burning in Northwestern Colorado during 1995. Chemosphere no. 43 (8):1141-1151. doi: http://dx.doi.org/10.1016/S0045-6535(00)00171-5.

Weingartner, E., Saathoff, H., Schnaiter, M., Streit, N., Bitnar, B., and Baltensperger, U. 2003. Absorption of light by soot particles: determination of the absorption coefficient by means of Aethalometers. Journal of Aerosol Science no. 34 (10):1445-1463. doi: http://dx.doi.org/10.1016/S0021-8502(03)00359-8.

Weber, R. J., Sullivan, A. P., Peltier, R. E., Russell, A., Yan, B., Zheng, M., de Gouw, J., Warneke, C., Brock, C., Holloway, J. S., Atlas, E. L., and Edgerton, E. 2007. A study of secondary organic aerosol formation in the anthropogenic-influenced southeastern United States. Journal of Geophysical Research: Atmospheres no. 112 (D13):D13302. doi: 10.1029/2007JD008408.

World Health Organization [WHO]. 2012. Diesel Engine Exhaust Carcinogenic. Available from http://press.iarc.fr/pr213_E.pdf.

Xu, L., Guo H., King, L., Verma V., Weber, R. and Ng, N. L. A Study of Secondary Organic Aerosol Formation Influenced by Mixed Anthropogenic and Biogenic Emissions in Atlanta Area by High Resolution Mass Spectrometer. In preparation.

Zhang, Q., Jimenez, J. L., Canagaratna, M. R., Allan, J. D., Coe, H., Ulbrich, I., Alfarra, M. R., Takami, A., Middlebrook, A. M., Sun, Y. L., Dzepina, K., Dunlea, E., Docherty, K., DeCarlo, P. F., Salcedo, D., Onasch, T., Jayne, J. T., Miyoshi, T., Shimono, A., Hatakeyama, S., Takegawa, N., Kondo, Y., Schneider, J., Drewnick, F., Borrmann, S., Weimer, S., Demerjian, K., Williams, P., Bower, K., Bahreini, R., Cottrell, L., Griffin, R. J., Rautiainen, J., Sun, J. Y., Zhang, Y. M., and

Worsnop, D. R. 2007. Ubiquity and dominance of oxygenated species in organic aerosols in anthropogenically-influenced Northern Hemisphere midlatitudes. Geophysical Research Letters no. 34 (13):L13801. doi: 10.1029/2007GL029979.

Zhang, Q., Jimenez, J., Canagaratna, M., Ulbrich, I., Ng, N., Worsnop, D., and Sun, Y. 2012. Understanding atmospheric organic aerosols via factor analysis of aerosol mass spectrometry: a review. Analytical & Bioanalytical Chemistry no. 401 (10):3045-3067. doi: 10.1007/s00216-011-5355-y.

CHAPTER 5

CONCLUSIONS AND FUTURE RESEARCH

5.1. Conclusions

The impact of the aerosol emissions from Inman and Tilford rail yards on local concentrations of $PM_{2.5}$ was quantified. BC and $PM_{2.5}$ fuel-based emission factors from the rail yards were estimated by carbon balance using high time resolution monitoring. A composition profile of the rail yard aerosols was identified using chemical speciation techniques. A local BC and $PM_{2.5}$ emissions inventory was calculated and dispersion modeling was applied to assess the impact of the rail yards. Baseline information that will allow evaluation of the improvement in local air quality after locomotives operating in the rail yards are replaced by cleaner technologies was generated.

5.1.1. Fuel-based fine particulate and black carbon emission factors from a rail yard area in Atlanta.

In-use emission factors were quantified for diesel-electric engines and supporting activities at the Inman-Tilford rail yard complex in Atlanta, Georgia, using near-source high-time resolution monitoring of ambient concentrations at two monitoring sites.

Three approaches were used to estimate the emission factors. The delta approach was based on the downwind–upwind difference in concentrations, the wavelet approach analyzed spikes of black carbon (BC), fine particulate ($PM_{2.5}$), and carbon dioxide (CO_2) concentrations, and the regression approach utilized events of correlated BC and CO_2 concentrations. The delta and the wavelet approaches are thought to represent emissions of a broad mix of rail yard sources, whereas the regression approach is likely to represent emissions from switchers and line-haul engines passing by monitoring sites. The average

estimated emission factors from the delta and wavelet approaches are 0.6 ± 0.03 g of BC and 1.3 ± 0.1 g of $PM_{2.5}$ per gallon of diesel fuel burned at DX and 0.8 ± 0.03 g of BC and 1.7 ± 0.1 g of $PM_{2.5}$ per gallon of diesel fuel burned at FS. Emission factors estimated by the delta and wavelet approaches were statistically similar. The regression approach yielded an average emission factor of 2.8 ± 0.2 g of BC and 6.0 ± 0.5 g of $PM_{2.5}$ per gallon of fuel.

Rail yard emissions led to average enhancements of approximately 1.7 ± 0.1 $\mu g/m^3$ of $PM_{2.5}$ and approximately 0.85 ± 0.01 $\mu g/m^3$ of BC on an annual basis. Events of high BC concentrations, likely generated by switchers and line-haul engines in the rail yards, lead to a typical increase of about 3 $\mu g/m^3$ of BC and about 6 ppm of CO_2 above baseline.

Uncertainties not quantified in these results arise in part from variability in downwind–upwind differences, differences in emissions of the diverse zones within the rail yards, and influence of on-road mobile sources other than the ones of interest.

5.1.2. Impacts on fine particulate, black carbon and health of converting rail yard locomotives to lower emission technologies.

Local air quality impacts of $PM_{2.5}$ and BC emissions from line-haul and switcher activities at the Tilford and Inman rail yards were determined using dispersion modeling and site-specific emission characterization. Emissions from these activities were calculated with previously measured emission factors and reported fuel consumption for switchers and line-haul locomotives. Model evaluation found agreement between measured and simulated concentrations. Simulations found that line-haul and switcher activities the Tilford and Inman rail yards account for approximately for 0.5 $\mu g/m^3$ and

0.7 $\mu g/m^3$ of BC, and for approximately 1 $\mu g/m^3$ and 1.6 $\mu g/m^3$ of $PM_{2.5}$ at FS and DX respectively.

Retrofitting the switcher locomotives at the Tilford and Inman rail yards with new generator sets would reduce $PM_{2.5}$ and BC emissions by 9.4±0.9 and 3.8±0.6 t/year. Replacing traditional switchers with mother-slug sets would reduce $PM_{2.5}$ and BC emissions by 7.8±0.9 and 2.4±0.6 t/year. A reduction of approximately 0.4±0.1 $\mu g/m^3$ and 0.6±0.2 $\mu g/m^3$ of $PM_{2.5}$ and approximately 0.2±0.1 $\mu g/m^3$ and 0.3±0.1 $\mu g/m^3$ of BC at FS and DX respectively can be achieved. Greater reductions are located over the rail yards and to the northeast of the domain. Primary $PM_{2.5}$ and BC impacts from the rail yards are reduced by 38% and 29%.

The spatial distribution of annual average BC concentrations resembles the rail yard layout whereas distributions of $PM_{2.5}$ also show structure near industrial sources. BC concentrations of approximately 1 $\mu g/m^3$ outline the rail yards up to 2 km from the center of the complex. The spatial distribution of annual average $PM_{2.5}$ concentrations over the domain indicates hot spots, 2 - 5 $\mu g/m^3$ above background, at the center of the rail yard complex and near specific industrial sources. Higher impacts of $PM_{2.5}$ from the line-haul and switcher activities at the rail yards are located to the northeast of the domain. Annual average $PM_{2.5}$ concentrations from these activities at the rail yards are about 1 $\mu g/m^3$ up to 1 km northeast from the center of the complex. Modeling results indicate that at FS emissions from on-road mobile sources on Marietta Blvd. and other important surface roads in the domain have 1/4 and 1/3 of the impact of the emissions from rail yard line-haul and switchers sources on $PM_{2.5}$ and BC concentrations respectively.

Significant reductions in $PM_{2.5}$ and BC concentrations over the domain can be achieved by converting switcher locomotives at Inman and Tilford rail yards to lower emission technologies. Greatest reductions, about 1 $\mu g/m^3$, are located over the rail yards. Reductions extend mostly toward the northeast of the domain. Reductions in $PM_{2.5}$ concentrations can save approximately $24 million in annual avoided health costs and premature mortality. The measure has a positive net present value of about $179 million through a ten year period.

5.1.3. Aerosol chemical speciation and source impact analysis near rail yards

The Inman and Tilford rail yard complex in Atlanta, GA is an important source of hydrocarbon like organic aerosols (HOA) and black carbon from fuel (BCf). On average during the monitoring period they were been simultaneously measured, 1.2 and 1 $\mu g/m^3$ of HOA and BC_f respectively, came from the direction of the rail yards. Elemental carbon (EC) concentrations from wind sector selective filter based measurements confirm downwind upwind continuous measurements and dispersion modeling results for $PM_{2.5}$ BC, indicating that the rail yards were responsible for about 0.6 ± 0.4 $\mu g/m^3$ of EC during the filter based campaign at FS, for an annual average enhancement of 1 $\mu g/m^3$ of $PM_{2.5}$ BC concentrations during 2011 at FS, and for about $0.5\pm0.1 \mu g/m^3$ of BC from modeling results respectively. A ratio of BCf/HOA of 0.8 af FS from ACSM and Aethalometer measurements and a downwind upwind EC/OC ratio of 0.9 from wind sector selective measurements might be characteristic for rail yard emissions from the Atlanta complex. Wind sector selective filter based samples indicate that the rail yards is a source of Lead, Antimony and Barium likely from a welding facility located inside the complex. The main sources of oxidized organic aerosols (OOA), biomass burning organic aerosols

(BBOA), sulfates, nitrates and ammonia in the area of this study were not located in the direction of the rail yard complex.

5.2 Future research

Assessment of changes in air quality after the implementation of cleaner technologies at the Inman and Tilford rail yard complex is a key topic for future research to complement the present work. Approaches developed here could be applied and extended to address this matter. Fuel-based emission factors for the new technologies should be obtained. High time-resolution monitoring, as used here, was found to be an effective approach to develop in-use emission factors for a source such as the rail yards. Additional monitoring sites near the rail yard complex could facilitate the calculation of emission factors and impact evaluation. Monitoring coverage could be augmented using low cost BC, $PM_{2.5}$ and CO_2 micro sensors which could simplify the location of new monitoring sites around the railyard complex.

The regression approach used here could be extended by monitoring NO_x concentrations and accessing or retrieving information on rail yard activity. NO_x concentration measurements could further the detection of high concentrations events coming from the rail yards, given that locomotive activity near monitoring sites should increase NO_x, CO_2 and BC concentrations simultaneously and all three should be well correlated. Monitoring NO_x concentrations may be used to differentiate between new switcher and line-haul locomotives. New switchers are thought to have low BC and NO_2 emissions but given low background of NO_x in the area this contaminant might be easier to detect than low BC concentrations coming from cleaner switcher locomotives. If no information on rail yard activity is provided by the industry, small motion sensor cameras

with night vision could be placed at the monitoring sites to record locomotive traffic and link it to pollutant concentrations as was done here.

Fuel-based emission factors could be measured for other rail yards and similar sources. Expanded monitoring capacity permitted by the recent developments in miniaturization and simplification of monitoring sensors for CO_2, CO, BC, NO_x could provide sufficient data at low cost and with improved spatial coverage to permit successful application of the approaches taken here. This could help lower uncertainties in emission inventories.

Evaluation of impacts of rail yard emissions by dispersion modeling could benefit from including emissions from other surface streets in the area, such as James Jackson Parkway NW, Hollywood Road NW, Chattahoochee Ave NW and Howell Mill Road. Estimates of emissions from these roads and the much larger roads already included in this work could reduce discrepancies between simulated and measured concentrations and better capture the morning rush hour peaks and other short-term features in the concentrations of simulated contaminants.

Analysis of monitoring data from the Atlanta Rail Yard Study (ARYS), a campaign carried out by Georgia Tech, EPA and Aerodyne Research Inc. during May 2012 will supplement the present work. Data on aerosol chemical speciation, aerosol size and number distributions, O_3, BC, NOx, CO, CO_2, formaldehyde and VOCs was collected and has yet to be analyzed. It will further elucidate the chemical composition of aerosols and gases emitted by rail yard activities. Specific chemical profiles for rail yard locomotives, trucks and cranes, other various in-yard sources might be extracted. Measurements of spatial gradients of gas and particulate near the rail yard complex done

in the ARYS campaign will help to further evaluate results of dispersion modeling presented in this work.

APPENDIX A

SUPPORTING INFORMATION FOR CHAPTER 2

A.1. Photos of Rail yard Activity

Rail yard operations were recorded from the DX site, flanking the tracks of the arrival section of Inman Yard. A Hero Gopro 960 camera was used to take pictures every minute on 42 days between 9/15/2011 and 11/14/2011 for a total of 60,384. Photos were look at one by one to identify rail yard activity. Photos corresponding to low light conditions during night time were unusable. Photos show trains, accelerating, idling or passing by before an event of overlapping signals of concentrations of BC and CO_2 were registered. Photos also showed that when no locomotives were present and the wind was from blowing from the direction of the rail yards, BC and CO_2 concentrations were poorly correlated.

Table A.1. Dates of photographic surveillance of Inman rail yard.

Initial Date	End Date	# Days
9/15/2011 9:37	9/18/2011 15:19	3
9/20/2011 16:38	9/27/2011 9:25	7
9/28/2011 11:27	10/1/2011 11:08	4
10/1/2011 12:03	10/7/2012 21:34	7
10/10/2011 16:56	10/17/2011 15:05	7
10/21/2011 9:49	10/27/2011 14:44	7
11/8/2011 12:30	11/14/2011 17:43	7

A.2. Algorithm for wavelet analysis

The Matlab algorithm to separate the high and low frequency components of the signals is presented next. Comments of each step are provided with in the code.

```
function [baselineCorrected, smoothSpec, baselineEst] =
WavletDenoiseBaselineRemove3(P,tolerance)
% baselinecorected is to be the high frequency components of the signal
% corrected for background concentrations
% smoothSpec is the pollutant signal smoothed by application of wavelet
% decomposition.
% baselineEst is the approximation of the background concentration obtained
% from lineal regressions between local minima.
% P is the variable to denoise and correct baseline. In our case it is BC,
% CO2 or PM2.5 data.
% tolerance is the level of concentration allowed to be disregarded when is
% below the baseline approximation. We used 0.5 ug/m3 for PM2.5 and BC and
% 1 ppb for CO2

iempty=isnan(P);
P(iempty)=mean(P(~iempty));
% nans are patched with the mean pollutant concentration, to be able to do
% the wavelet decomposition. The array of empty data is saved to discard the
% patched data later on.


L=5;
% L is the decomposition level.  A typical value of 5 was used.

[c,l] = wavedec(P,L,'db8');
% Matlab function wavedec performs a multilevel one-dimensional wavelet
analysis using either a specific wavelet, in this case db8 Daubechies wavelet
filter. The output decomposition structure contains the wavelet decomposition
vector c and the bookkeeping vector l.

a(length(P),L)=1;
% preallocate variable “a” to storage reconstructions of the signal at
different % levels

for i=1:L;
a(:,i)= wrcoef('a',c,l,'db8',i);
end
% Reconstruct approximation at level L, from the wavelet decomposition
% structure [c,l].

base=a(:,L);
% L Level is selected to construct the baseline approximation

d=diff(base);
% Matlab function diff(x)calculates differences between adjacent elements of
% x, that can be used approximate derivatives to identify local minima.

q(:,1)=d<=0;
q(:,2)=d>0;
k(1,length(base))=0;
% preallocate variables q, and k to storage minima localization
```

```
for j=3:length(q(:,1))-3;
 if ((q(j,1)>=1)&&(q(j,2)<=0))&&((q(j+1,1)<=0)&&(q(j+1,2)>=1))
     k(j+1)=1;
 end
end
% locate local minima

x = find(k>0); x=x';
y = base(x);
% assigns local minima to construct initial baseline estimation
xi = 1:1:length(base); xi=xi';
yi = interp1(x,y,xi,'linear');

% Matlab function interp1(x,Y,xi) does a lineal interpolation to find yi, the
% values of the underlying function Y at the points in the vector or array
% xi.

offset=yi-base;
% Offset is defined as the concentration data that is under the initial
% baseline approximation.

tol=sum(offset>=0);
% initial value of a tolerance level

while tol>100;
    Arraycopy = offset;
    for j = 1:500
       [~, IND(j)] = max(Arraycopy);
       Arraycopy(IND(j)) = 0;
    end
    k(IND)=1;
    x = find(k>0); x=x';
    y = a(x,3);
    xi = 1:1:length(a(:,3)); xi=xi';
    yi = interp1(x,y,xi,'linear');
    offset=yi-a(:,3);
    tol=sum(offset>=tolerance);
end
% this while cycle looks for the baseline approximation accounting for as
% much concentration data as possible, minimizing signal loss.
smoothSpec=a(:,1);
smoothSpec(iempty)=nan;
% assigns the first level reconstruction to output smoothSpec and eliminates
% data previously patched.
baselineEst=yi;
baselineEst(iempty)=nan;
% assigns the estimated base line reconstruction to output baselineEst and
% eliminates data previously patched.
baselineCorrected = smoothSpec - baselineEst;
% assigns the high frequency components minus the estimated base line to
% output baselineEst.
```

A.3. Histograms and time series plots of Downwind/Upwind data

To visualize the effectiveness of the delta approach to calculate emission factors and the origin of the variability of the results we plotted the time series of the downwind and upwind data. In green is the upwind data and in red de downwind data at both monitoring sites.

Whereas time series and histograms show a clear difference for BC downwind vs. upwind concentrations the same is harder to see in the CO_2 and $PM_{2.5}$ time series.

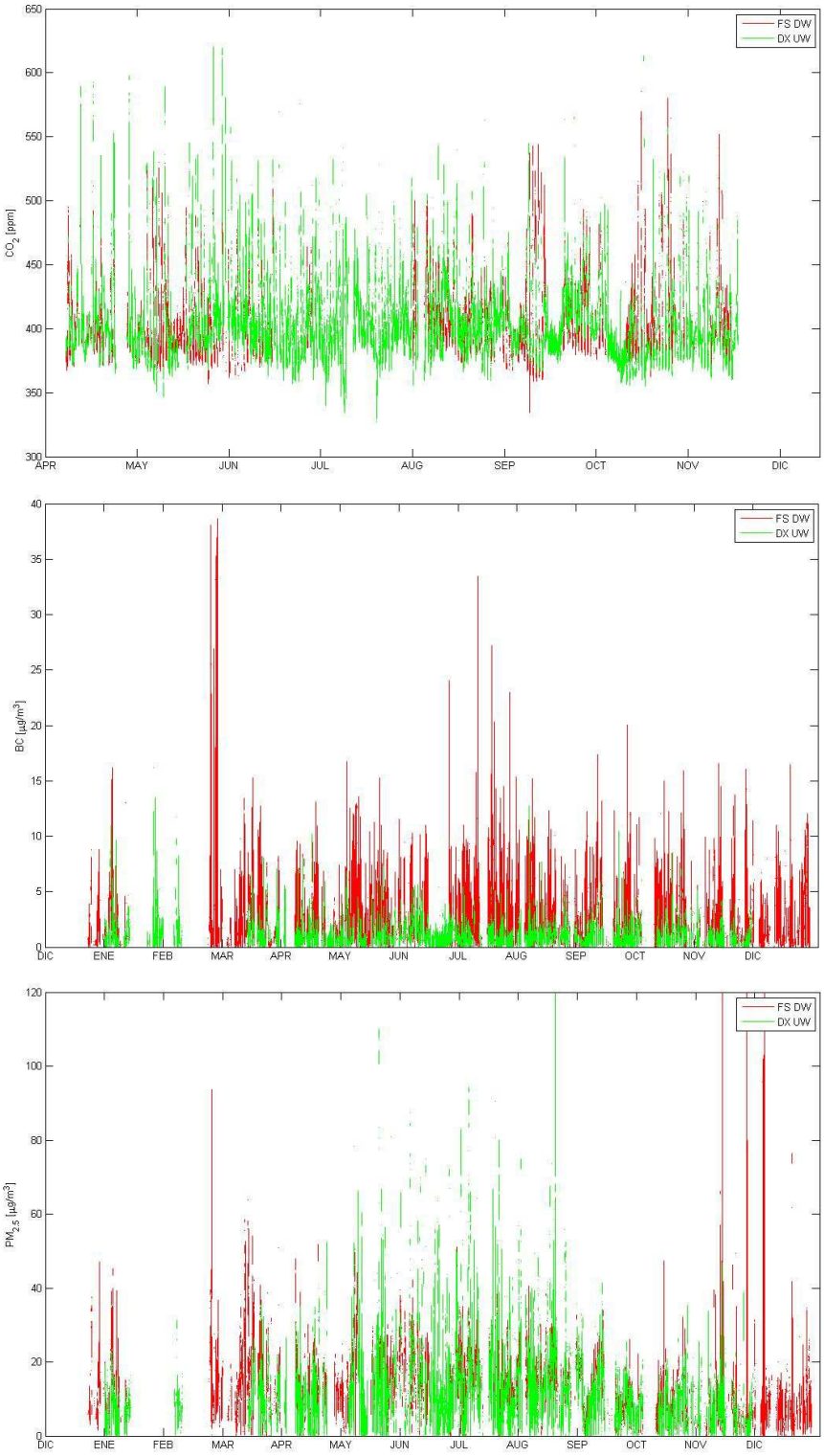

Figure A.1. CO_2, BC and $PM_{2.5}$ time series for FS downwind conditions.

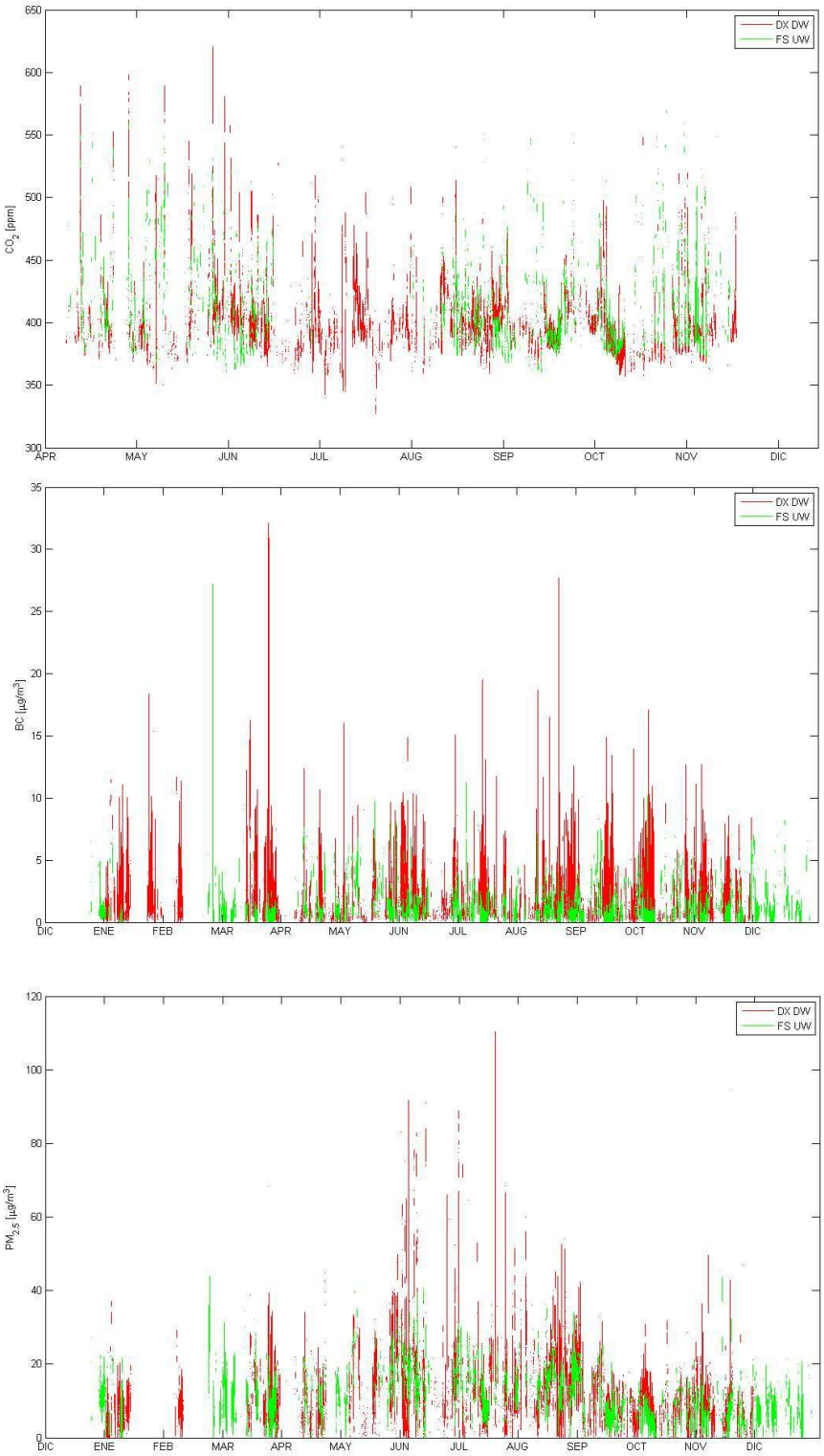

Figure A.2. CO_2, BC and $PM_{2.5}$ time series for DX downwind conditions.

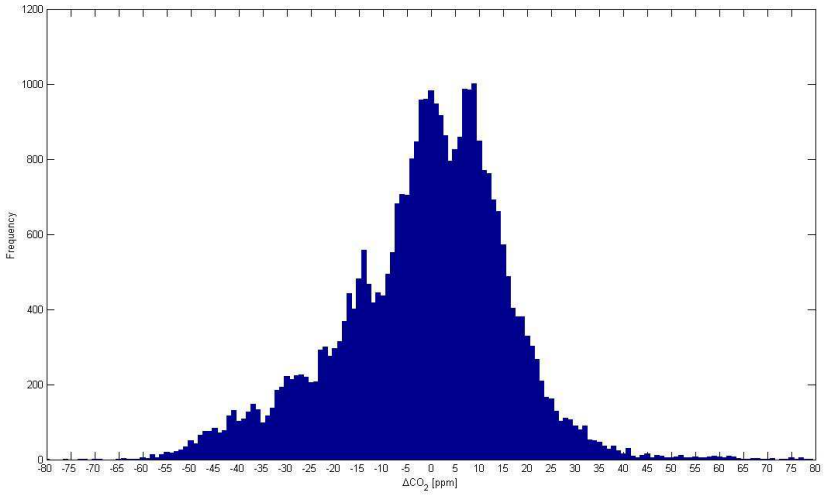

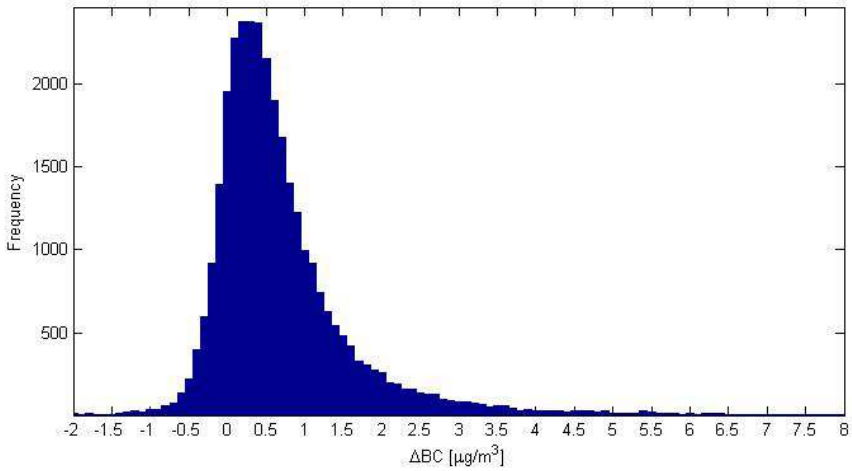

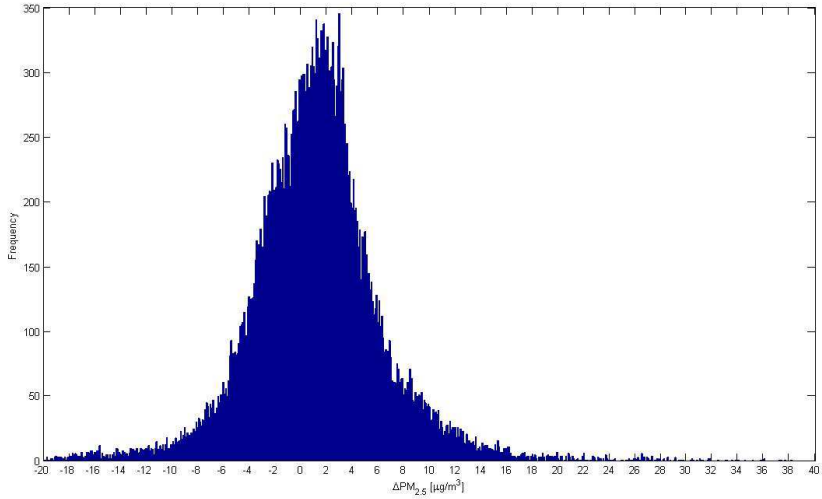

Figure A.3. Histograms of CO_2, BC and $PM_{2.5}$ for FS downwind conditions.

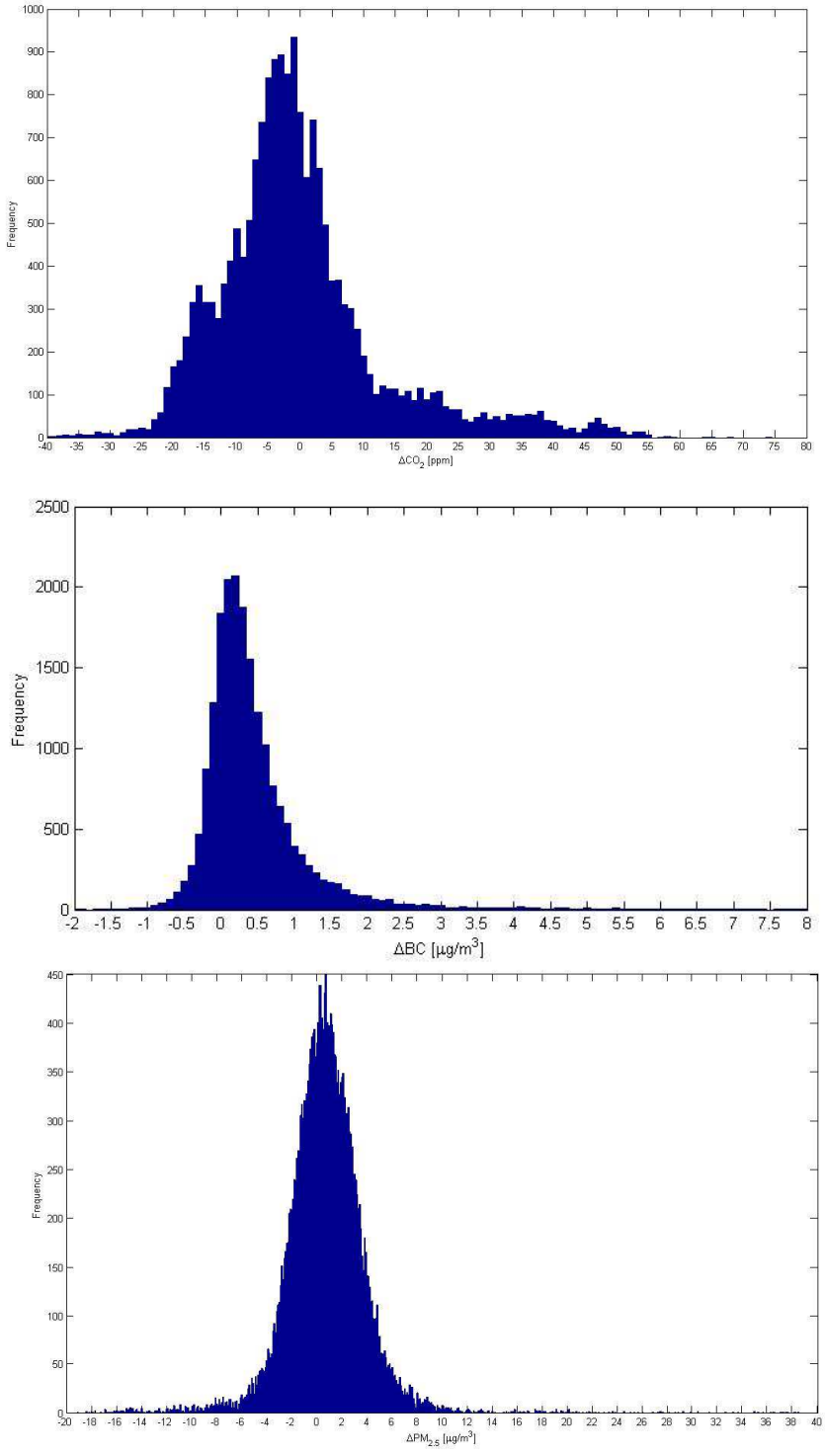

Figure A.4. Histograms of CO_2, BC and $PM_{2.5}$ for DX downwind conditions.

A.4. Boxplots of BC emission factors

To explore whether the FS spikes may be partly attributed to the near-field emissions along Marietta Blvd. we plotted the emission factors at both sites by the time of day and day of week at both sites, during conditions of wind from the rail yard area. Traffic on Marietta Blvd. during weekends and by night and early morning is scarce. The plots tell us that there is no significant difference between events detected at different times of the day or at different days of the week. Behavior of emission factors calculated does not appear to match peak hours or valleys of traffic, or to be different during the weekends.

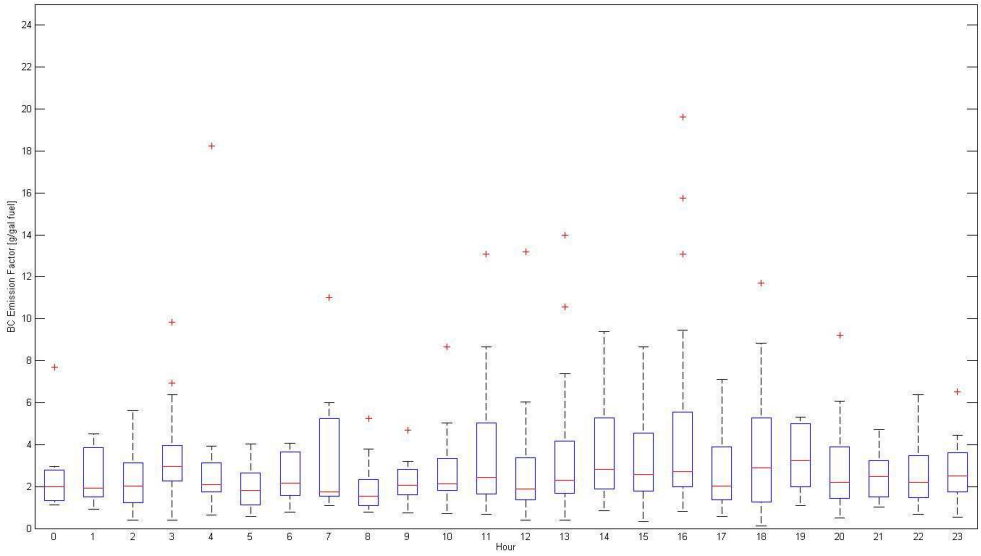

Figure A.5. Boxplot of BC emission factor by hour of the day at DX site.

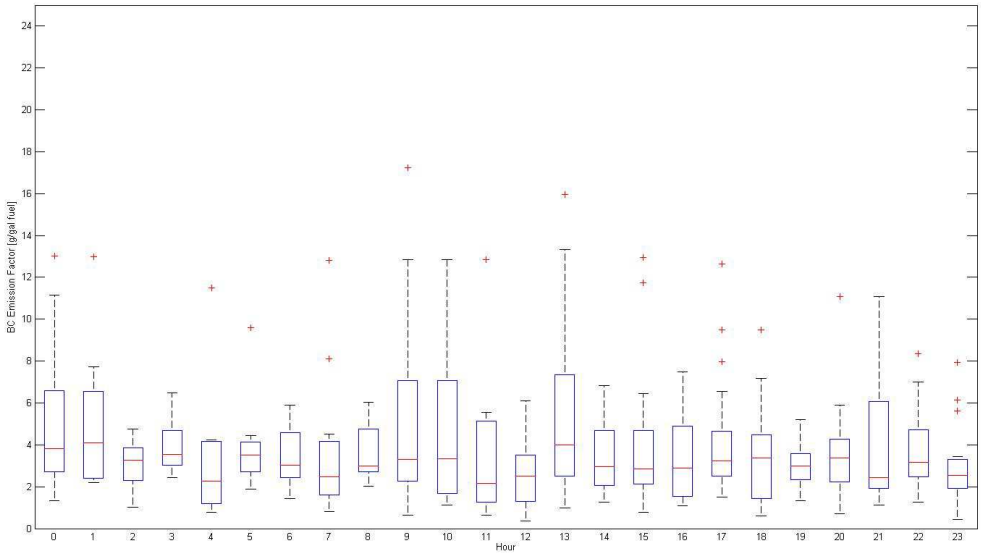

Figure A.6. Boxplot of BC emission factor by hour of the day at FS site.

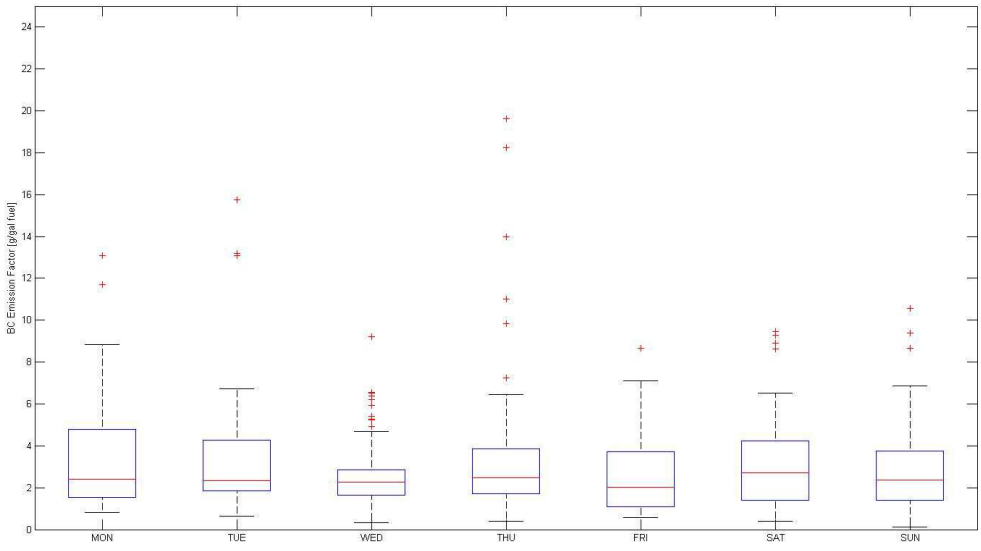

Figure A.7. Boxplot of BC emission factor by day of the week at DX site.

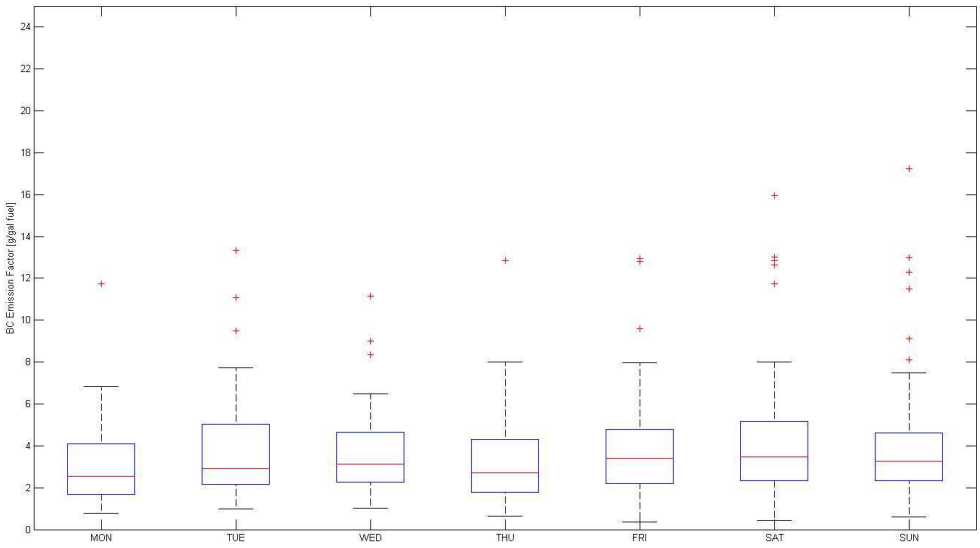

Figure A.8. Boxplot of BC emission factor by day of the week at FS site.

A.5. Emission factors results calculated when the wind was not blowing from the rail yards

The Delta method implies uncertainties. One way to check that the results obtained from this method are meaningful is to calculate emission factors when the wind was not blowing from the rail yards, between 110◦ and 170◦ for FS downwind, and 280◦ and 320◦ for DX downwind. Emission factors obtained this way are very small in comparison with the results when the wind blows from the rail yards.

Table A.2. Control Emission factors.

	Downwind Site	
	DX	FS
EF_{BC} [g of BC /gal fuel]	0.02±0.03	0.04±0.07
$EF_{PM_{2.5}}$ [g of $PM_{2.5}$ /gal fuel]	0.1±0.2	0.3±0.6

APPENDIX B

SUPPORTING INFORMATION FOR CHAPTER 3

B.1. Surface characteristics

Surface characteristics are used by AERMET in the computation of the fluxes and stability of the atmosphere. The albedo is the fraction of total incident solar radiation reflected by the surface back to space without absorption. The Bowen ratio is the ratio of the sensible heat flux to the latent heat flux it is an indicator of surface moisture. The surface roughness length is the height at which the mean horizontal wind speed is zero. It relates to the height of obstacles to the wind flow.

Table B.1. Surface characteristics generated with AERSURFACE.

Season	Section	Albedo	Bowen Ratio	Surface Roughness (m)
Winter	0-30	0.17	1.09	0.093
	30-60	0.17	1.09	0.069
	60-90	0.17	1.09	0.050
	90-120	0.17	1.09	0.035
	120-150	0.17	1.09	0.047
	150-180	0.17	1.09	0.122
	180-210	0.17	1.09	0.145
	210-240	0.17	1.09	0.087
	240-270	0.17	1.09	0.037
	270-300	0.17	1.09	0.056
	300-330	0.17	1.09	0.082
	330-360	0.17	1.09	0.093
Spring	0-30	0.16	0.90	0.094
	30-60	0.16	0.90	0.074
	60-90	0.16	0.90	0.057
	90-120	0.16	0.90	0.042
	120-150	0.16	0.90	0.057
	150-180	0.16	0.90	0.139
	180-210	0.16	0.90	0.168
	210-240	0.16	0.90	0.102
	240-270	0.16	0.90	0.046
	270-300	0.16	0.90	0.062
	300-330	0.16	0.90	0.086
	330-360	0.16	0.90	0.094
Summer	0-30	0.16	0.70	0.095
	30-60	0.16	0.70	0.078
	60-90	0.16	0.70	0.062
	90-120	0.16	0.70	0.048
	120-150	0.16	0.70	0.066
	150-180	0.16	0.70	0.151
	180-210	0.16	0.70	0.185
	210-240	0.16	0.70	0.114
	240-270	0.16	0.70	0.052
	270-300	0.16	0.70	0.067
	300-330	0.16	0.70	0.088
	330-360	0.16	0.70	0.095
Fall	0-30	0.16	1.08	0.094
	30-60	0.16	1.08	0.074
	60-90	0.16	1.08	0.057
	90-120	0.16	1.08	0.042
	120-150	0.16	1.08	0.058
	150-180	0.16	1.08	0.141
	180-210	0.16	1.08	0.175
	210-240	0.16	1.08	0.103
	240-270	0.16	1.08	0.046
	270-300	0.16	1.08	0.062
	300-330	0.16	1.08	0.086
	330-360	0.16	1.08	0.094

B.2. Modeling parameters for non-road and on-road mobile sources

AERMOD algorithms need the following parameters for the mobile sources modeled in this work: The source ID is the identification of the source, the source type, the location in the domain X and Y in meters and Z in meters above mean sea level, the release height (center of volume) above ground in meters, Sigma Y0 the initial lateral dimension of the volume in meters, and Sigma Z0 the initial vertical dimension of the volume in meters. These parameters were determined using EPA (1995) and GAEPD (2012). Switching and line-haul activities were defined to occupy the same location, and have the same source parameters, but emissions rates for each are different.

Table B.2. Modeling parameters for non-road and on-road mobile sources.

Rail yard line-haul							
Source ID	Source Type	X (m)	Y (m)	Z (MAMSL)	Height (m)	Sigma Y0 (m)	Sigma Z0 (m)
HINMNA	VOLUME	735660	3743145	274	4.6	115.11	1.7
HINMNB	VOLUME	736580	3742440	278	4.6	97.29	1.7
HTLFDA	VOLUME	735635	3743825	264	4.6	80.56	1.7
HTLFDB	VOLUME	736720	3742972	275	4.6	44.12	1.7
Rail yard switchers							
Source ID	Source Type	X (m)	Y (m)	Altitude (MAMSL)	Height (m)	Sigma Y0 (m)	Sigma Z0 (m)
SINMNA	VOLUME	735660	3743145	274	4.6	115.11	1.7
SINMNB	VOLUME	736580	3742440	278	4.6	97.29	1.7
STLFDA	VOLUME	735635	3743825	264	4.6	80.56	1.7
STLFDB	VOLUME	736720	3742972	275	4.6	44.12	1.7

Table B.2. (continued). Modeling parameters for non-road and on-road mobile sources.

Other mobile non-road and on-road sources							
Source ID	Source Type	X (m)	Y (m)	Altitude (MAMSL)	Height (m)	Sigma Y0 (m)	Sigma Z0 (m)
HOWELLS	VOLUME	738850	3742690	278	4.6	115.11	1.7
BOLTON1	VOLUME	733940	3744220	272	2.44	16.48	1.7
BOLTON2	VOLUME	734586	3744670	263	2.44	16.48	1.7
BOLTON3	VOLUME	735200	3745210	235	2.44	15.85	1.7
MRTRD1	VOLUME	735390	3744400	251	2.44	21.97	1.7
MRTRD2	VOLUME	736560	3743400	285	2.44	21.97	1.7
MRTRD3	VOLUME	737220	3742200	277	2.44	21.97	1.7
MRTBLV01	VOLUME	736165	3744868	254	2.44	30.81	1.7
MRTBLV02	VOLUME	736921	3744475	267	2.44	28.13	1.7
MRTBLV03	VOLUME	737053	3744202	257	2.44	28.13	1.7
MRTBLV04	VOLUME	737096	3743996	254	2.44	17.79	1.7
MRTBLV05	VOLUME	737124	3743884	251	2.44	17.79	1.7
MRTBLV06	VOLUME	737154	3743766	253	2.44	17.79	1.7
MRTBLV07	VOLUME	737190	3743647	255	2.44	17.79	1.7
MRTBLV08	VOLUME	737225	3743530	256	2.44	17.79	1.7
MRTBLV09	VOLUME	737255	3743446	257	2.44	11.48	1.7
MRTBLV10	VOLUME	737266	3743400	259	2.44	11.48	1.7
MRTBLV11	VOLUME	737277	3743355	260	2.44	11.48	1.7
MRTBLV12	VOLUME	737294	3743306	261	2.44	11.48	1.7
MRTBLV13	VOLUME	737312	3743257	262	2.44	11.48	1.7
MRTBLV14	VOLUME	737325	3743210	265	2.44	11.48	1.7
MRTBLV15	VOLUME	737341	3743165	265	2.44	11.48	1.7
MRTBLV16	VOLUME	737358	3743118	265	2.44	11.48	1.7
MRTBLV17	VOLUME	737375	3743071	265	2.44	11.48	1.7
MRTBLV18	VOLUME	737398	3743025	265	2.44	11.48	1.7
MRTBLV19	VOLUME	737421	3742980	266	2.44	11.48	1.7
MRTBLV20	VOLUME	737462	3742904	267	2.44	17.79	1.7
MRTBLV21	VOLUME	737521	3742796	267	2.44	17.79	1.7
MRTBLV22	VOLUME	737580	3742688	266	2.44	17.79	1.7
MRTBLV23	VOLUME	737638	3742581	265	2.44	17.79	1.7
MRTBLV24	VOLUME	737693	3742474	266	2.44	17.79	1.7
MRTBLV25	VOLUME	737793	3742292	271	2.44	28.13	1.7
MRTBLV26	VOLUME	737932	3742027	278	2.44	28.13	1.7
MRTBLV27	VOLUME	738073	3741150	283	2.44	32.35	1.7

B.3.Modeling parameters for industrial sources

AERMOD algorithms need the following parameters for the point sources defined in this work: The source ID is the identification of the source, the source type, the location in the domain X and Y in meters and Z in meters above mean sea level, the stack height which is the release height above ground in meters, the stack gas exit temperature in Kelvin, the stack gas exit velocity in m/s, and the stack inside diameter in meters. Ennis plant was defined as a volume source following the above description for that type of source.

Table B.3. Modeling parameters for industrial sources.

Point sources

Source ID	Source Type	X (m)	Y (m)	Z (MAMSL)	Stack Height (m)	Stack Temperature (K)	Stack exit velocity (m/s)	Stack Diameter (m)
GAPOWER	POINT	733900	3745661	240	254.8	405.4	20.27	7.9
LAFARGE	POINT	734534	3745561	240	13.4	389.8	20.98	0.7
SHBRICK	POINT	732475	3743547	233.5	20.1	586	13.1	1.98
SUTTON	POINT	735080	3746126	238	17.7	302	8.99	0.55
RMCLYTN	POINT	735565	3745276	242	9.76	302.6	18.29	0.4
MEADPKG	POINT	738760	3741287	290	44.2	312.6	7.01	1.06
CMETAL1	POINT	739930	3740537	300	16.8	298.15	15.02	1.37
CMETAL2	POINT	739930	3740537	300	16.5	298.15	35.22	0.91
CMETAL3	POINT	739930	3740537	300	9.76	1283.15	7.6	0.61

Volume sources

Source ID	Source Type	X (m)	Y (m)	Z (m)	Height (m)	Sigma Y0 (m)	Sigma Z0 (m)
ENNISPT	VOLUME	737418	3743629	257	6	16.44	2.78

B.4. Emissions from rail yards

Emission factors correspond to previous works (Galvis et al., 2013; Georgia-EPD 2009; EPA 2010; Honc et al. 2006) and also where obtained from personal communication with Michelle Bergin. Class I railroad operations of Norfolk Southern (NS) which operates Inman and CSX Transportation (CSXT) which operates Tilford were split into two categories: line-haul and switching activity. Line-haul emissions were estimated using data from the surface transportation board R-1 annual reports (NS, 2012; CSXT, 2012). Switcher emissions were obtained from GAEPD (2012b). There are 17 switchers in Inman, 10 in Tilford, and 1 in Howells yard. Emissions rates must be converted to g/s for use in AERMOD.

Table B.4. Emissions from rail yards.

Emission factors R_{EF}	Units	TILFORD	INMAN
BC	g/gal	2.4	3.1
$PM_{2.5}$	g/gal	4.8	7.2
BC and $PM_{2.5}$ after GenSet retrofit	g/gal	0.8	0.8
BC and $PM_{2.5}$ after conversion to Mother-slug sets	g/gal	2.9	1.6

	Units	TILFORD	INMAN
R-1 schedule 750 line 1 system diesel oil consumption	[gal/year]	4.51E+08	4.40E+08
R-1schedule 755 line 104 system-wide gross ton miles	[GTM]	4.56E+11	3.92E+11
System-wide fuel combustion efficiency η	[GTM /gal/year]	1.01E+03	8.91E+02
County-level GTM from NS and CSX reports to GA-EPD Fulton Cobb	[GTM]	 2.71E+09 2.44E+09	 1.74E+09 1.87E+09
County level track miles (T_C) Fulton Cobb	[miles]	 67 37	 23 17
Domain Level Track miles (T_D) Fulton Cobb	[miles]	 14.0 3.4	 14.2 2.3
Gross ton miles transported in the modeling domain (G_D) Fulton Cobb	[GTM]	 5.66E+08 2.21E+08	 1.08E+09 2.64E+08
Line-Haul Domain-level Fuel consumption ($LHFC_D$) Fulton Cobb Total	[gal/year]	 5.60E+05 2.19E+05 7.79E+05	 1.21E+06 2.97E+05 1.51E+06

Table B.4.(Continued). Emissions from rail yards.

Line-haul rail yard emissions	Units	TILFORD	INMAN
Switchers fuel use in the domain SFC_D	[gal/year]	6.00E+05	1.01E+06
Switchers fuel use in the domain SFC_D after GenSet retrofit	[gal/year]	4.50E+05	4.89E+05
Switchers fuel use in the domain SFC_D after conversion to mother-slugs sets	[gal/year]	4.75E+05	5.59E+05

Line-haul rail yard emissions	Units	TILFORD	INMAN
BC	[t/year]	1.9	4.7
$PM_{2.5}$		3.7	10.9
Switchers rail yard emissions	Units	TILFORD	INMAN
BC	[t/year]	1.4	3.1
$PM_{2.5}$		2.9	7.2
Switchers rail yard emissions after upgrades	Units	TILFORD	INMAN
GenSet BC and $PM_{2.5}$	[t/year]	0.3	0.4
Mother-slug sets BC and $PM_{2.5}$		1.4	0.9

BC emissions	**Inman A [g/s]**	**Inman B [g/s]**	**Tilford A [g/s]**	**Tilford B [g/s]**	**Howells [g/s]**
Line-Haul	0.0741	0.0741	0.0395	0.0198	0.0021
Switchers	0.0495	0.0495	0.0304	0.0152	0.0016
Switchers after GenSet retrofit	0.0059	0.0059	0.0072	0.0036	0.0004
Switchers after conversion to mother-slug sets	0.0145	0.0145	0.0290	0.0145	0.0015
$PM_{2.5}$ emissions	**Inman A [g/s]**	**Inman B [g/s]**	**Tilford A [g/s]**	**Tilford B [g/s]**	**Howells [g/s]**
Line-Haul	0.1722	0.1722	0.0790	0.0395	0.0041
Switchers	0.1150	0.1150	0.0609	0.0304	0.0032
Switchers after GenSet retrofit	0.0059	0.0059	0.0072	0.0036	0.0004
Switchers after conversion to mother-slug sets	0.0145	0.0145	0.0290	0.0145	0.0015

B.5. Emissions from on-road mobile sources.

Table B.5. Emissions from on-road mobile sources.

Road	$PM_{2.5}$ [t/year]	BC [t/year]
Bolton 1 (between James Jackson Parkway and Hollywood Road)	0.11	0.03
Bolton 2 (between Hollywood Road and Marietta Road)	0.12	0.03
Bolton 3 (between Marietta Road and Marietta Boulevard)	0.07	0.02
Marietta Boulevard	1.23	0.36
Marietta Road	0.36	0.10

Table B.5. (continued). Emissions from on-road mobile sources.

Road Segment	$PM_{2.5}$ [g/s]	BC [g/s]
BOLTON1	0.00337	0.00097
BOLTON2	0.00368	0.00106
BOLTON3	0.00221	0.00064
MRTRD1	0.00384	0.00109
MRTRD2	0.00384	0.00109
MRTRD3	0.00384	0.00109
MRTBLV01	0.00939	0.00277
MRTBLV02	0.00196	0.00058
MRTBLV03	0.00196	0.00058
MRTBLV04	0.00078	0.00023
MRTBLV05	0.00078	0.00023
MRTBLV06	0.00078	0.00023
MRTBLV07	0.00078	0.00023
MRTBLV08	0.00078	0.00023
MRTBLV09	0.00033	0.00010
MRTBLV10	0.00033	0.00010
MRTBLV11	0.00033	0.00010

Road Segment	$PM_{2.5}$ [g/s]	BC [g/s]
MRTBLV12	0.00033	0.00010
MRTBLV13	0.00033	0.00010
MRTBLV14	0.00033	0.00010
MRTBLV15	0.00033	0.00010
MRTBLV16	0.00033	0.00010
MRTBLV17	0.00033	0.00010
MRTBLV18	0.00033	0.00010
MRTBLV19	0.00033	0.00010
MRTBLV20	0.00078	0.00023
MRTBLV21	0.00078	0.00023
MRTBLV22	0.00078	0.00023
MRTBLV23	0.00078	0.00023
MRTBLV24	0.00078	0.00023
MRTBLV25	0.00196	0.00058
MRTBLV26	0.00196	0.00058
MRTBLV27	0.01036	0.00305

B.6. Emissions from industrial sources.

Table B.6. Emissions from industrial sources.

Facility Name	AIRS No.	Latitude	Longitude	$PM_{2.5}$ [t/year]	BC [t/year]
Georgia Power Company McDonough/Atkinson Plant	06700003	33.820865	-84.484080	132.4	50.3
General Shale Brick Inc. Plant	12100004	33.808896	-84.486768	40.8	0.8
Lafarge Building Materials, Inc.	12100401	33.821937	-84.471987	24.9	0.5
Cobb County R.L. Sutton water reclamation facility	06700018	33.829254	-84.459795	36.6	0.7
Central Metals Co.	12100033	33.777804	-84.408952	9.5	0.2
Mead Packaging Co	12100070	33.784353	-84.422530	19.1	0.4
Atlanta R.M. Clayton water reclamation facility	12100268	33.821438	-84.456540	2.4	0.05
Ennis Paint, Inc.	12100617	33.805794	-84.436891	3.6	0.07

B.7. Concentration-response functions.

Table B7. Concentration-response functions.

Health endpoint | Age group	Author	Function
Mortality, All Cause | 30-99	Krewski et al.	(1-(1/EXP(Beta*DELTAQ)))*Incidence*POP
Mortality, All Cause | 25-99	Lepeule et al.	(1-EXP(-Beta*DELTAQ))*Incidence*POP
Mortality, All Cause | infants	Woodruff et al.	(1-(1/((1-Incidence)*EXP(Beta*DeltaQ)+Incidence)))*Incidence*POP
Emergency Room Visits, Asthma | 0-99	Mar et al.	(1-EXP(-Beta*DELTAQ))*Incidence*POP
HA, All Respiratory |65-99	Zanobetti et al	(1-EXP(-Beta*DELTAQ))*Incidence*POP
HA, Asthma |0-17	Sheppard	(1-(1/EXP(Beta*DELTAQ)))*Incidence*POP
HA, Chronic Lung Disease | 18-94	Moolgavkar	(1-(1/EXP(Beta*DELTAQ)))*Incidence*POP
HA, All Cardiovascular (less Myocardial Infarctions) | 65-99	Zanobetti et al	(1-EXP(-Beta*DELTAQ))*Incidence*POP
HA, All Cardiovascular (less Myocardial Infarctions) | 18-64	Moolgavkar	(1-(1/EXP(Beta*DELTAQ)))*Incidence*POP
Work Loss Days | 18-64	Ostro	(1-(1/EXP(Beta*DELTAQ)))*Incidence*POP
Minor Restricted Activity Days | 18-64	Ostro and Rothschild	(1-(1/EXP(Beta*DELTAQ)))*A*POP
Acute Bronchitis | 8-12	Dockery et al.	(1-(1/((1-Incidence)*EXP(Beta*DeltaQ)+Incidence)))*Incidence*POP
Lower Respiratory Symptoms | 7-14	Schwartz and Neas	(1-(1/((1-A)*EXP(Beta*DeltaQ)+A)))*A*POP
Upper Respiratory Symptoms | 9-11	Pope et al.	(1-(1/((1-A)*EXP(Beta*DeltaQ)+A)))*A*POP*Prevalence
Asthma Exacerbation, Cough | 6-18	Mar et al.	(A - (A/((1-A)*exp(Beta*DELTAQ)+A)))*POP*Prevalence
Asthma Exacerbation, Shortness of Breath | 6-18	Mar et al.	(A - (A/((1-A)*exp(Beta*DELTAQ)+A)))*POP*Prevalence
Asthma Exacerbation, Wheeze | 6-18	Ostro et al.	(1-(1/((1-A)*EXP(Beta*DeltaQ)+A)))*A*POP*Prevalence

B.8. Concentration-response functions.

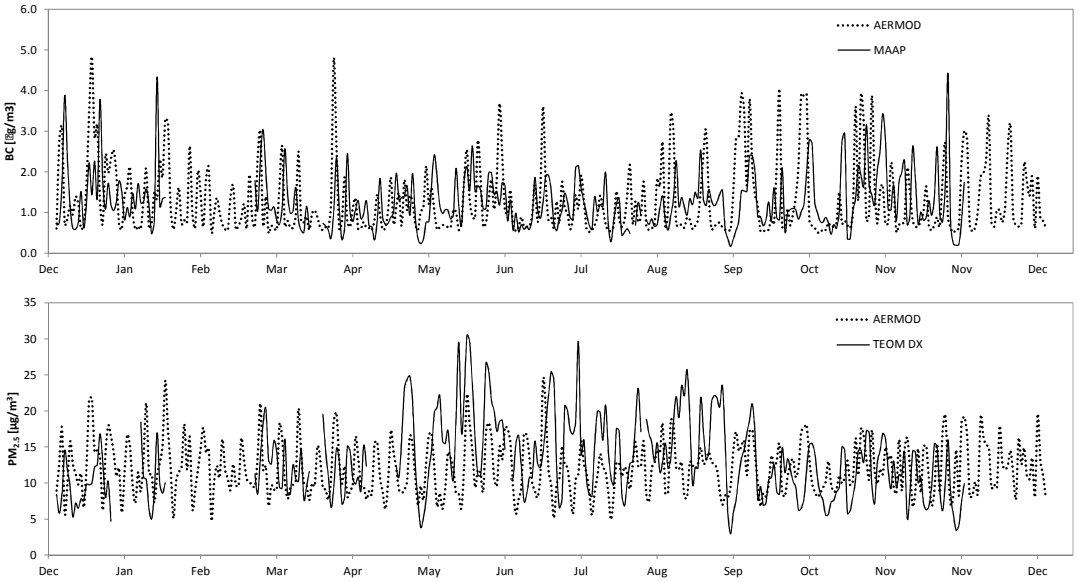

Figure B.1. Simulated and measured daily averages of BC and $PM_{2.5}$ at DX.

B5. References

CSXT. 2012. Class I Railroad Annual Report, [accessed Dec, 2012]. http://www.stb.dot.gov/econdata.nsf/f039526076cc0f8e8525660b006870c9/8775aca41ef66efb852579db004c9dee?OpenDocument.

EPA. 1995. USER'S GUIDE FOR THE INDUSTRIAL SOURCE COMPLEX (ISC3) DISPERSION MODELS VOL1, [accessed Oct, 2012]. http://www.epa.gov/scram001/userg/regmod/isc3v1.pdf.

EPA. 2010. Exhaust and Crankcase Emission Factors for Nonroad Engine Modeling Compression Ignition [accessed Jan, 2013].

Dockery, D.W., J. Cunningham, A.I. Damokosh, L.M. Neas, J.D. Spengler, P. Koutrakis, J.H. Ware, M. Raizenne and F.E. Speizer. 1996. Health Effects of Acid Aerosols On North American Children - Respiratory Symptoms. Environmental Health Perspectives. Vol.

Georgia Environmental Protection Division [GAEPD]. 2009. Voluntary Reduction of Emissions from Railyards in Metro Atlanta Region, [accessed Oct, 2012]. http://www.georgiaair.org/airpermit/downloads/planningsupport/regdev/sips_and_revisions/atlanta_8hr_ozone/appendixt.pdf.

Georgia Environmental Protection Division [GAEPD]. 2012. Guideline for Modeling PM10 Ambient Concentration in Areas Impacted by Quarry Operation Producing Crushed Stone, [accessed Feb, 2013]. http://www.georgiaair.org/airpermit/downloads/sspp/modeling/quarryguideline_august2012.pdf

Georgia Environmental Protection Division [GAEPD]. 2012b. Railroad Emission Inventories. Locomotive Emission Inventories for the United States from ERTAC Rail., [accessed Mar, 2013].

Galvis, B., M. Bergin, and A. G. Russell. 2013. Fuel-based fine particulate and black carbon emission factors from a railyard area in Atlanta. Journal of the Air & Waste Management Association (In press).

Honc, Randell L., Steven G. Fritz, Michael B. Schell, Andrew Tarnow, and Adam Bennett. 2006. Fuel Consumption and Exhaust Emissions From a 1,125 kW Multiple Genset Switcher Locomotive. ASME Conference Proceedings no. 2006 (42606):1-8. doi: 10.1115/ICEF2006-1515.

Krewski D, Jerrett M, Burnett R, et al. 2009. Extended Follow-Up and Spatial analysis of the American Cancer Society Linking Particulate Air Pollution and Mortality. Health Effects Institute, Cambridge MA

Lepeule J, Laden F, Dockery D, Schwartz J. Chronic exposure to fine particles and mortality: an extended follow-up of the Harvard Six Cities study from 1974 to 2009. Vol 120(7). 965-970

Mar, T. F., J. Q. Koenig and J. Primomo. 2010. Associations between asthma emergency visits and particulate matter sources, including diesel emissions from stationary generators in Tacoma, Washington. Inhal Toxicol. Vol. 22 (6): 445-8. http://www.ncbi.nlm

Mar, T. F., T. V. Larson, R. A. Stier, C. Claiborn and J. Q. Koenig. 2004. An analysis of the association between respiratory symptoms in subjects with asthma and daily air pollution in Spokane, Washington. Inhal Toxicol. Vol. 16 (13): 809-15.

Mar, T. F., T. V. Larson, R. A. Stier, C. Claiborn and J. Q. Koenig. 2004. An analysis of the association between respiratory symptoms in subjects with asthma and daily air pollution in Spokane, Washington. Inhal Toxicol. Vol. 16 (13): 809-15.

Moolgavkar, S.H. Air Pollution and Hospital Admissions for Chronic Obstructive Pulmonary Disease in Three Metropolitan Areas in the United States. Inhalation Toxicology, 2000. 12(Supplement 4): p. 75-90.

Moolgavkar, S.H. Air pollution and hospital admissions for diseases of the circulatory system in three U.S. metropolitan areas. J Air Waste Manag Assoc, 2000. 50(7): p. 1199-206.

Norfolk Southern [NS]. 2012. Class I Railroad Annual Report, [accessed Nov, 2012]. http://www.stb.dot.gov/econdata.nsf/f039526076cc0f8e8525660b006870c9/d945e6d27425d1f6852579db004cfdbd?OpenDocument.

Ostro, B., M. Lipsett, J. Mann, H. Braxton-Owens and M. White. 2001. Air pollution and exacerbation of asthma in African-American children in Los Angeles. Epidemiology. Vol. 12 (2): 200-8.

Ostro, B.D. Air Pollution and Morbidity Revisited: A Specification Test. Journal of Environmental Economics and Management, 1987. 14: p. 87-98.

Ostro, B.D. and S. Rothschild. Air Pollution and Acute Respiratory Morbidity - an Observational Study of Multiple Pollutants. Environ Res, 1989. 50(2): p. 238-247.

Pope, C.A., et al. Respiratory Health and Pm10 Pollution - a Daily Time Series Analysis. American Review of Respiratory Disease, 1991. 144(3): p. 668-674.

Schwartz, J. and L.M. Neas. 2000. Fine particles are more strongly associated than coarse particles with acute respiratory health effects in schoolchildren. Epidemiology. Vol. 11 (1): 6-10.

Sheppard, L. Ambient Air Pollution and Nonelderly Asthma Hospital Admissions in Seattle, Washington, 1987-1994. In: Revised Analyses of Time-Series Studies of Air Pollution and Health. 2003, Health Effects Institute: Boston, MA. p. 227-230.

Woodruff, T.J., J. Grillo and K.C. Schoendorf. 1997. The relationship between selected causes of postneonatal infant mortality and particulate air pollution in the United States. Environmental Health Perspectives. Vol. 105 (6): 608-612.

Zanobetti, A., M. Franklin and J. Schwartz. 2009. Fine particulate air pollution and its components in association with cause-specific emergency admissions. Environmental Health Vol. 8: 58-60.

Zanobetti, A., M. Franklin and J. Schwartz. 2009. Fine particulate air pollution and its components in association with cause-specific emergency admissions. Environmental Health Vol. 8: 58-60.

APPENDIX C

DATABASE OF MEASUREMENTS

A data base with measurements for $PM_{2.5}$, BC, CO_2 wind speed and direction and tables with metals, EC/OC and Ions filter based measurements is contained in digital format as Appendix C. There are data base tables for each of the pollutants continuous measurements at each of the two monitoring sites. Two instruments were used to measure BC at fire station 8 sites, an Aethalometer and a multi-angle absorption photometer. An access table is provided for the measurements of each of these instruments. Data is marked with time stamps, formatted month day year hour: minute (mm-dd-yyy hh:mm).

VITA

Boris Galvis

BORIS GALVIS was born in San Gil, Santander, Colombia. He received a B.S. in Chemical Engineering from the Industrial University of Santander, Bucaramanga, Colombia in 1998. He worked for several environmental government agencies in Colombia. He was married in 2001 to Luz Dary Carreño. He obtained a M.S. in Environmental Engineering from University of the Andes, Bogota, Colombia in 2006. He joined Environmental Engineering faculty at Universidad de La Salle in Bogota in 2006. In 2008, he decided to pursue a doctorate in Environmental Engineering with full support of his wife. The Colombian Institute for the Development of Science and Technology awarded him a fellowship to aid him in this endeavor. He came to Georgia Tech pursuing a Doctorate and also obtained a M.S. in Environmental Engineering, in 2010. Boris enjoys very much using environmental monitoring instruments and tinkering with them. He also likes to ride his bike and to take road trips with his family to small towns, beaches, natural parks and museums. He enjoys dancing with his wife, reading to his daughter and going to the movies with his son.